

Exploring the role of endogenous TDP-43 SUMOylation in mice: Implications for Amyotrophic Lateral Sclerosis and Frontotemporal Dementia.

Caroline Part

A thesis submitted to the University of Ottawa in partial fulfillment of the requirements for the Master's degree in Neuroscience.

Department of Cellular and Molecular Medicine
Faculty of Medicine
University of Ottawa

© **Caroline Part, Ottawa, Canada, 2024**

Abstract

As the most common motor neuron disease, Amyotrophic lateral sclerosis (ALS) affects around 4 in every 100,000 people worldwide with reports of increasing prevalence over the years.

Characterized by progressive degeneration of motor neurons, ALS patients suffer impairments of movement and typically die from respiratory failure 2-5 years after diagnosis. Curiously, ALS exists on a disease continuum with Frontotemporal Dementia (FTD) where 30-50% of patients will be diagnosed with both diseases. In FTD, degeneration of cortical neurons results in diverse behavioural changes including deficits in executive and social skills as well as language and memory. A central connection between ALS and FTD is TDP-43 (encoded by *TARDBP*), an essential DNA/RNA binding protein known to serve critical functions in numerous cellular processes. Despite mutations in *TARDBP* constituting a small percentage of familial cases, TDP-43 nuclear-to-cytoplasmic mislocalization is a pathological hallmark of most ALS-FTD cases.

Therefore, therapeutic targets to rectify pathology and disease may be uncovered by identifying factors that regulate TDP-43. While it is currently established TDP-43 is ubiquitinated and phosphorylated in diseased states, our lab recently found TDP-43 is SUMOylated in response to stress. Of note, perturbations in the stress response are becoming increasingly implicated in neurodegenerations. Furthermore, TDP-43 plays critical roles in the stress response which become perturbed in ALS/FTD. We developed a TDP-43 “SUMO dead” mouse allele to gain an understanding of how disrupting this may contribute to the pathogenesis of ALS-FTD.

Longitudinal characterization of the model explored behavioural and histological *in vivo* consequences following loss of TDP-43 SUMOylation. However, the phenotypes observed in the mutant mice were less robust in comparison to established ALS/FTD mouse models. Mutant mice did not have consistent differences in tests for similar outcomes, trials of the same test, or across age. Female mutant mice presented with early hyperactivity and disinhibition along with

altered social grooming behaviour. At later age, these female mice developed impairments in spatial working memory. Male mice developed apathetic behaviour and motor deficits at the middle age timepoint. Histologically, various forms of pathological TDP-43 were observed in the absence of neurodegeneration. These data reveal that TDP-43 SUMOylation may play an important role in ALS/FTD pathogenesis.

Acknowledgements

I would first like to thank my supervisor, Dr. Maxime Rousseaux, for welcoming me into his lab and for his mentorship throughout my degree. Your passion and support shaped me as a scientist, and I am grateful for the many opportunities you provided me during my graduate studies. I would also like to thank my two lab mentors, Terry Suk and Haley Geertsma, for their technical support in the lab as well as guidance on all things related to academia and graduate school. Many thanks to all the members of the Rousseaux lab for their support and friendship. A special thank you to Steve Callaghan for his excellence in managing the lab, allowing me to complete my experiments.

I would like to sincerely thank the member of my thesis advisory committee, Dr. Diane Lagace and Dr. Rashmi Kothary, who provided me with expertise and encouragement throughout my graduate school journey.

Many thanks to the Behaviour Core staff, in particular Dr. Kerstin Ure and Sarah Kealey, who never got tired of my endless questions and always enthusiastically supported my new ideas.

I would also like to thank the patients living with ALS who I had the upmost privilege to meet at ALS Canada Society events. Hearing your stories has been a constant driving force behind my research. And thank you to Shirely, for the moments we spent together and our lovely chats. I will carry your memory with me as inspiration for the rest of my career.

I would not be the ‘mouse whisperer’ if I did not thank all my mice who gave the greatest sacrifice for this research and the advancement of health research. We as a scientific community could not save lives without them and should be eternally grateful. It is my deepest wish that

non-aversive handling and cage enrichment will become the standard, not the exception in the near future for animal work.

Last, but definitely not least, I am immensely grateful to my family for all of their support on my academic journey. I knew I could always turn to you in times of frustration, stress or sadness. I could not have made my accomplishments with you all.

Funding

I would like to express my sincerest gratitude to my funding sources, who helped make this research possible. Firstly, I would like to acknowledge the **Canadian Institute of Health Research** and **The Ontario Graduate Scholarship Program**. Receiving the “Canadian Graduate Scholarship – Master’s” and “Ontario Graduate Scholarship” was a great honour and has inspired me to continue to pursue medical research,

List of Figures

Figure 1. TDP-43 is SUMOylated at K408 in a stress-dependent manner.....	17
Figure 2. TDP-43 SUMOylation is blocked <i>in vivo</i> with K408R mutation but not does not affect viability or breeding ratios.....	45
Figure 3. <i>Tdp-43</i> ^{K408R} mutant mice do not display overt development impairment.....	47
Figure 4. <i>Tdp-43</i> ^{K408R} mutant mice do not display deficits in forelimb grip strength or hanging wire.....	48
Figure 5. Male <i>Tdp-43</i> ^{K408R} mutant mice display deficits in rotarod deficits at middle age.....	50
Figure 6. Male <i>Tdp-43</i> ^{K408R} mutant mice display mild marble burying deficits at middle age.....	51
Figure 7. <i>Tdp-43</i> ^{K408R} mutant mice behavioural alterations in open field testing.....	53
Figure 8. <i>Tdp-43</i> ^{K408R} mutant mice do not show changes in light-dark box and beam break.....	54
Figure 9. Female <i>Tdp-43</i> ^{K408R} mutant mice show changes in habituation behaviour at middle age in beam break.....	56
Figure 10. <i>Tdp-43</i> ^{K408R} mutant mice display reduced dominance within cages at old age.....	57
Figure 11. <i>Tdp-43</i> ^{K408R} mutant female mice have cognitive deficit in Y-maze at old age.....	60
Figure 12. <i>Tdp-43</i> ^{K408R} mutant mice do not display changes in emotional processing.....	61
Figure 13. <i>Tdp-43</i> ^{K408R} mutant mice neuromuscular impairments but female mice show changes in barbering behaviour.....	62
Figure 14. <i>Tdp-43</i> ^{K408R} mutant female mice do not display cortical neurodegeneration at 5-months.....	64
Figure 15. <i>Tdp-43</i> ^{K408R} mutant female mice do not display loss of upper motor neurons.....	65
Figure 16. <i>Tdp-43</i> ^{K408R} mutant female mice do not display significant hippocampal pathology at 5-months.....	66
Figure 17. <i>Tdp-43</i> ^{K408R} mutant female mice do not display central nervous system demyelination at 5-months.....	68
Figure 18. <i>Tdp-43</i> ^{K408R} mutant female mice display pathological TDP-43 at 5-months.....	69
Figure 19. <i>Tdp-43</i> ^{K408R} mutant mice display mislocalized TDP-43 at 9-months.....	71
Supplementary Figure 1. Wild-type mice display motor decline in rotarod and open field with age.....	85
Supplementary Figure 2. Number of arm entries during Y-maze test at 16-months.....	86

List of Tables

Table 1. Scoring for Hindlimb Clasping Phenotype.....	83
Table 2. Scoring for Kyphosis Phenotype.....	83
Table 3. List of Primary Antibodies Used in this Study.....	84

Abbreviations

MND - Motor neuron disease
ALS – Amyotrophic Lateral Sclerosis
PLS – Primary lateral sclerosis
SBMA – Spinal and bulbar muscular atrophy
PPS – Postpolio Syndrome
UMN – Upper motor neuron
LMN – Lower motor neuron
MRI – Magnetic resonance imaging
ALSFRS-r – ALS Functional Rating Scale revised
ALS-MiToS – Milan Torino Staging system
TDP-43 – Trans-activation response DNA-binding protein 43 kDA
SOD1 - Superoxide dismutase 1
FUS – Fused in Sarcoma
C9orf72 – Chromosome 9 open reading frame 72
FTD – Frontotemporal dementia
FTLD- Frontotemporal lobar degeneration
bvFTD – Behavioural variant of FTD
SD - Semantic dementia of FTD
PNFA – Progressive nonfluent aphasia of FTD
MAPT – Microtubule associated protein tau
SQSTM1 – Sequestosome-1 or p62
Nfl – Neurofilament light chain
STMN2 – Stathmin 2
UNC13A – Unc-13 homolog A
POLDIP3 - DNA Polymerase delta interacting protein 3
SORT1 - Sortilin 1
PFKP - Phosphofructokinase, platelet
RRM1 and 2 – RNA recognition motifs 1 and 2
NLS – Nuclear localization signal
NES – Nuclear export signal
SUMO – Small ubiquitin-like modifiers
SENPs – SUMO-specific proteases

Table of Contents

Abstract.....	ii
Acknowledgments.....	iv
Funding.....	vi
List of Figures.....	vii
List of Tables.....	viii
Abbreviations.....	ix
1. Introduction.....	1
1.1 Amyotrophic Lateral Sclerosis.....	1
1.1.1 Epidemiology.....	1
1.1.2 Symptoms and Progression.....	1
1.1.3 Diagnosis, Staging, and Treatment.....	2
1.1.4 Genetics.....	6
1.2 Frontotemporal Dementia.....	7
1.2.1 Epidemiology.....	7
1.2.2 Clinical Presentation, Diagnosis, and Treatment.....	8
1.2.3 Pathological Subgroups.....	10
1.3 The ALS/FTD Clinical Spectrum.....	14
1.3.1 Biomarkers.....	15
1.4 TDP-43.....	16
1.4.1 TDP-43 Pathology in ALS/FTD.....	16
1.4.2 Structure and Function.....	17
1.4.3 TDP-43 Mediated Toxicity: Loss or Gain of Function?.....	18
1.4.4 TDP-43 Mouse Models of ALS/FTD.....	22
1.5.4 Post-translational Modifications of TDP-43.....	23
1.5 SUMOylation.....	24
1.5.1 SUMOylation and ALS/FTD.....	25
1.6 Rationale for the <i>Tdp-43</i> ^{K408R} Mouse Line.....	26
2. Hypothesis.....	28
3. Aim.....	28

4. Contributions to the Project.....	28
5. Materials and Methods.....	28
5.1 General Information for Animal Work and Ethics Statement.....	28
5.2 <i>Tdp-43</i> ^{K408R} Mouse Line Generation.....	29
5.3 Genotyping.....	29
5.4 Mouse Wellness Monitoring.....	30
5.5 Behaviour Testing.....	31
5.5.1 General Information.....	31
5.5.2 Developmental Testing.....	32
5.5.3 Beam Break.....	32
5.5.4 Digigait.....	33
5.5.5 Fear Conditioning.....	33
5.5.6 Grip Strength.....	34
5.5.7 Grooming.....	35
5.5.8 Hanging Wire.....	35
5.5.9 Light Dark Box.....	35
5.5.10 Marble Burying.....	36
5.5.11 Nest Building.....	36
5.5.12 Open Field.....	36
5.5.13 Rotarod.....	37
5.5.14 Spontaneous Y-Maze.....	37
5.5.15 Tail Suspension.....	37
5.5.16 Three Chamber Sociability.....	38
5.5.17 Tube Test of Social Dominance.....	38
5.6 Tissue Collection and Processing.....	39
5.7 Histology.....	39
5.7.1 General Information.....	39
5.7.2 Immunofluorescence Staining.....	40
5.7.3 Chromogenic Dye Staining.....	40
5.6.4 Image Acquisition and Analysis.....	41

5.8 Statistical Analysis.....	32
6. Results.....	32
6.1 Tdp-43 ^{K408R} Mouse Line Validation.....	32
6.2 Behavioural Characterization.....	33
6.2.1 <i>Tdp-43</i> ^{K408R} Mice Development.....	33
6.2.2 Motor Function of <i>Tdp-43</i> ^{K408R} Mice.....	34
6.2.3 Naturalistic Behaviour of <i>Tdp-43</i> ^{K408R} Mice.....	36
6.2.4 Testing Exploration, Locomotion and Anxiety of <i>Tdp-43</i> ^{K408R} Mice.....	49
6.2.5 Social Behaviour of <i>Tdp-43</i> ^{K408R} Mice.....	52
6.2.6 Working Memory of <i>Tdp-43</i> ^{K408R} Mice.....	58
6.2.7 Emotional Processing of <i>Tdp-43</i> ^{K408R} Mice.....	58
6.2.8 Wellness Monitoring of Adult <i>Tdp-43</i> ^{K408R} Mice.....	59
6.3 Histological Characterization.....	63
6.3.1 Cortical Neurodegeneration in 5-Month Female <i>Tdp-43</i> ^{K408R} Mice.....	63
6.3.2 Hippocampal Pathology in 5-Month Female <i>Tdp-43</i> ^{K408R} Mice.....	63
6.3.3 CNS Myelination in 5-Month Female <i>Tdp-43</i> ^{K408R} Mice.....	67
6.3.4 Pathological TDP-43 in 5-Month Female <i>Tdp-43</i> ^{K408R} Mice.....	67
6.3.5 Lower Motor Neurons in 9-Month <i>Tdp-43</i> ^{K408R} Mice.....	70
6.3.6 C-Terminal TDP-43 in 9-Month <i>Tdp-43</i> ^{K408R} Mice.....	70
5. Discussion.....	72
5.1 TDP-43 Animal Models have Variable Onset of ALS and FTD Disease Features.....	73
5.1.1 Investigation Limitations.....	74
5.2 Future Directions.....	77
5.2.1 Sex Differences in ALS/FTD.....	77
5.2.1 Environmental Insults and Stress in ALS/FTD.....	78
5.2.3 Biomarker Development for ALS/FTD.....	80
5.3 Conclusion.....	82
6. References.....	87

1. Introduction

1.1 Amyotrophic Lateral Sclerosis

1.1.1 Epidemiology

Motor neuron diseases (MNDs) consist of a collection of diseases with degeneration of motor neurons producing loss of skeletal muscle function.¹ Globally, the incidence of MND is approximately 1 to 3 per 100, 000 with a lifetime risk of approximately 1 in 400 people.^{2,3} Amongst MNDs, the most common, making up around 80% of all cases, is Amyotrophic Lateral Sclerosis, with more than 200, 000 individuals across the globe living with the disease.⁴⁻⁶ Epidemiological data of ALS cases varies by geographical region, but globally the incident rate for ALS is approximately 2 per 100, 000.^{7,8} Advancing age is the biggest risk factor for the development of ALS.⁹ Globally, the age of onset is around 50 to 65 years old. Male sex has also been identified as a risk factor for ALS with studies reporting a male to female bias between 1 and 3.¹⁰ Interestingly, the rates of ALS are significantly more similar between males and females with age adjusted data.¹⁰

1.1.2 Symptoms and Progression

Amyotrophic Lateral Sclerosis (ALS) is a progressive, fatal neurodegenerative disease with heterogeneous clinical and biological features. ALS is characterized by the selective loss of motor neurons and the consequent denervation and dysfunction of the associated somatic muscles. In ALS, degeneration of both the upper and lower motor neurons is present over the diseases course.¹¹ The cell bodies of upper motor neurons are in layer V of the motor cortex. Their axons descend as the corticospinal and corticobulbar tracts to synapse with lower motor

neurons. Spinal motor neurons are found in the ventral horn of the spinal cord and cranial motor neurons in the brainstem, respectively. The spinal and cranial lower motor neurons send descending axons as nerves to innervate target muscles. The loss of upper motor neurons produces symptoms of spasticity, increased muscle tone and hyperreflexia whereas loss of lower motor neurons produces muscle weakness, atrophy, and fasciculations.¹² Most ALS patients die due to weakness of the diaphragm resulting in respiratory insufficiency within 5 years of diagnosis.¹³ The onset of ALS is often focal muscle weakness which spreads as the disease progresses, but patients can be classified by regional differences in symptom onset.¹⁴ Almost two-thirds of patients will have spinal onset, presenting with weakness in the upper or lower limbs.^{14,15} For spinal-ALS patients with onset in the upper limb, the majority will present with asymmetrical weakness in their dominant limb.¹⁶ Most patients experience these symptoms in distal muscles prior to those proximal in the affected limb.¹⁴ Patients with spinal onset have an average life expectancy of 3-5 years.¹⁵ Alternatively, approximately one-third of patients have bulbar onset where muscles of mastication, speech, and swallowing are affected producing dysphagia and dysarthria. Bulbar-onset ALS has a more rapid decline, with patients having a life expectancy of around 2 years after diagnosis.¹⁷ Respiratory onset ALS, affecting a minority (~3%) of patients results in weakness of the diaphragmatic muscles is early in the course of the disease.^{14,18,19} These patients experience dyspnea and succumb to disease within 2 years of diagnosis.

In addition to motor deficits, as many as 50% of ALS patients will also experience cognitive and behavioural deficits.²⁰⁻²² ALS patients with bulbar onset or who are women have been found to be more likely to experience cognitive symptoms over the course of their disease.²³ At the time of diagnosis, most patients perform normally on neuropsychiatric testing and cognitive

symptoms present with progression to advanced stages of ALS.²⁴ This has been suggested to reflect the spreading of pathology from motor to nonmotor areas within the nervous system.²⁵ Unfortunately, the appearance of cognitive symptoms has been associated with a more rapidly progressing disease.²⁶

1.1.3 Diagnosis, Staging, and Treatment

The diagnosis of ALS remains challenging due to the lack of specific tests or biomarkers and thus, requires the exclusion of other diseases, especially other motor neuron diseases with similar phenotypes.²⁷⁻²⁹ These diseases, often referred to as ALS mimics, include primary lateral sclerosis (PLS), spinal and bulbar muscular atrophy (SBMA), and Postpolio Syndrome (PPS).³⁰ PLS is characterized by only UMN degeneration, whereas SBMA is an X-linked disease and PPS is a disease secondary to poliovirus infection, with both having lower motor neuron degeneration.³⁰ The diagnostic process includes a battery of blood tests, brain and spinal cord imaging like magnetic resonance (MRI), muscle biopsies and electrophysiological recordings in conjunction with the clinical history, signs and symptoms.^{31,32} Genetic testing may be ordered if there is a relevant family history of familial ALS. Adding to the diagnostic challenge, the first presenting symptoms are subtle, vague and less associated with ALS including malaise and fatigue in addition to walking difficulties and muscle weakness. Misdiagnosis has resulted in ALS patients receiving unnecessary, often invasive procedures.^{33,34} ALS patients have been found to undergo spinal, knee, carpal tunnel, shoulder, tonsillectomy, ulnar nerve transposition, and sinus surgeries prior to their diagnosis. The symptoms preceding the surgeries did not resolve afterwards. Currently, ALS patients experience a diagnostic delay of 8-22 months which has not improved for a decade despite recognition that prompt diagnosis may improve patient quality of life.^{35,36}

The first diagnostic criteria, the El Escorial, for ALS was established in 1994 to classify patients by diagnostic certainty for clinical studies of disease.³⁷ This system was revisited to improve its use by clinicians in addition to research purposes.³⁸ This system considers both UMN and LMN signs across four topographical regions: bulbar, cervical, thoracic, and lumbar. The four diagnostic categories include possible ALS, probable ALS, laboratory-supported ALS, and definite ALS.²⁹ In 2008, the Awaji-Shima criteria was established and has been found to improve diagnostic sensitivity by incorporating electrophysiological data along with clinical signs.^{39,40} Still, many clinicians are not using these systems in the diagnosis of ALS as they were developed for research purposes and to inform decisions on including and monitoring patients in clinical trials.¹⁴ Most recently in 2019, the Gold Coast diagnostic criteria were developed specifically for the diagnosis of ALS with only a binary interpretation.^{41,42} These criteria have been validated for sensitivity and specificity and may be used more commonly in clinic.

Staging systems have been developed to quantify disease progression in ALS patients and assess novel biomarkers and treatments in clinical trials.⁴³ However, with the heterogeneity of the disease, it has been challenging for a system to cover all patients uniformly. Previously, the most commonly used scale for both physicians and researchers was the revised ALS Functional Rating Scale (ALSFRS-r).^{44,45} This scale is made up of 12 points for scoring and assessed the bulbar, respiratory, upper and lower limb domains. However, several limitations have been identified with the use of the ALSFRS-r including its non-linear progression, lack of correlation with prognosis, and poorly defined categories.⁴⁶ More recently, the Kings College and the Milan Torino (ALS-MiToS) staging systems are increasingly used as the *de factor* clinical scales.^{47,48} The Kings College is a 5 point scale based on anatomical spread of disease across neurological regions. Stage 1-3 focus on weakness and dysfunction in regions affected by motor neuron loss,

stage 4 focuses on nutritional and respiratory failure, and stage 5 corresponds to death. The MiToS is a 6-point scale which assess functional impairment and incorporates the ALSFRS-r. Studies have found that these two staging systems are not redundant but instead complimentary in their information and should be used together.⁴⁹ Specifically, the Kings College was found to have higher resolution in early disease stages, and the MiToS for later disease stages.⁴⁹

Despite decades of research with advances in genetic and molecular understanding of the disease, there are minimal treatment options for ALS patients and currently no curative treatment.⁵⁰ There exists a need for the development of treatment to reduce the rate of disease progression to improve both quality and quantity of life for patients. In Canada, there are currently three approved pharmacological disease modifying therapies for ALS.⁵¹ Firstly, Riluzole, an anti-glutamatergic agent aimed to reduce excitotoxicity.⁵² In clinical trials it was shown to increase survival by 3 months.⁵² However, more recent studies have found this may be as high as 19 months in real-world settings outside of clinical trials.⁵³ In comparison to randomized-controlled trials, real-world data is collected from multiple sources with varying methodologies and is not bound by narrow patient eligibility or exclusion criteria.^{53,54} Real world evidence can be more relevant to patient populations. Secondly, Edavarone, a free radical scavenger designed to reduce neuroinflammation and oxidative stress, can reduce the loss of physical function by 33% over a 24-week treatment period and recent reports have also found it can improve survival up to 30 months.^{55,56} Lastly, Tofersen is a novel antisense oligonucleotide drug specifically for the treatment of ALS patients with a *SOD1* mutation (discussed on Section 1.14).⁵⁷

Presently, specialized supportive multidisciplinary care is recommended for ALS patients to manage symptoms and has been found to improve their quality of life and survival.^{32,58} Supportive care varies by the individual needs of each patient.⁵⁹ For mobility related concerns, physical therapy helps to reduce fatigue and muscle stiffness whereas occupational therapy uses devices and strategies to assist in everyday tasks.^{59,60} Patients can participate in speech therapy for both communication and eating difficulties. With the progression of the disease, they may switch to the use of technological devices for communication. Additionally, as many ALS patients experience a decline in body weight because of challenges eating and swallowing, they may take nutritional supplements or undergo a gastrostomy.^{61,62} Most patients will undergo invasive ventilation procedures in the later stage of disease as respiratory symptoms worsen.⁶³ Generally, tracheostomy ventilation has been found to improve survival of ALS while still providing them with acceptable quality of life. However, it is associated with a high burden of care.⁶³ Finally palliative care is aimed at reducing the symptoms and stress associated with ALS while overall improving patient quality of life.^{64,65} Palliative care teams often assist patients in making informed decisions about their health over the course of their illness. More recently, it has been recommended that patients receive palliative care early after diagnosis, as opposed to historically being offered at end-stage of the disease, to maximize its benefit.^{64,65}

1.1.4 Genetics

While causative genetic mutations have been identified for the smaller subset of familial ALS cases (~10%), the underlying cause(s) and mechanism(s) of disease development in sporadic cases (~90%) remain unclear and are suggested to involve both genetic and environmental factors.⁶⁶⁻⁶⁹ Proposed mechanisms implicated in the pathogenesis of ALS include changes in protein homeostasis, mitochondrial dysfunction, impaired cell stress pathways, perturbations in

RNA processing, reduced axonal transport, glutamate mediated excitotoxicity, and autophagy.³² Currently, mutations in around 30 genes are linked with ALS, however 4 genes have been identified to account for the majority of familial ALS cases which include *SOD1* (encoding superoxide dismutase 1), *FUS* (encoding RNA-binding protein Fused in Sarcoma, FUS), *C9orf72* (Chromosome 9 open reading frame 72), and *TARDBP* (encoding Trans-activation response (TAR) DNA-binding protein 43 kDA, TDP-43).⁷⁰ Interestingly, while *TARDBP* only contributes to around 4% of familial cases, a hallmark of almost all (~97%) ALS cases is the nuclear-to-cytoplasmic mislocalization and aggregation of TDP-43.^{20,67,71-75}

1.2 Frontotemporal Dementia

1.2.1 Epidemiology

Frontotemporal dementia (FTD) is a neurodegenerative disorder with clinical and pathological heterogeneity.⁷⁶ Dementia is a broad term for many diseases which are caused by impaired cognitive functioning. FTD is the second most common presenile dementia with an average age of onset of 58.⁷⁷ Globally, FTD has an incidence of around 3 per 100, 000 with this increasing to 9 per 100,000 for the above 60 age group.⁷⁸ However, recent studies have found that in some population up to 70% of patients initially misdiagnosed with another psychiatric condition and thus, the epidemiological data for this disease may be under represented.⁷⁷ The sex ratio for FTD is not well characterized. Some studies have reported an almost 5-fold greater prevalence in males, whereas others have found an equal distribution across the sexes, or a 3:1 female prevalence.^{76,79} These discrepancies may be explained by reports that females with FTD are significantly more likely to be misdiagnosed with other psychiatric conditions than males.⁷⁹ Survival time after diagnosis is highly variable ranging from 3-14 years.^{76,78,80,81} The most

common cause of death for FTD patients is aspiration pneumonia with others including infection, dehydration, gastrointestinal problems, and complications from falls.⁸²

1.2.2 Clinical Presentation, Diagnosis, and Treatment

The pathological process underlying the clinical manifestation of FTD, is frontotemporal lobar degeneration (FTLD) with neurodegeneration of the frontal and temporal cortices.⁸³ There are three categories of FTD based on the clinical presentation where these symptoms are determined by the pattern of neurodegeneration.⁸⁰ These three categories include the behavioural variant (bvFTD), and primary progressive aphasia which is further categorized into semantic dementia (SD) and progressive nonfluent aphasia (PNFA).⁸⁴ Diagnostic criteria for each of the three FTD variants was originally published in 1998, however this was revised to address limitations by the Frontotemporal Dementia Consortium 2011.^{76,85} Diagnosis of FTD is complex and currently there exists no singular test. Instead, physicians rely on clinical presentation, laboratory tests, batteries of neuropsychiatric tests, neuroimaging, and sometimes genetic testing to diagnosis patients with FTD while excluding other causes.⁸⁰

i. Behavioural Variant

The bvFTD is the most common form of FTD constituting more than half of all the cases. However, they are commonly misdiagnosed with depression or personality disorders.³⁸ There are three levels of diagnostic certainty including possible, probable, and definite bvFTD.⁸³ Patients with bvFTD suffer a diverse range of disturbances in personality, behaviour, and cognition while performing

normally in the domains of memory, language and visuospatial processing on neuropsychiatric tests.⁸¹ Possible bvFTD requires patients to have progressive impairment in at least of the following: disinhibition, apathy, impaired executive function, lack of empathy, compulsions, and disordered eating.^{81,83,86,87}

Neuroimaging studies have found that patients with bvFTD display atrophy in the frontal and anterior temporal cortices including the orbitofrontal cortex, prefrontal cortex, anterior cingulate and insular cortex.^{87,88} Patients with neuroimaging findings consistent with these features are classified as probable bvFTD. Definite bvFTD requires confirmation through genetic testing or post-mortem pathological examination.

ii. Semantic Dementia (SD)

Semantic dementia (SD) accounts for around a quarter of all FTD cases.^{81,86,87} SD patients experience the loss of semantic knowledge and language deficits. While their language is fluent, they develop problems with word finding and comprehension as well as recognizing faces and objects.⁸¹ Atrophy of the temporal lobe including the fusiform and inferior temporal gyri are most implicated.^{87,88} Notably, the pattern of degeneration early in the disease course is usually asymmetrical with greater atrophy of the left hemisphere producing language deficits while the atrophy of the right hemisphere produces deficits in recognition.⁸⁷ As the disease progresses, atrophy becomes more widespread to the other cortical lobes. There also three levels of diagnostic certainty for SD: clinical diagnosis, neuroimaging-supported diagnosis, and definite.⁸³ While language must be the primary symptom of impairment, they must also present with at least

two of the following symptoms for a specific diagnosis of SD: surface dyslexia, dysgraphia, spared repetition, spared speech production, and impaired object knowledge.

iii. Progressive nonfluent aphasia

The remaining 25% of FTD cases are classified in the subtype of progressive nonfluent aphasia (PNFA).⁸¹ These patients experience agrammatism and apraxia of speech which results in their speaking being nonfluent, effortful, slow with sound distortions.^{81,89} The agrammatical features are correlated with degeneration in the left hemisphere language network across the inferior frontal, temporal and parietal lobes whereas degeneration in premotor and motor cortices including Broca's area result in apraxia^{36,38}. The left inferior gyrus is affected earliest in PNFA and atrophy to the other areas progresses with the disease course.⁸⁷ The PNFA has the same levels of diagnosis certainty as SD.⁸⁹ However, these patients must have at least two of the following features: spared object knowledge, spared single-word comprehension, and impaired comprehension of syntactically complex sentences.

1.2.3 Pathological Subgroups

Contributing to its heterogeneity, FTD can also be subdivided by the predominant protein which accumulates in pathological intraneuronal inclusions.^{84,89} There are three categories based on the three proteins: tau (FTLD-tau), TAR DNA binding protein 43 (TDP-43, FTLD-TDP), and fused in the sarcoma (FUS, FTLD-FUS).

i. FTLD-Tau

Tau is a microtubule associated with important functions supporting axonal transport and structural stability for neurons as well as glia.⁸⁹ In pathological conditions collectively known as tauopathies, tau is hyperphosphorylated and forms insoluble cytoplasmic aggregates. Across the different tauopathies there are differences in the level of hyperphosphorylation, isoforms and other modifications of the tau protein. Several of these diseases are classified as FTD (FTD-tau).

Sporadically, FTD patients can have Pick's disease which includes the presence of swollen neurons called Pick cells, and large argyrophilic cytoplasmic inclusions in neurons and sometimes glia called Pick bodies.⁸⁹ While Pick's disease is most associated with the bvFTD, it can be present in any of the clinical subtypes.

Familial cases of FTLD-tau are also found with patients having mutation in the tau encoding gene, *MAPT*. Upwards of 30% of all familial cases of FTD have mutations in this gene.

ii. FTLD-FUS

FUS is an RNA-binding protein with known roles in regulating transcription, splicing, and DNA repair.⁸⁹ In neurodegenerative disorder, there has been support for both gain and loss of function mediating FUS toxicity.⁹⁰ Patients with FUS pathology make up the smallest percentage, 10% of all cases, and at the histopathological level develop cytoplasmic FUS inclusions in neurons and to a lesser extent glia.⁸⁹ More recently, aggregates of the other members of the FET protein family, to which FUS belongs, have been found in FTLD-FUS inclusions.⁹¹ Currently, no causative genetic mutations in the encoding gene have

been identified in patients.⁹² Unlike the other molecular subtypes, FTLN-FUS has only been associated with the bvFTD and not PPA.^{91,93} Additionally, these patients have a younger average age of onset at 40 with more severe clinical symptoms and degeneration in association brain regions.⁹⁴ Interestingly, FTLN-FUS patients specifically have greater atrophy of the caudate, which has been proposed as a potential diagnostic biomarker.⁹⁰

iii. FTLN-TDP

Trans-activation response (TAR) DNA-binding protein 43 kDA (TDP-43) is a ubiquitously expressed ribonuclear protein which has been found to be involved in several cellular functions. In FTLN-TDP, the predominately nuclear TDP-43 mislocalizes and aggregates in the cytoplasm of neurons and glia.^{89,91,93} These inclusions include TDP-43 which is hyperphosphorylated and immunoreactive to ubiquitin. However, this pathology is not exclusive to FTLN.⁸⁹ FTLN-TDP makes up the majority, at around 50% of all cases despite familial mutations in its encoding gene being of very low percentage.⁸⁹ Similarly, to FTLN-tau, this pathology is predominately associated with the bvFTD.⁹⁵ The FTLN-TDP classification can further broken down into FTLN-TDP type A-D based on pathological features, clinical phenotypes, and causative mutations.

A. FTLN-TDP Type A

Type A cases are particularly associated with neuronal cytoplasmic inclusions of TDP-43 in the superficial neocortical layers.^{91,96}

However, pathology is also found within regions of the hippocampus.

At the clinical level, FTLN-TDP-43 Type A can manifest as bvFTD or NFPA.⁹⁶

B. FTLN-TDP Type B

Type B pathology includes TDP-43 cytoplasmic inclusions throughout the cortex.⁹¹ Importantly, FTLN cases with TDP-43 pathology in lower motor neurons are almost exclusively Type B even when no other features of ALS are present. These cases are most likely to develop ALS-FTD.⁹⁶

C. FTLN-Type C

In Type C, there are little to no TDP-43 intraneural cytoplasmic inclusions in the cortex, however, dystrophic neurites become abundant.^{91,96} In subcortical structures including the dentate gyrus and striatum there is numerous cytoplasmic TDP-43 inclusions in neurons.⁹⁶ Clinically, this subtype is associated with SD.

D. FTLN-Type D

For Type D cases, there is an absence of cytoplasmic TDP-43 pathology across cortical and subcortical regions.^{91,96} Throughout, dystrophic neurons and intranuclear inclusions can be identified. This subtype is only found in patients with a genetic mutation in VCP, and is most often associated with the bvFTD.^{91,96}

As with many types of dementia, developing treatment is challenging, and currently there are no approved disease-modifying therapies for patients with FTD.^{80,84,97,98} Pharmacological and non-

pharmacological approaches focus on alleviating the symptoms of the disease. Antipsychotics and mood stabilizers are commonly used to treat symptoms of agitation and aggression and their use is supported by studies finding improvement in behavioural domains.^{78,86,99} More research is needed to determine the benefits of other psychiatric drugs.⁷⁸ Numerous non-pharmacological interventions for behavioural management of FTD patients are employed including physical exercise, speech therapy, music therapy, changes in the environment to address both sensory and safety needs.¹⁰⁰

1.3 The ALS/FTD Clinical Spectrum

While ALS and FTD are both neurodegenerative disorders, the manifestations of their clinical symptoms appear distinct. However, increasing evidence has been found in support of an overlap between these two diseases at the clinical, genetic, and pathological level.¹⁰¹ They are now said to exist on a spectrum. Of the ALS patients who experience cognitive impairment, approximately 20% will fit the diagnostic criteria for FTD. Additionally, around 10% of patients initially diagnosed with FTD, will go on to develop motor symptoms characteristic of ALS. While mutations in genes can produce pure forms of either ALS (e.g. *SOD1*) or FTD (e.g. *MAPT*), there also exists genes whose mutations can cause either disease.⁸⁴ Most notably these include chromosome 9 open reading frame 72 (*C9orf72*), Sequestosome-1 or p62 (*SQSTM1*), and TDP-43 (*TARDBP*).⁷⁰ The hexanucleotide expansion repeat in *C9orf72* is the most common genetic mutation for both familial and sporadic forms of ALS and FTD.¹⁰² However, despite mutations in TDP-43 making up a small percentage of both ALS and FTD cases, given the high predominance of patients displaying TDP-43 pathology, it has become known as a pathological hallmark of

these neurodegenerative diseases.^{74,75} Thus, TDP-43 is the point of convergence between genetics and pathology in ALS and FTD.

1.3.1 Biomarkers

ALS and FTD are both diseases which are challenging to diagnose early and lack disease modifying interventions. One of the contributing factors is the lack of biomarkers. As defined by the UK Medical Research Council, biomarkers are any objective measure which can give indication of a biological or pathological process, or pharmacological to a therapeutic intervention.¹⁰³ There are different categories of biomarkers depending on their clinical benefit. Diagnostic biomarkers aid in discrimination between diseases. Biomarkers can be predictive or prognostic for progression of diseases or be used to monitor the effectiveness of a novel therapeutic. A reliable biomarker would aid in clinical trials to monitor progression of patients and response to novel treatments in conjunction with the current staging systems and clinical tests. In recent years there has been growing effort to identify biomarkers for ALS/FTD in many areas including neuroimaging, electrophysiological, and biofluids including blood and cerebrospinal fluid (CSF). An ideal biomarker would be sensitive and specific to the disease of interest, be detectable early in the disease course prior of significant levels of degeneration, and practical to measure in patients.¹⁰³ Presently, the most studied biomarker for ALS and FTD is Neurofilament light chain (Nfl).¹⁰⁴ Nfl is a part of the axonal cytoskeleton providing structural support and specific to neurons.¹⁰⁵ Upon damage or degeneration to the axon, Nfl is released from the neuron where it can then be detected in the blood and CSF.^{104,105} Higher levels of Nfl in the blood or CSF are not specific to ALS or FTD but can be found in other degenerative diseases.¹⁰⁶ However, Nfl in ALS patients has been found to be significantly higher than ALS disease mimics up to 6 months after symptom onset.^{107,108} With this discriminative capacity it

can aid in earlier diagnosis. Additionally, its levels in ALS patients have been found to be correlated with the ALSFRS-R over the progression of the disease. For FTD, Nfl levels were higher allowing differentiation between Alzheimer's patients and were correlated with frontal and temporal lobe atrophy from neuroimaging.^{104,109} While Nfl as a biomarker has promising benefits, there are limitations to its utility. As mentioned, it is not specific to ALS or FTD, and the differences in levels compared to other diseases is not completely understood. Additionally, whether Nfl can serve as a presymptomatic biomarker is still being investigated. While some studies report no difference in Nfl between presymptomatic ALS genetic risk carriers, others have found Nfl begins to increase prior to symptom onset, however this may be for aggressive forms of the disease.¹¹⁰ Overall, more work is needed in the development of biomarkers for ALS and FTD to benefit patients.

1.4 TDP-43

1.4.1 TDP-43 Pathology in ALS/FTD

Known as a pathological hallmark, the nuclear to cytoplasmic mislocalization and subsequent aggregation of TDP-43 is a key feature in 97% of ALS and over 50% of FTD cases.

Neuropathological features of TDP-43 in disease include nuclear depletion, cytoplasmic accumulation, and formation of insoluble aggregates in neurons and to a lesser extent glia.

Additionally, it has been found that these inclusions contain TDP-43 which is hyper-ubiquitinated and hyper-phosphorylated (Serine 403/404 and 409/410), as well as 25 and 35kDa truncated C-terminal fragments of the full-length protein. These aggregates have also been found to be positive for p62.^{111,112}

1.4.2 Structure and Function

TDP-43 is 414 amino acid residues in length and a highly conserved member of the heterogeneous nuclear ribonucleoprotein family.^{67,113-115} TDP-43 is ubiquitously expressed in many tissues including the nervous system and is essential for embryonic development.¹¹⁶ Structurally, TDP-43 is comprised of four domains: an N-terminal, two RNA recognition motifs (RRM1 and RRM2), and a low complexity glycine -rich C-terminal domain.^{114,117,118} Within the linker between the N-terminal domain and the RNA-binding domains is the bipartite nuclear localization signal (NLS) and a nuclear export signal (NES) within RRM2.¹¹⁴ The NLS and NES shuttle TDP-43 between the nucleus and the cytoplasm, despite it being predominately found in the nucleus. However, the NES remains controversial with some studies suggesting it is not functional.¹¹⁹ Finally, the C-terminal domain is known as the low-complexity domain being unstructured and prone to pathological aggregation.¹²⁰ Curiously, the majority of ALS and FTD mutations are found within this domain and are generally thought to increase cytoplasmic localization and aggregation propensity.¹²¹

TDP-43 has several roles within the nucleus and cytoplasm. Most functions of TDP-43 relate to its ability to bind nucleic acids, binding hundreds of RNA species, for RNA metabolism and include mRNA stabilization, splicing, transcription and translation.^{67,113,122,123} TDP-43 also regulates its own mRNA levels via a negative feedback loop. In binding its own transcript at the 3' untranslated region, it triggers the destruction of the mRNA and tightly autoregulates TDP-43 protein levels.^{124,125} Importantly, TDP-43 plays a role in the cellular stress response. In stress conditions, cytoplasmic TDP-43 has been found to be associated with stress granules.¹²⁶⁻¹²⁸

Stress granules are transient membrane-less organelles that form in response to various stressors including heat, osmotic, or oxidative.¹²⁹ They promote cell survival during these periods of stress by stalling translation and triaging mRNA critical for cellular survival for translation.¹³⁰ With the resolution of the stress, stress granules disassemble.^{126–128} The relationship between TDP-43 and stress granules is not completely understood. TDP-43 has been found to be recruited to stress granules and to regulate stress granule assembly by stabilising RNA transcripts.^{131–133} However, TDP-43 loss of function can reduce the formation of stress granules and promote cell death.¹³⁴ While stress granules disassemble under acute stress, in chronic stress they have been found to persist.¹²⁹ It has been hypothesized that these chronic stress granules arise in neurodegenerative diseases and may act as seeds for aggregation of TDP-43, as seen in ALS/FTD, and contribute to cell death.^{135,136} Stress granule markers have been detected to associate with TDP-43 aggregates of ALS and FTD patients.¹³⁵ However, there is also evidence for an independent model of TDP-43 aggregation not requiring stress granules.¹³⁷ Overall, there is support for TDP-43 and the stress response implicated in ALS/FTD pathogenesis.

1.4.3 TDP-43 Mediated Toxicity: Loss or Gain of Function?

The exact mechanisms of TDP-43 toxicity that are linked to neurodegeneration is not yet completely understood especially as this pathology is not unique to patients with TDP-43 mutations. However, evidence has found support for both loss of nuclear and gain of cytoplasmic TDP-43 functions as contributors in disease.

i. Loss of Function

The nuclear depletion of TDP-43 in ALS and FTD patients suggests that the loss of TDP-43 nuclear function may contribute to neurodegeneration.

There has been support for this from animal models. The loss of nematode TDP-43 ortholog in *C. elegans*, impairs growth and locomotion activity, however, it also extends the lifespan.¹³⁸ In flies, loss of TDP-43 homolog (*TBPH*) results in premature lethality, deficits in motor behaviour, and impairs synaptic connectivity.¹³⁹ Similarly, knocking out TDP-43 (*Tardbp*) and its paralogue (*Tardbp-like*) in Zebrafish leads to muscle degeneration, reduces axonal outgrowth length of motor neurons, and shortens the lifespan of the animals.¹⁴⁰ While murine TDP-43 knockout models are embryonically lethal, targeted depletion of TDP-43 in lower motor neurons recapitulates ALS features in mice.¹⁴¹

Molecular evidence for loss of functions toxicity relates to the role of TDP-43 as a splicing repressor.¹⁴² TDP-43 depletion results in the inclusion of cryptic exons which are splice variants with erroneous frameshifts or stop codons in the mature RNA.¹⁴³ Numerous studies have identified cryptic exons in post-mortem ALS and FTD patient tissues.^{144,145} Two note-worthy cryptic exons with their relevance to disease include *STMN2* (Stathmin 2) and *UNC13A* (Unc-13 homolog A).¹⁴⁴ *STMN2* encodes a microtubule associated protein and the inclusion of the cryptic exon reduced levels of the functional protein and impaired axonal regeneration.^{144,146} Loss *STMN2* in mice produces denervation of neuromuscular junctions and impaired motor behaviour.¹⁴⁶ It is therefore thought to play a role in ALS pathogenesis by playing a critical role in the

health of motor neurons. *UNC13A* is involved in various aspects of synaptic transmission and knockouts in mice result in mortality soon after birth.^{144,147,148} The loss of TDP-43 was found to result in the inclusion of cryptic exons in *UNC13A*, providing a mechanistic link to *UNC13A* as a strong genetic risk factor for ALS.^{144,147,148} However, it is important to note that for both *STMN2* and *UNC13A*, the cryptic exons are not conserved in mice. Therefore, humanized models will be required to understand whether blocking the cryptic exon rescues the TDP-43 loss of function. However, TDP-43 regulates splicing of conserved exons *POLDIP3* (DNA Polymerase delta interacting protein 3), *SORT1* (Sortilin 1), and *PFKP* (Phosphofructokinase, platelet). Altered splicing can be used to study TDP-43 nuclear loss of function in mice.¹⁴⁴

ii. Gain of Function

With its widespread but critical functions for the cell, TDP-43 protein levels are highly regulated. Clinically, higher levels of TDP-43 have been found in biofluids of ALS and FTD patients which suggests that perturbations in autoregulation may contribute to disease pathogenesis through gain of function mechanisms.¹⁴⁹ The importance of maintaining TDP-43 levels has been demonstrated using a transgenic mouse line which modestly overexpresses the protein.¹⁵⁰ With TDP-43 less than 60% above endogenous levels in the central nervous system, these mice develop features of ALS including neurodegeneration.¹⁵⁰ Furthermore, a knock-in mutation in TDP-43 was found to perturb autoregulation while producing

cognitive impairment in the mice.¹⁵¹ In other animal models including *C. elegans* and flies, overexpression of TDP-43 equivalents lead to similar toxic phenotypes as depletion.^{139,152} Supporting that both mechanisms play a role in disease.

Studies have also specifically investigated whether the localization of TDP-43 to the nucleus is directly toxic. Using rat cortical neurons, a point mutation of TDP-43 (A315T) or a disruption in the NLS increased mislocalization, and these cells had reduced viability.¹⁵³ Additionally, a mutation in the NES alleviated the toxicity of the A315T mutant. In transgenic models, the expression of human TDP-43 with a disrupted NLS modelled histological and behavioural features of ALS.^{154,155} These mice exhibited phosphorylated cytoplasmic TDP-43 inclusions, brain atrophy, loss of motor neurons, muscle denervation, and premature mortality. Behaviourally, deficits in locomotion and motor behaviour as well as cognitive abilities and social performance were observed. TDP-43 can exert toxicity in the cytoplasm by impairing protein synthesis of mitochondrial proteins in motor neurons.¹⁵⁶ Importantly, the contribution of mislocalization and aggregation of TDP-43 in the cytoplasm is still not completely understood. Studies *in vitro* have shown, that while intrinsically prone to aggregation through the C terminal domain, disease linked mutations in TDP-43 accelerate this process.¹⁵⁷ This increased number of aggregates promotes toxicity by causing enhanced cell death.

However, while the mislocalization of TDP-43 is toxic to neurons in culture with increased cytoplasmic mutant TDP-43 resulting in cell death, the formation of aggregates independently is not.¹⁵³ Overall, understanding the regulation of TDP-43 localization is critical for the development of effective treatments to mitigate toxicity.

1.4.4 TDP-43 Mouse Models of ALS/FTD

Mouse models of ALS date back to 1956 and the Wobbler mouse.¹⁵⁸ This mouse model arose by spontaneous mutation and developed many features of ALS including motor neuron degeneration, reduced body weight, gait impairments and muscle atrophy. It was later discovered that this mouse had a mutation in the *Vps54* gene which is not associated with ALS or other motor neuron diseases.^{158,159} Now, sixty-seven years later, numerous models of ALS and FTD have been created often targeting genetic mutations found in patients. Given its predominant role in disease pathogenesis, numerous approaches for TDP-43 mouse models have been developed to investigate whether the ALS/FTD phenotypes can be recapitulated. These models include overexpression of humanized wild-type and mutant forms of TDP-43, temporal and spatial conditional knockouts of TDP-43, as well as endogenous knock-in mutations of TDP-43.¹⁶⁰ Despite the many models available, there is currently still a great need to develop models with greater translational capacity to patients.¹⁶¹ While the models listed above can all provide informative insight into TDP-43 pathobiology in disease, there are also limitations in reflecting what is observed in patients which is critical for the development of therapeutics and biomarkers. Overexpression models of mutant and wild-type TDP-43 often present with rapid and aggressive disease progression with very early death. There is also currently no evidence that TDP-43 is

overexpressed in patients. Similarly, knock-out models can develop ALS/FTD phenotypes but does not reflect patients because TDP-43 is essential. Lastly, knock-in mutations only reflect a small subset of patients who have the specific mutation that is being modelled. Across the board, TDP-43 models of ALS and FTD are variable in their behavioural impairments and pathological findings including the presence of TDP-43 pathology. More work is needed to develop a model which reproduces the prevalent phenotypes found in patients to facilitate clinical advancements.

1.4.5 Post-translational Modification of TDP-43

As previously mentioned, TDP-43 undergoes key post-translational modifications in ALS/FTD including phosphorylation and ubiquitination.^{74,75}

While phosphorylation of proteins plays critical roles in healthy states, it is proposed to be toxic in ALS/FTD.^{162,163} Phosphorylation of full length TDP-43 specifically at Serine residues 403/404 and 409/410 are consistently detected in post-mortem patient cytoplasmic aggregates.⁹² Additionally, increased levels of phosphorylated TDP-43 in patient biofluids have been detected.¹⁶⁴ Despite most evidence supporting phosphorylation as toxic and driving neurodegeneration, there is some evidence that suggests it may play a protective role by preventing aggregation.¹⁶⁵

Akin to phosphorylation, ubiquitinated TDP-43 is also consistently detected in pathological TDP-43 aggregates. Causative mutations in machinery of the ubiquitin-proteasome system (UPS) are known in ALS/FTD.¹⁶⁶ In healthy states, TDP-43 can be cleared by the UPS, and there is strong support for dysfunction of the system in disease. Ubiquitination of TDP-43 promotes aggregation into cytoplasmic inclusions.¹⁶⁷

Besides phosphorylation and ubiquitination, several other post-translational modifications of TDP-43 are being investigated including acetylation, cysteine oxidation, and PARylation.^{114,163,168} These modifications have been found to alter the solubility, particularly promoting TDP-43 accumulation in insoluble aggregates, impair its ability to bind RNA and regulate splicing, and intracellular localization. Overall, post-translational modifications play a clear role in regulating aspects of TDP-43 biology and dysfunction can be implicated in disease pathology. This provides rationale to explore less studied modifications of TDP-43, like SUMOylation, and potential links to ALS/FTD.

1.5 SUMOylation

Conserved across eukaryote evolution, SUMOylation is an essential process which involves the covalent attachment of small ubiquitin-like modifier (SUMO) proteins to lysine residues of a target protein.^{114,169} There are 5 SUMO isoforms in humans (SUMO1-SUMO5) and the first 3 are conserved in mice and ubiquitously expressed.¹⁷⁰⁻¹⁷² In short, once SUMO proteins are cleaved at the C terminus by SUMO-specific proteases (SENPs) in a maturation process, it is activated in an ATP-dependent manner by an E1 enzyme.^{173,174} Next, the activated SUMO will be delivered to an E2 conjugating and often an E3 ligating enzyme to catalyze its binding to the target protein generally at lysine residues in the SUMO consensus motifs (Ψ -K-x-D/E; Ψ , large hydrophobic amino acid).¹⁷⁵ This process is reversible with SENPs completing deSUMOylation of target proteins.^{173,174} SUMOylation has been found in numerous cellular functions including protein trafficking, subcellular localization, stability, solubility, and protein interactions.¹⁷⁰

1.5.1 SUMOylation and ALS/FTD

There is an increasing body of evidence that SUMOylation regulates proteins critical in the pathogenesis of various neurodegenerative diseases, including some implicated in ALS/FTD.^{173,176,177} This is particularly interesting considering the role of SUMOylation in the cellular stress response.¹⁶⁹ However, the role of SUMOylation of TDP-43 in the context of ALS is currently not clear. When either full length TDP-43 or a mutant form lacking the C terminal domain was over-expressed in primary neuronal cultures an increase in SUMO2/3 co-localization with insoluble TDP-43 positive aggregates in the nucleus and to a lesser extent in the cytoplasm.¹⁷⁸ Cultured motor neurons overexpressing wild-type TDP-43 treated with anacardic acid, a known inhibitor of the E1 SUMO activating enzyme, had improved cell viability and neuritogenesis whereas the number of cytoplasmic TDP-43 aggregates was reduced.¹⁷⁹ However, the overexpression of either SENPs or a TS-1 cell permeable peptide which promote deSUMOylation lead to increased cytosolic localization of TDP-43.¹⁸⁰ Importantly, SUMOylation regulates many proteins, and these experiments did not specifically disrupt an interaction with TDP-43 which may account for the divergent results. Furthermore, these studies mutated a bioinformatically predicted SUMOylation consensus site on TDP-43 at Lysine 136 (K136).^{179,180} They found this mutated TDP-43 had impaired splicing activity and nucleocytoplasmic localization, remaining in the nucleus upon exposure to stress and was associated with less toxicity. However, it is important to note that no studies have demonstrated biochemical evidence that K136 is a SUMOylation or that mutating this site reduces TDP-43 SUMOylation. Therefore, the loss of SUMOylation may not be responsible for the results in these studies. Additionally, it has been found that up to 40% of SUMOylation sites are non-consensus sequences.¹⁸¹ Overall, more comprehensive study of SUMOylation and cellular

mislocalization and toxicity associated with TDP-43 aggregates in ALS is required. What's more, no animal models exist to study it in the context of ALS and FTD to address this gap in the field.

1.6 Rational for the *Tdp-43^{K408R}* Mouse Line

With the overlapping roles of TDP-43 and SUMOylation, a co-immunoprecipitation assay with GFP-tagged TDP-43 and HA-tagged SUMO2 was used to investigate TDP-43 SUMOylation (Figure 1A). When cells were treated with sodium arsenite stress, there was a robust increase in TDP-43 SUMOylation from the minimal levels at basal conditions (Figure 1B). Using bioinformatics, predicted TDP-43 SUMOylation sites at K136 (consensus) and K408 (non-consensus) were identified. These residues were mutated from Lysines to Arginines to block SUMOylation but maintain structure. Following stress, TDP-43 K136R could be SUMOylated to wild-type levels, but TDP-43 K408R could not. This result suggests that K408 is a stress-dependent SUMOylation site of TDP-43. This is tantalizing since the K408 residue is within a SUMOylation site dependent on phosphorylation, a hallmark feature of TDP-43 pathology, and a region of the C terminal domain that is highly conserved among vertebrates. To explore the *in vivo* consequences of blocking SUMOylation, the Tdp-43 “SUMO dead” mouse model (*Tdp-43^{K408R}*) was generated.

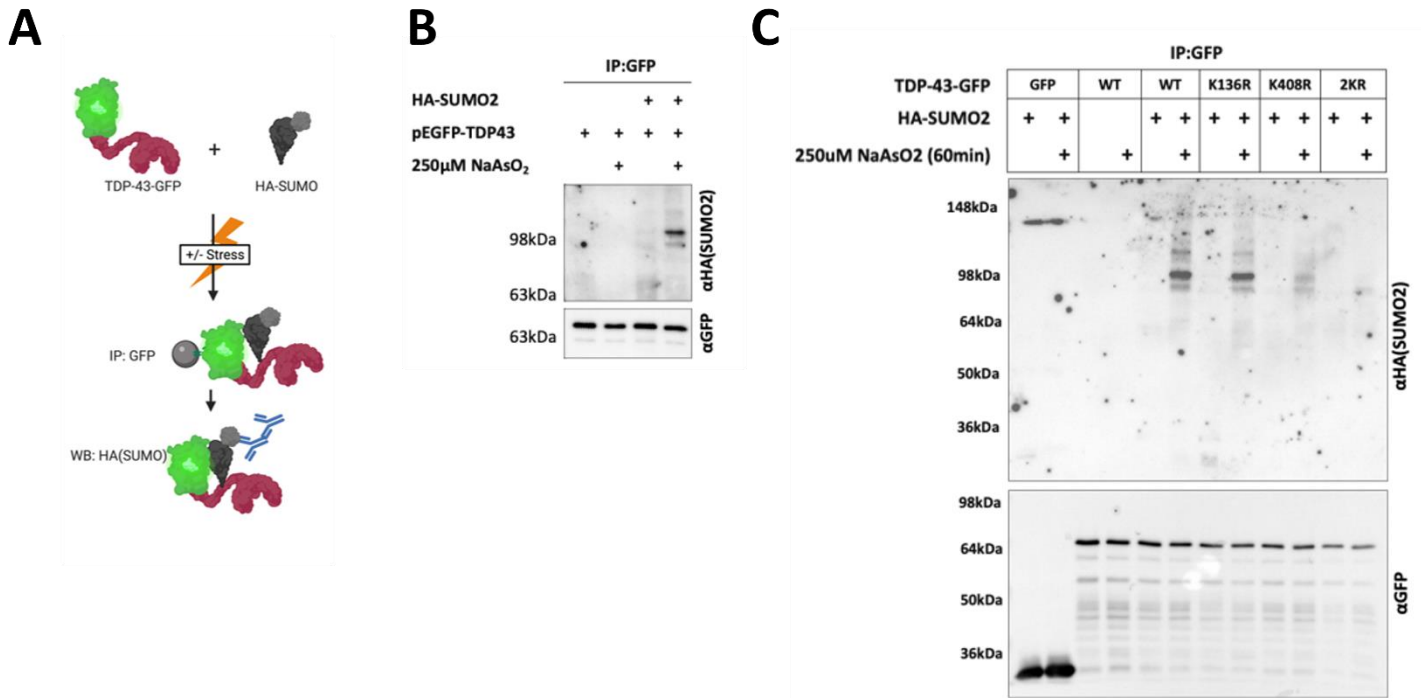


Figure 1. TDP-43 is SUMOylated at K408 in a stress-dependent manner. A) Schematic representation of co-immunoprecipitation experiment for GFP-tagged TDP-43 and HA-tagged SUMO2 following cellular stress. **B)** Western blot results for co- immunoprecipitation with and without sodium arsenite stress. **C)** Western blot results for co-immunoprecipitation experiment with TDP-43 K136R, K408R, or double mutant compared to wildtype TDP-43.

2. Hypothesis

Disruption of Tdp-43 SUMOylation is predicted to induce motor and cognitive behavioural features and neuropathology associated with ALS-FTD spectrum.

3. Aim

1. Characterization of the *Tdp-43^{K408R}* mouse wellness and behaviour as a model of ALS and FTD

2. Characterize the *Tdp-43^{K408R}* mouse for histological features of ALS and FTD

4. Contributions to the Project

Generation, genotyping, and maintenance of the breeding colony of the *Tdp-43^{K408R}* mouse line was completed by Terry Suk (Ph.D. Candidate, Rousseaux Lab, University of Ottawa). During tissue collection, Terry completed the dissection and weighing of the brain. Terry Suk completed work for Figure 1 and 2. All other experiments were completed by me.

5. Materials and Methods

5.1 General Information for Animal Work and Ethics Statement

All mouse procedures were carried out in accordance with the Canadian Council on Animal Care and approved by the University of Ottawa Animal Care Committee. All mice were group housed (3-5 per mice cage) with access to food and water *ad libitum* on a standard 12-hour light dark cycle. Exceptions included adult male mice who were separated and single housed if persistent fighting and fight wounds were observed in the cage. All experimental mice were given crinkle paper in addition to the standard nestlet and hut enrichment material. Husbandry was completed

by University of Ottawa Animal Care and Veterinary Services except for cohorts actively undergoing behaviour testing for which husbandry was completed by the experimenter.

5.2 *Tdp-43*^{K408R} Mouse line Generation

At The Centre of Phenogenomics, the *Tdp-43*^{K408R} (C57BL6/N background) mice were generated based on the methods described in Gertsentein and Nutter (2018) using CRISPR/Cas9-mediated gene editing of the endogenous *Tardbp* locus. In brief, spCas9 loaded with an sgRNA to target exon 6 of *Tardbp* (MGI:2387629; 5'-TGGGGGCTTTGGCTCGAGCA-3') was electroporated into embryos alongside a single stranded oligonucleotide (ssODN) repair template (5'-CTAAATCTACCTAACCTAATAACCAACCTACTAACCACCCCCACCACCTACATTCCCCAGCCAGAAGACcTAGAATCCATGgaCGAGCCAAAGCCCCATTAAAACCACTGCCCGATCCTGCATTTGATGCTGACCCCCAACCAAGGGGGGC-3'). Embryos were screened via allelic discrimination (see Genotyping below) to identify founders. 4 founders were crossed to C57BL6/N mice to ensure germline transmission of knock-in allele.

5.3 Genotyping

Tail samples were collected prior to weaning and again postmortem for genomic DNA (gDNA) isolation and genotyping. Tails were solubilized in 300 µL solubilization buffer (10X SET, 100 mM NaCl, 100 µg/mL Proteinase K (Bio Basic PB0451-250)) at 55 °C overnight. Cell debris was precipitated by adding 150 µL of “Tail Salts Buffer” (4.31M NaCl, 0.63M HCl, 10 mM Tris-HCl, pH) then samples were centrifuged at ~21,000g for 15 minutes at 4 °C. Supernatant containing gDNA was transferred into 600 µL of chilled 100% ethanol to precipitate nucleic acids which were then pelleted by centrifugation for 10 minutes at ~21,000g at 4 °C. The supernatant was carefully removed, and the pellet was washed in 600 µL of chilled 70% ethanol

then centrifuged at ~21,000g at 4°C for 5 minutes. The supernatant was carefully removed, and residual supernatant was left to evaporate for 5 minutes. The gDNA pellet was resuspended in double distilled H₂O at 55 °C for 10 minutes.

Genotyping reaction was prepared in a 10 µL reaction containing ~5ng of gDNA, 250nM Tardbp Forward primer (5'-CCACCATCTAAATCTACCTAACCTAATA-3'), 250nM Tardbp Reverse primer (5'-GGATCGGGCAGTGGTTTTA-3'), 125nM Wild Type Locked Nucleic Acid (LNA) probe (*HEX-TCT+A+A+GT+CT+TCT+GGC-IowaBlack FQ*), 125nM K408R LNA probe (*FAM-TCT+A+G+GT+CT+T+CT-IowaBlack FQ*), and 2X PerfeCTa qPCR Tough Mix (QuantaBio). Reactions were run on a BioRad CFX96 qPCR thermocycler with the following cycling parameters: Initial annealing at 95°C for 2 minutes, followed by 40 cycles of 95°C for 15 seconds then 60°C for 60 seconds. Results were analyzed via allelic discrimination in the BioRad Maestro software.

5.4 Mouse Wellness Monitoring

Mice were monitored weekly starting at age P21 and included assessment of hindlimb clasping, kyphosis, weight, and general health. The hindlimb function was assessed based on methods described by Miedel et al. 2017.¹⁸² Briefly, the mouse was suspended in the air for approximately 5-10 seconds by the base of the tail. Features of the limbs were assessed to give a score from 0-4 as described in Table 1. Kyphosis was assessed by allowing the mice to briefly walk on the flat tabletop in the housing room and visually observing the straightness of the spine. A score of 0-3 was given based on methods previously described by Guyenet et al. 2010 in Table 2.¹⁸³ Weight was measured every other week by placing individual mice on a digital weigh scale. Notably, mice exhibiting barbered patches were monitored and recorded.

5.5 Behaviour Testing

5.5.1 General Information

The main behaviour cohort consisted of males and females with 12-15 animals per sex per genotype. Over the course of the study, one mouse reached endpoint prior to the 9-month testing timepoint and twelve mice reached endpoint prior to the 16-month testing timepoint.

Additionally, two mice were excluded from the hanging wire test at 16-months due to large ventral masses. Established TDP-43 knock-in mouse models have found differences between heterozygous and homozygous mutant mice.¹⁸⁴ Thus, both heterozygous (*Tdp-43^{K408R/+}*) and homozygous (*Tdp-43^{K408R/K408R}*) mutant mice were included in the study to understand the consequences of losing SUMOylation on one or both alleles of TDP-43.

All adult behaviour testing was performed in the University of Ottawa Behaviour and Physiology Core. During behaviour testing periods the mice were minimally disturbed: food and water were only added/changed as needed and cages were changed by the experimenter with a transfer of old bedding material. Apart from nesting and Beam Break testing, all behaviour tests were performed in the light phase of the cycle. The experimenter was blinded to the genotype of the mice during behaviour testing and until the mice were end pointed. Mice were brought to the testing room to habituate in dim white light at least 30 minutes prior to commencing testing with the exceptions of nest building and fear conditioning for which there was no habituation period.

Behaviour testing was completed in the same order at each age point which was as follows: light dark box, open field, grooming, tube test of social dominance, 3-chamber social interaction, marble burying, spontaneous Y-maze, beam break, nesting, grip strength, hanging wire, Digigait, rotarod, and tail suspension. Tests were ordered such that tests of anxiety were first, followed by

cognitive, motor, and finally aversive tests. Importantly fear conditioning was only conducted at the 16-month age point for the main behaviour cohort. Two separate cohorts for fear conditioning at 2- and 9-months of age were used to ensure no influence on other behaviour testing. These cohorts had a sample size of 4-15 animals per sex per genotype. All mice used in behaviour testing had been backcrossed three times to C57BL/6N background.

5.5.2 Developmental Testing

A small battery of behaviour tests was completed at P8 and P21. At P8, these tested included weight, righting reflex, hindlimb suspension, and forelimb suspension.¹⁸⁵

- i. Weight: Weight was measured every other week by placing individual mice on a digital weigh scale.
- ii. Righting Reflex: Mice were placed on their back on a tabletop and timed for how long it took them to right themselves onto their paws.
- iii. Hindlimb Suspension: Mice were placed facing downward in a 50mL Falcon tube (VWR 21008-940) and timed for their latency to fall.
- iv. Forelimb Suspension: Mice were placed to grasp a wire suspended by a pencil holder and timed for latency to fall.

At P21, hanging wire was performed in which the mouse was allowed to grasp a wire 30cm off the ground and time for its latency to fall.¹⁸⁶ Each mouse completed three trials with a maximum time of 60 seconds.

5.5.3 Beam Break

The Beam Break test was used to assess general locomotor activity and habituation to a novel cage environment.¹⁸⁷ The apparatuses used to record and analyze the mice activity included the Micromax analyzer/Fusion Software (Omnitech Electronics; Columbus, OH, USA) at the 2-month time point and the Photobeam Activity System (San Diego Instruments; San Diego, CA, USA) at the 9 and 16-month timepoints. Clean cages with only a thin layer of corncob bedding, food, and water were loaded into the recording frame. Mice were singly housed in one of these cages 2 hours prior to the start of their dark cycle. For a 24-hour period at the standard 12-hour dark/light cycle, the activity of the mice was monitored by infrared beam emitters and receptors. When the test was completed, the sum of the infrared beam breaks in 5-minute, 1-hour, and 24-hour sampling bins was analyzed.

5.5.4 Digigait

The Digigait treadmill Imager and Analysis Software (Mouse Specifics Inc.) were used to record and analyze parameters of gait, respectively.^{188,189} Mice were placed on the unmoving treadmill surface and once recording was started the speed was increased to 18cm/s with 0degree incline. A 3 second video of each mouse walking continuously, with no stopping or starting, was captured. A mouse was excluded from the test if it was unable to walk for 3 seconds at the 18cm/s speed.

5.5.5 Fear Conditioning

Contextual and cued fear conditioning were tested using a 3-day protocol to assess associative fear learning and memory.^{189,190} Prior to each testing timepoint of fear conditioning, a separate cohort of naïve age and sex matched mice were used to determine the optimal shock value. Mice

were exposed to incrementally increasing shock amperage and the experimenter observed signs of flinching, movement, jumping, or vocalization in the mouse. The maximal shock value in which a mouse displayed two of the four behaviours twice in a row was selected for testing. The shock value used at all testing time points was 0.3 mAmps. On day 1 (training), the mice were placed into a Phenotyper box (Noldus Information Technology) with a grid shock floor (Med Associates). The testing room was set to 60lux light level and 70dB of white noise (context A). The mice were left in the apparatus for 6 minutes during which they receive 3 tone-shock pairings (30 seconds tone co-terminated with a 2 second foot shock). On day 2 (Context), the mice were placed in the same apparatus (Context A) with no tone or foot shock delivered for the 6 minute trial. On day 3 (cue), the animals were placed in the test apparatus with an altered context (context B) including red light, no white noise, vanilla scent, textured mat covering the shock floor and plastic inserts in the apparatus. The mice are allowed to explore this context with no tone for 3 minutes, and then are presented with the same tone from Day 1 for the last 3 minutes. The time freezing was analyzed with EthoVision software for all 3 testing days.

5.5.6 Grip Strength

A grip strength meter (Chatillon DFE II, Columbus Instruments) was used to assess the maximal forelimb grip strength of the mice.¹⁹¹ The grip strength meter was rotated vertically and temporarily mounted on a flat surface prior to testing.¹⁹² The mouse was brought near the triangular attachment and allowed to grasp the lower bar with its forepaws. The mouse was pulled directly downward, by the tail, in one smooth motion. Each mouse was tested, and the grip strength recorded for 5 consecutive trials with a 1-minute intertrial interval. If a trial was deemed unsuccessful by the blinded experimenter, the trial was redone. Causes of an

unsuccessful trial included the mouse prematurely losing its grip on the bar or grasping the bar with its hindfoot. The average grip strength for the 5 successful trials was analyzed.

5.5.7 Grooming

Spontaneous self-grooming was evaluated by individually placing mice in a clean cage with no bedding.¹⁵⁵ Each mouse was allowed to habituate to the cage for 10 minutes and was then recorded by a camera mounted on a tripod for 10 minutes. The cumulative time spent grooming was analyzed by The Observer XT software (Noldus Information Technology).

5.5.8 Hanging Wire

The hanging wire test was used to assess muscle strength and coordination.¹⁸⁶ A metal wire was secured to the top of a tall plastic box with padding on the bottom. The mouse was brought near and allowed to grasp the wire with its forepaws. A timer was started once the experimenter released the mouse to allow it to hang freely. When the mouse fell from the wire the time was recorded. Mice had three trials and were allowed to hang for a maximum of 600 seconds with a 60 second intertrial interval in between. If a mouse hung for 600 seconds, it did not complete any additional trials. The maximum hanging time from the trials was used for analysis.

5.5.9 Light Dark Box

The light dark paradigm was used to assess anxiety-like or disinhibited, exploratory behaviour.¹⁹³ The testing apparatus (Med Associates) has two equal sized rectangular compartments the mouse can move freely between. The one is fully illuminated whereas the other is covered by a black plastic insert. The position of the mouse in the apparatus testing field is recorded using infrared beams. To start the test, the mice are placed into the lit side and allowed to explore for 10

minutes. The time spent in each compartment and number of entries into each compartment was recorded and analyzed by Activity Monitor software (Med Associates).

5.5.10 Marble Burying

Digging and burrowing are innate behaviours for mice.¹⁹⁴ The marble burying assay can assess the motor function required to bury objects as well as cognitive changes related to apathy or perseverance.¹⁵¹ Cages were filled with 10cm of fresh corncob bedding and one mouse was placed to habituate for 5 minutes. After habituation, 20 glass marbles were laid out evenly in a 4 by 5 pattern. The mouse was returned to the cage and left alone for 30 minutes in 60 lux light. With the completion of the trial, the number of marbles buried by at least two thirds was scored by a blinded experimenter.

5.5.11 Nest Building

Nest building is an innate behaviour of mice in their daily lives. This complex behaviour requires both executive planning and sensorimotor coordination. Directly following Beam Break testing, a single square nestlet (5cm² cotton pad) was placed in each Beam Break cage for 16 – 18 hours, of which 12 of these hours was during the dark cycle. At the end of the test, images were taken of the nests and scored blindly for quality as previously described on a scale from 1-5.¹⁹⁵

5.5.12 Open Field

The open field test was used to assess anxiety and locomotor activity in a novel environment.¹⁵⁵ The apparatus consists of white plastic square arenas measuring 45cm on each side. The mice were placed in a corner of the arena and allowed to freely explore for 10 minutes with light

levels at 300 lux. The distance travelled, time spent in the corners and center of the field was recorded and analyzed by EthoVision software (Noldus Information Technology).

5.5.13 Rotarod

The rotarod (IITC Life Science, Ugo Basile) was used to test the motor performance of mice including coordination and resistance to fatigue.¹⁵⁵ Mice were placed in the stationary rotarod bar for 10 seconds before the rotarod program was initiated. The bar accelerated from 4rpm to 40rpm for 5 minutes and the latency to fall for each mouse was recorded. The time was stopped when the mouse fell from the bar or rotated passively. Mice were completed four trials per day, with a 10-minute intertrial interval in their home cage, for 3 consecutive days.

5.5.14 Spontaneous Y-Maze

The spontaneous Y-Maze test was used to assess spatial working memory.¹⁵⁵ The Y-shaped maze has three identical arms at 120degrees around a center point triangle. The mice were placed in the center point and allowed to freely explore the arms for 8 minutes. The movement of the mouse was tracked including the sequence of arm entries by EthoVision (Noldus Information Technology). An alternation is defined as the mouse making consecutive, sequential entries into each of the three arms without revisiting an arm. The alternation index was calculated as $(\text{number of alternations}/(\text{total number of arm entries minus two}))$ and reported as a percent.

5.5.15 Tail Suspension

The automated Tail Suspension apparatus (Med Associates) was used to assess apathetic-like behaviours of the mice.¹⁹⁶ Mice were taped and suspended by the tail to a vertical steel bar which measures strain gauge as the mouse moves during a 6-minute trial. The cumulative time spent

immobile, hanging passively (below lower threshold of) was measured by the Tail Suspension software.

5.5.16 Three Chamber Sociability

The Three Chamber test was conducted to measure the sociability of mice when allowed to interact with a novel mouse or a similarly sized inanimate object.¹⁹⁶ The testing apparatus is a 19 x 45cm plastic box divided into three equal chambers with clear plastic wall dividers. The two external chambers each have a single weighted metallic mesh pencil holder and the central chamber is empty. The mice are habituated to the apparatus for 5 minutes by being placed in the central chamber and allowed to freely explore and enter all chambers. The mouse has a 5-minute intertrial interval in its home cage. In the test trial, a sex and age matched wild-type mouse (social target) is placed beneath one mesh pencil holder, and an inanimate plastic toy (non-social target) is placed beneath the other. To commence the test trial, the mouse is placed in the central chamber. The time spent in each chamber and interacting with the social or non-social target is recorded and analyzed by EthoVision software (Noldus Information Technology).

5.5.17 Tube Test of Social Dominance

The tube test was used to assess social dominance and within cage social hierarchy.^{197,198} Mice from the same cage were paired against each other for testing in a round-robin design. The tube test was conducted on a flat tabletop, which the mice were allowed to run around on for 5 minutes prior to commencing the testing. One foot of vinyl tubing was used. Mice were habituated to the tube prior to testing on the same day by encouraging them to run through the empty tube from either side 5 times. A blinded experimenter placed a mouse on either end of the tube, and released their tails when they completely entered the tube. The first mouse to step its

hind paws out of the tube lost the battle. The battle was redone if after 2 minutes no mouse had won.

5.6 Tissue Collection and Processing

Mice were euthanized by isoflurane inhalation. A V-cut was made through the skin and abdominal wall to expose the diaphragm which was cut along the rib cage to fully expose the heart. The right aorta was cut to allow blood to drain into the chest cavity. A 1ml syringe (without a needle) was used to collect blood and placed into VACUETTE® TUBE 5 ml CAT Serum Separator Clot Activator tubes (VWR 95057-389). Mice were then decapitated, and the brain was removed. Using a razorblade, the brain was cut into left and right hemispheres. The body was eviscerated prior to making an incision at the level of the hips. Through an 18-gauge needle (Fisher Scientific 14-826-5D), phosphate buffer saline (PBS) 1x was pushed into the caudal end of the spinal cavity with a 10 ml syringe to extract the spinal cord. The lumbar enlargement was visually identified and dissected out. The right hemispheres and lumbar enlargements were immediately placed in 10% buffered formalin for fixation. After 72 hours, the tissue was transferred into 70% ethanol and delivered to the University of Ottawa Louise Pelletier Histology Core Facility for paraffin embedding. The lumbar spinal cords were sectioned on a microtome (Microm HM 330) at 5µm.

5.7 Histology

5.7.1 General Information

Histology experiments included tissue from *Tdp-43*^{+/+} (wildtype; WT) and homozygous mutant mice. Histology tissue for the 5-month timepoint was collected from animals which were backcrossed once to C57BL6/6 background. This cohort consisted of only female mice with 3-5

animals per genotype. Histology tissue from the 9-month timepoint was collected from animals which were backcrossed three times to C57BL6/N background. This cohort consisted of both males and females with 3-4 animals per sex per genotype.

5.7.2 Immunofluorescence Staining

Brain and spinal cord slides were deparaffinized in two consecutive rounds of 100% xylenes (Fisher Scientific X3P-1GAL) for 10 minutes each. The slides were then rehydrated in descending ethanol solutions: two 5 minutes rounds in 100%, 5 minutes in 70%, and 5 minutes in 50%. The slides were then immersed in PBS 1x solution for at least 5 minutes. Antigen retrieval, to expose antigens affected by fixation, was performed by placing slides in 1X sodium citrate buffer (2.94g sodium citrate 0.5mL Tween-20 in 1L 1X PBS, pH6) at 95°C for 30 minutes. To block nonspecific binding, the slides were incubated in 10% cosmic calf serum and 1% Triton-X for 2 hours at room temperature. Following blocking the slides were incubated with primary antibody (listed with dilution in Table 3) overnight at 4°C. The next day the slides were washed twice in PBS 1X + 0.1% Triton-X for 5 minutes each and then for 3 times in PBS 1X for 5 minutes each. The slides were then incubated in secondary antibody at room temperature for 2 hours. Following another round of washes, the slides were covered with #1.5 coverslips (Thermo Fisher Scientific 12-544E) and fluorescent mounting media (Dako S3023).

5.7.3 Chromogenic Dye Staining

Brain and spinal cord slides were deparaffinized in two consecutive rounds of 100% xylenes (Fisher Scientific X3P-1GAL) for 10 minutes each. The slides were then rehydrated in descending ethanol solutions: two 5 minutes rounds in 100%, 5 minutes in 70%, and 5 minutes in 50%. For cresyl violet staining, slides were left in 0.1% cresyl violet acetate (Electron

Microscopy Sciences, Cedarlane 26681-02) for 5 minutes. Slides were then rinsed in one change of distilled H₂O, and then differentiated in two rounds of 100% ethanol for three minutes each. For Luxol Fast Blue (Electron Microscopy Sciences, Cedarlane 26681-01) staining, slides were left in the stain for 16 hours at 55°C in a water bath. The slides were then rinsed in 95% ethanol for 3 minutes, 0.05% Lithium Carbonate (Electron Microscopy Sciences, Cedarlane 26681-04) for 30 seconds, and 70% ethanol for 1 minute. For both dyes, the slides were dipped in 100% ethanol for 2 minutes and then 100% xylenes for 6 minutes. The slides were mounted with Permount mounting media (Fisher Scientific SP15-100) and covered with #1.5 coverslips (Thermo Fisher Scientific 12-544E).

5.7.4 Image Acquisition and Analysis

Stained slides were imaged on the Zeiss AxioObserver 7 or Zeiss LSM800 AxioObserver Z1 Confocal (University of Ottawa Cell Biology Image Acquisition Core) and processed and analyzed with FIJI ImageJ 1.54f.

Cresyl violet staining of the cortex was captured at 10x magnification. The measurement for cortical thickness was measured from layer I to VI. NeuN and Ctip2 staining was captured at 20x magnification. Cells were completed in a 0.5mm² area. Hippocampal cresyl violet and GFAP staining was captured at 40x and cells were counted within the anatomical limits of the dentate gyrus. Luxol Fast Blue staining was captured at 10x in both the brain and spinal cord regions. Full length TDP-43 staining in the cortex was captured at 20x and pS403/404 TDP-43 in the ventral spinal cord root was captured at 63x. ChAT staining in the ventral root of the spinal cord was captured at 40x. C-terminal TDP-43 in the ventral root of the spinal cord was captured at 20x.

5.8 Statistical Analysis

GraphPad Prism 10 was used for all statistical analyses and graphs (GraphPad, San Diego, CA, USA). All data in this study is represented as mean +/- standard error of the mean (SEM). For bar graphs, individual dots represent a mouse, and the bars represent the average for all the mice in the group. For line graphs, the points represent the average for each group. For behaviour experiments, Brown-Forsythe and Welch One-Way ANOVA was completed for comparisons of genotype only. If a significant main effect was found a Dunnett's post-hoc test was run for multiple comparisons. For analysis of genotype and age, trial, or time, a Two-Way ANOVA was used with Tukey's post-hoc test if a main effect was found. The tube test was analyzed by a One-Tailed binomial test for observed versus expected distributions with the expected distribution set to 50% wins for each genotype. For histological analysis, a Student's t-test was used for comparison between genotypes. For all statistical analysis, $p < 0.05$ was considered statistically significant.

6. Results

6.1 Tdp-43^{K408R} Mouse Line Validation

The Tdp-43^{K408R} mice were found to be viable and breeding crosses between Tdp-43^{K408R/+} mice produced litters with normal Mendelian ratios (Figure 2A). Additionally, from mouse embryonic fibroblast tissue, it was confirmed that there is a stress dependent reduction in SUMOylation of TDP-43 in the Tdp-43^{K408R} mutant mice via co-immunoprecipitation (Figure 2B). From 2-month-old mouse brains there were no differences in TDP-43 protein levels between Tdp-43^{+/+} and Tdp-43^{K408R/K408R} mice, suggesting that potential phenotypes will be neurodegenerative.

6.2 Behavioural Characterization

To determine whether blocking endogenous SUMOylation of TDP-43 in mice will recapitulate motor and cognitive phenotypes of ALS and FTD patients, the *Tdp-43^{K408R}* mouse line was characterized at the behavioural level. Established animal models with altered TDP-43 have varied outcomes in terms of motor and non-motor phenotypes and timing of their emergence. Therefore, a longitudinal approach to the characterization of the *Tdp-43^{K408R}* mouse model with regular wellness checks and an extensive battery of behavioural tests to encompass the full phenotypic spectrum of ALS-FTD. The battery of tests included assessments of motor function (rotarod, grip strength, hanging wire, Digigait), exploration and anxiety (light-dark box, open field, beam-break), social function (tube test of social dominance and 3 chamber social interaction), naturalistic behaviours (marble burying and best building), memory (Y-maze), and emotional processing (tail suspension and fear conditioning). With 12-15 animals per sex per genotype, this sample size provided statistical power and allowed for analysis of sex differences.

6.2.1 *Tdp-43^{K408R}* Mice Development

Aside from its role in neurodegenerative diseases, TDP-43 plays crucial roles in development. TDP-43 levels are high during embryonic development and gradually decline postnatally. Specifically, TDP-43 plays important roles in the development of the nervous system being highly expressed in the neuroepithelium and neural progenitor cells. Therefore, the first timepoint for wellness and behaviour testing of the mice was at P8 followed by P21 to provide a baseline assessment. For all measures, there was no significant differences across the genotypes for any of the tests performed at these ages (Figure 3). This suggests that the loss of TDP-43 SUMOylation did not produce gross developmental or motor deficits prior to adulthood.

6.2.2 Motor Function of *Tdp-43*^{K408R} Mice

Multiple tests were used to identify possible ALS-like motor deficits. These tests captured various features of motor performance and neuromuscular function including muscle strength, coordination, and resistance to fatigue. The forelimb grip strength of mice was tested using a modified setup where the force transducer meter is perpendicular to the floor, allowing the mouse being tested to be pulled vertically off the grate. The modified setup was previously shown to reduce inter-trial variability.¹⁹² At all testing ages, there was no significant differences between genotypes in forelimb grip strength (Figure 4A). All genotypes followed the same direction in grip strength amplitude across age. Interestingly, there was a significant main effect of genotype and age in the female mice, but *post-hoc* analysis revealed a non-significant trend for the *Tdp-43*^{K408R/K408R} mice having increased forelimb strength compared to wild type controls from the 2- to 16-month timepoint. For the hanging wire test, a mouse was placed on a single metal rod by its forelimbs and its maximum latency to fall time was recorded giving an indication of muscle strength and endurance. Each mouse is given 3 trials but if a mouse held on for the maximum of time, 300 seconds, this value is recorded, and no further trials conducted. Like grip strength, no significant differences in fall latency were found between genotypes at 2-, 9-, and 16-months (Figure 4B). There was a significant effect of genotype for females across time with a non-significant trend for increased hanging time in the *Tdp-43*^{K408R/K408R} mice compared to wild type control except at the oldest timepoint. The rotarod test was used to assess motor coordination and endurance. Mice completed 3 days of testing with 4 trials each day.

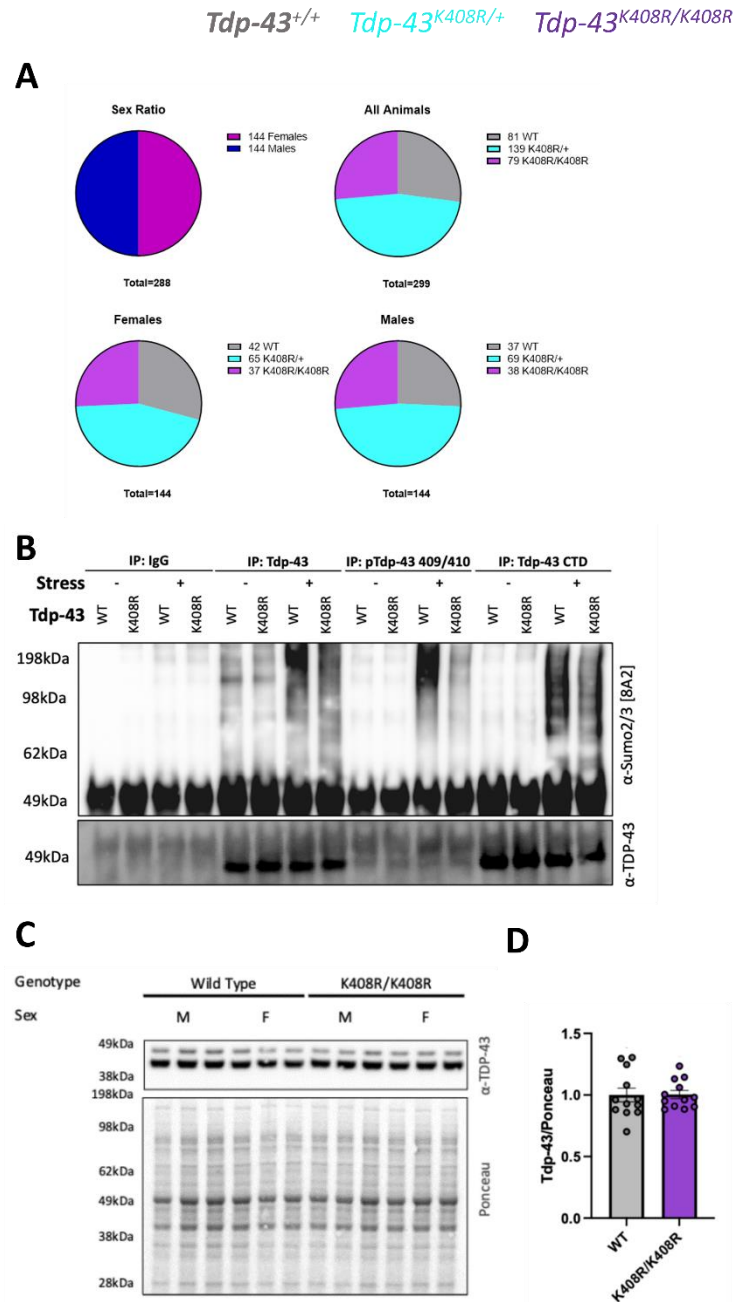


Figure 2. TDP-43 SUMOylation is blocked *in vivo* with K408R mutation but does not affect viability or breeding ratios. A) Sex and genotype ratios for *Tdp-43*^{K408R} mouse line for breeding crosses between *Tdp-43*^{K408R/+} animals. **B)** Western blot results for co-immunoprecipitation of TDP-43 and SUMO2/3 from *Tdp-43*^{K408R/K408R} mouse embryonic fibroblasts. **C)** Western blot **D)** and quantification of TDP-43 protein levels in mouse brain tissue at 2 months.

Motor impairment like in ALS mouse models reduce the fall latency off the rotarod. At the age of 2-months, genotype was not a main effect on latency to fall (Figure 5A). At the 9-month timepoint, there was a sex-specific effect in the rotarod result. Male, but not female, *Tdp-43^{K408R/+}* mice performed significantly worse than wildtype controls (Figure 5B, C). However, this deficit did not progress to the 16-month age. This result is likely due to 16-month wildtype mice having significantly worse performance on this test in comparison to their motor ability at the earlier age points (Supplementary Figure 1A).

6.2.3 Naturalistic Behaviour of *Tdp-43^{K408R}* Mice

Nesting building and marble burying are both tests of natural innate behaviours in mice. Nest building is imperative for temperature regulation, shelter from predators, and facilitates reproduction.^{199,200} It requires a complex combination of sensorimotor skills and reflects the overall wellbeing of the mouse. Similarly, marble burying assesses innate mouse digging behaviour which they use when foraging food or finding shelter. Abnormalities in either of these behaviours has been identified in mouse models of FTD. Improved nest building or marble burying reflects a perseverant, compulsive, or repetitive phenotype, whereas deficits can reflect apathetic behaviour baring motor or other impairments. Nest quality scores had no significant differences between genotypes at the 2-, 9-, or 16-month testing ages (Figure 6A). For the marble burying assay, no significant results were observed across the three age points when male and female mice were pooled together (Figure 6B). However, when split by sex, the male *Tdp-43^{K408R/+}* mice buried significantly less marbles compared to wildtype counterparts at 9-months of age (Figure 6D). Importantly, male mice displayed mild motor impairment on the rotarod task at this age point which could explain the lower percentage of marbles buried. With no deficits in

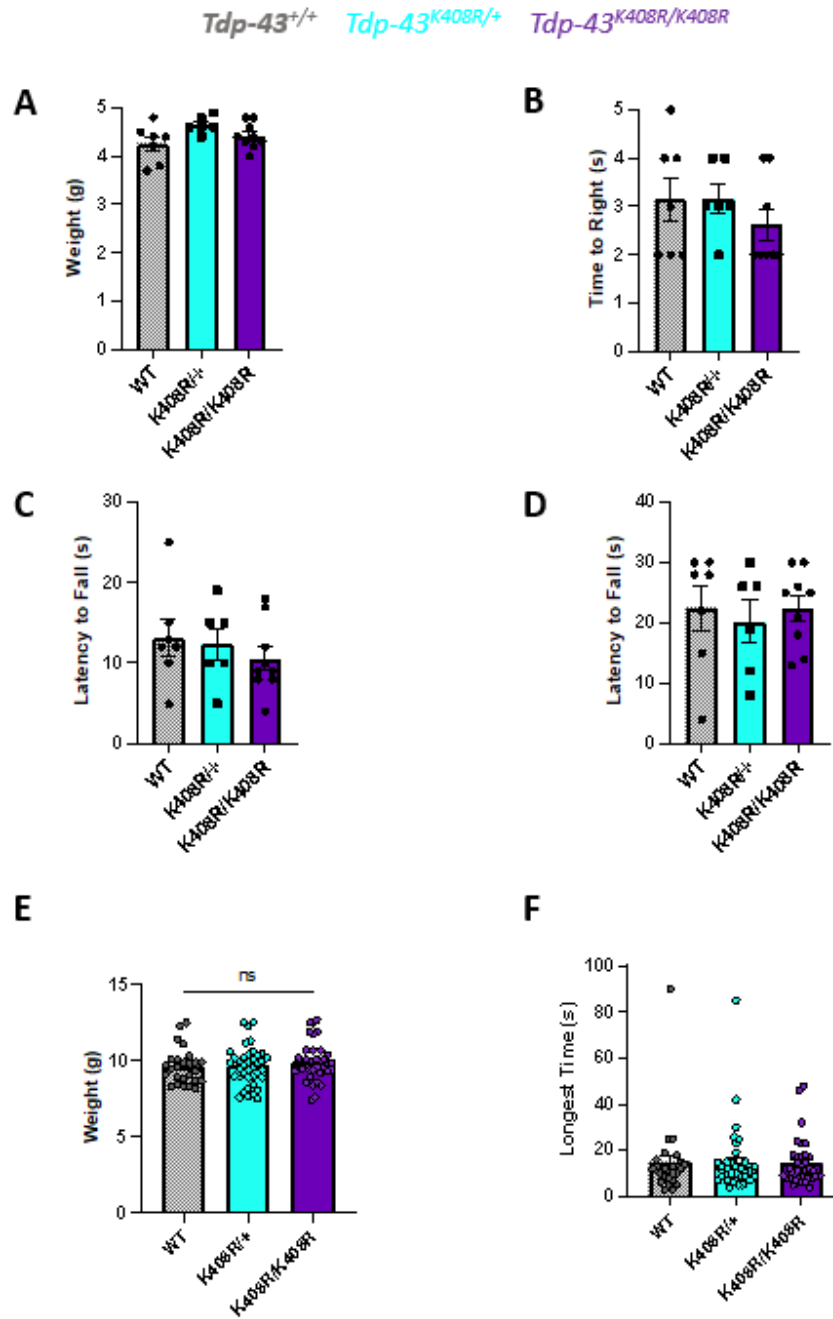


Figure 3. *Tdp-43^{K408R}* mutant mice do not display overt development impairment. At P8 **A**) body weight (grams), **B**) time to right (seconds). **C**) forelimb and **D**) hindlimb latency to fall (seconds) hanging test. At P21 **E**) body weight (grams) and **F**) longest hang time in hanging wire. All statistical analyses are via Brown-Forsythe and Welch One-Way ANOVA with Dunnett's post-hoc test. Mean +/- SEM is shown. Each dot represents one animal.

Tdp-43^{+/+} *Tdp-43*^{K408R/+} *Tdp-43*^{K408R/K408R}

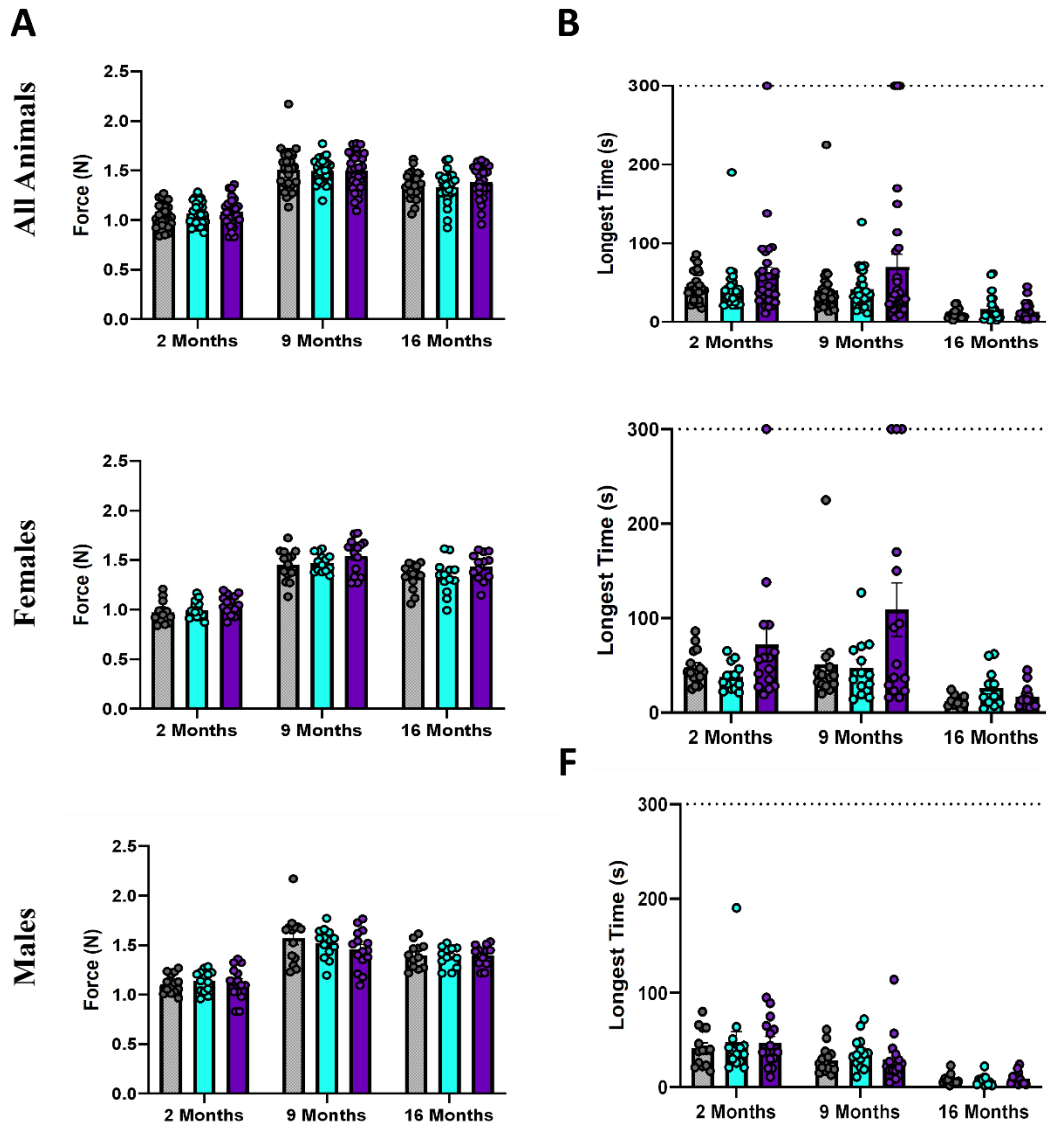


Figure 4. *Tdp-43*^{K408R} mutant mice do not display deficits in forelimb grip strength or hanging wire. **A)** Average force measurement (Newtons) for five trials of forelimb grip strength at 2-, 9-, and 16-months for all animals, females, and males only. **B)** Longest latency to fall (seconds) from three trials of hanging wire at 2-, 9-, and 16-months for all animals, females, and males only. All statistical analyses are via Two-Way ANOVA with Tukey’s post-hoc test. Mean +/- SEM is shown. Each dot represents one animal.

their ability to build nests, this may suggest the motor impairment was not severe to interfere with these naturalistic behaviours. However, this result did not persist at the 16-month testing age, suggesting only a mild cognitive change.

6.2.4 Exploration, Locomotion and Anxiety of *Tdp-43^{K408R}* Mice

To explore anxiety-related behaviour phenotypes observed in FTD patients and mouse models, the *Tdp-43^{K408R}* mice underwent open field, light-dark box, and beam break testing. For open field, mice were placed in an empty square arena under bright light and allowed to freely move about. Mice tend to avoid bright light and stay in the corners. At 2-months of age, female *Tdp-43^{K408R/K408R}* spent a significantly greater amount of time in the center of the arena (Figure 7E). They also travelled a significantly greater distance around the box during their trial (Figure 7B). These results suggest that young female *Tdp-43^{K408R/K408R}* mice display a hyperactive, disinhibited phenotype compared to controls. At the 9-month timepoint, there was a significant reduction in the distance travelled by all animals, suggestive of a mild motor impairment (Figure 7A). This result did not progress to the 16-month testing round, likely because the control mice had significantly reduced activity at this age compared to 2- and 9-months of age akin to rotarod (Supplementary Figure 1B). The light-dark box paradigm was the other measure of anxiety behaviour where mice are allowed to explore two connected boxes. The only difference between the box is that one is light, and one is dark. Mice usually find the light box aversive. Unlike the results from open field, there was no differences between genotypes for the time spent in or entries into the light box (Figure 8A, B).

Tdp-43^{+/+} *Tdp-43*^{K408R/+} *Tdp-43*^{K408R/K408R}

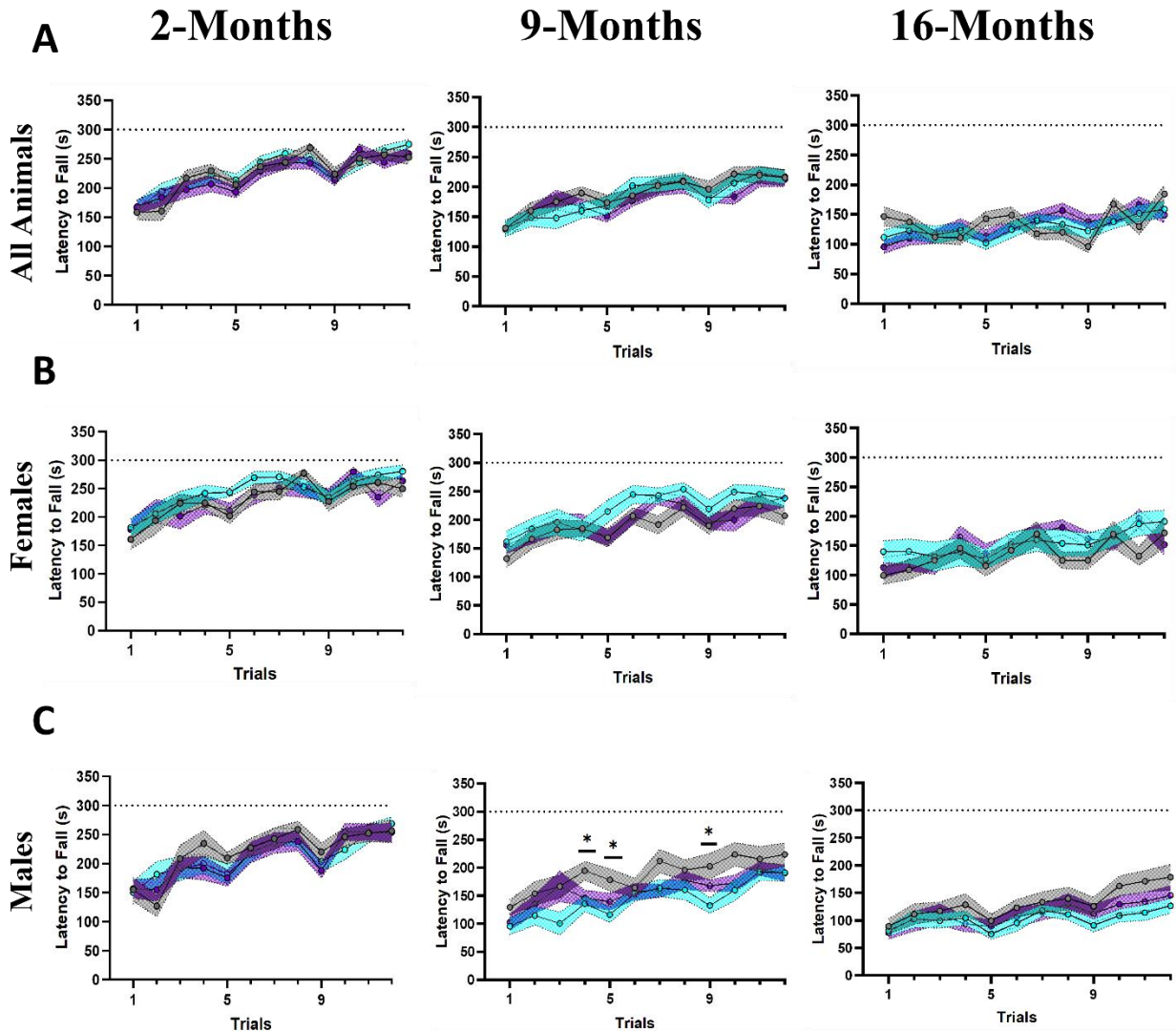


Figure 5. Male *Tdp-43*^{K408R} mutant mice display deficits in rotarod deficits at middle age. A) All animals **B)** females only **C)** and males only latency to fall (Seconds) from 3-day rotarod testing each with 4 trials per day for 2-, 9-, and 16-month testing ages. All statistical analyses are via Two-Way ANOVA with Tukey's post-hoc test. Mean +/- SEM is shown. (*P<0.05).

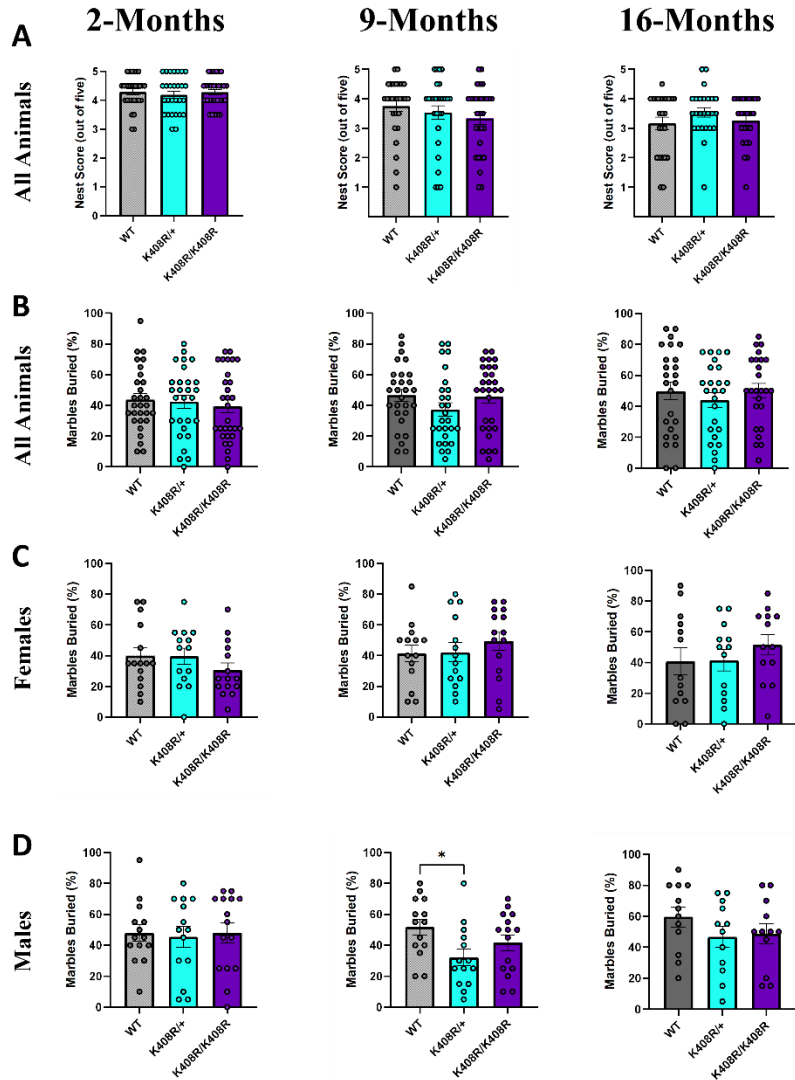


Figure 6. Male *Tdp-43*^{K408R} mutant mice display mild marble burying deficits at middle age.

A) Nesting scores (out of five) for all animals at 2-, 9-, and 16-month testing ages. **B)** All animals **C)** females only, and **D)** males only percentage of total marbles buried at 2-, 9-, and 16-month testing ages. All statistical analyses are via Brown-Forsythe and Welch One-Way ANOVA with Dunnett’s post-hoc test. Mean +/- SEM is shown. Each dot represents one animal. (*P<0.05).

In the beam break test, mice were singly placed into an empty cage and monitored for horizontal activity over a 24-hour period to assess general locomotion, circadian rhythm, and habituation in a novel cage environment. Firstly, there were no significant differences between genotypes at any age for the total horizontal activity (Figure 8C). Breaking this down into 1-hour bins across the 24 hours of testing, there were no significant difference in activity between genotypes at any age (Figure 8D). All animals across age displayed normal patterns of activity relative to the circadian cycle with higher activity during the dark hours. However, non-significant trends for activity differences were observed in the first 4 hours of testing. Therefore, to more closely investigate activity during this habituation period, the activity counts were further broken down into 5-minute bins for these initial testing hours. Specific to the 9-month age point, genotype was a main effect for the female mice. *Post hoc* analysis revealed that *Tdp-43^{K408R/K408R}* had significantly reduced activity counts at 65, 75, 105, 150, 190, 195, 220, and 225 minutes (Figure 9B). These results suggest these mice habituation to a novel cage environment more quickly compared to control mice. This reduced exploratory behaviour may indicate changes in motivational processing.

6.2.5 Social Behaviour of *Tdp-43^{K408R}* Mice

Animal models of FTD present with changes in social behaviour.²⁰¹ To assess this in the *Tdp-43^{K408R}* mice, the 3-chamber social interaction and tube test of social dominance were used. In the 3-chamber test, a mouse was first habituated to the empty apparatus, and subsequently reintroduced into the center chamber of the apparatus and allowed to explore either of the side chambers which either had a novel mouse (social chamber) or inanimate object (non-social

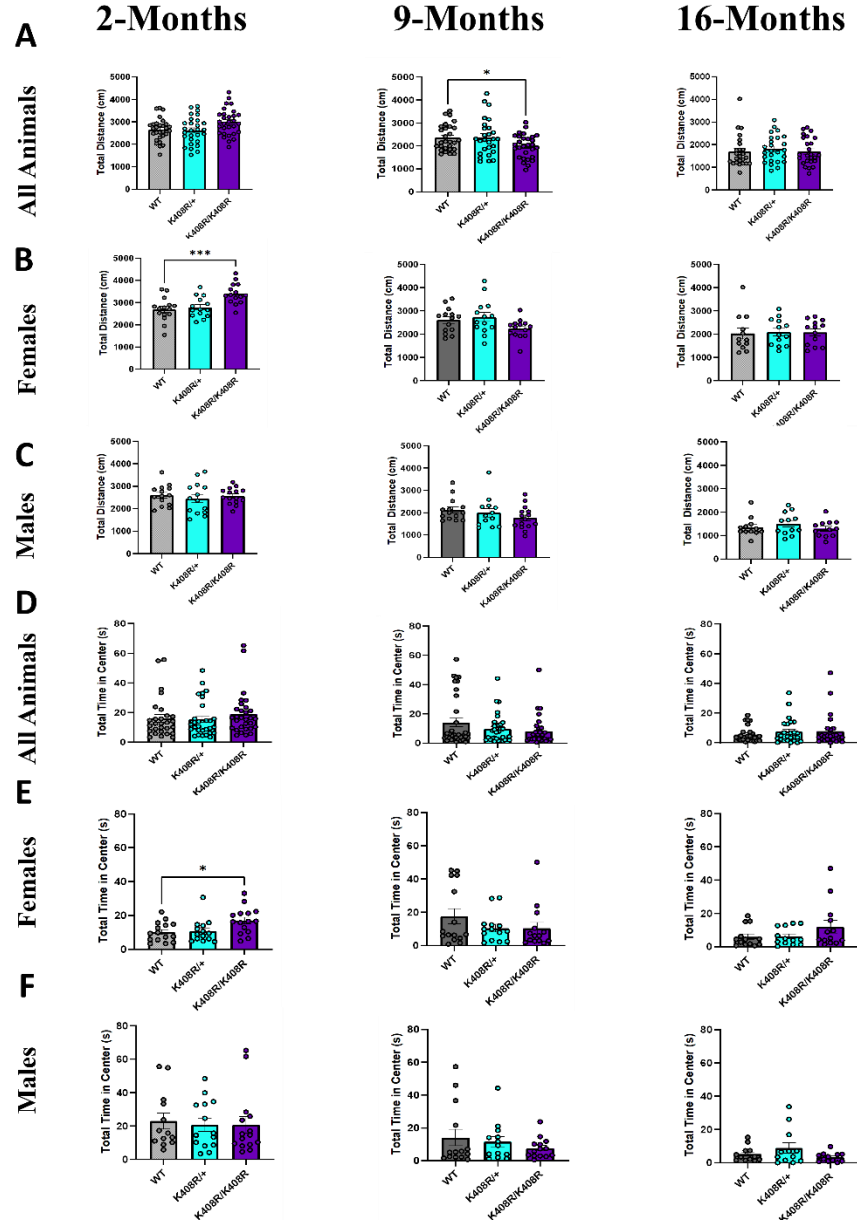


Figure 7. *Tdp-43*^{K408R} mutant mice behavioural alterations in open field testing. **A)** All animals **B)** females only **C)** and males only total distance travelled (centimeters) for 2-, 9-, and 16-month testing ages. **D)** All animals **E)** females only **F)** and males total time spent in the arena center (seconds) for 2-, 9-, and 16-month testing ages. All statistical analyses are via Brown-Forsythe and Welch One-Way ANOVA with Dunnett’s post-hoc test. Mean +/- SEM is shown. Each dot represents one animal. (*P<0.05 ***P<0.001).

Tdp-43^{+/+} *Tdp-43*^{K408R/+} *Tdp-43*^{K408R/K408R}

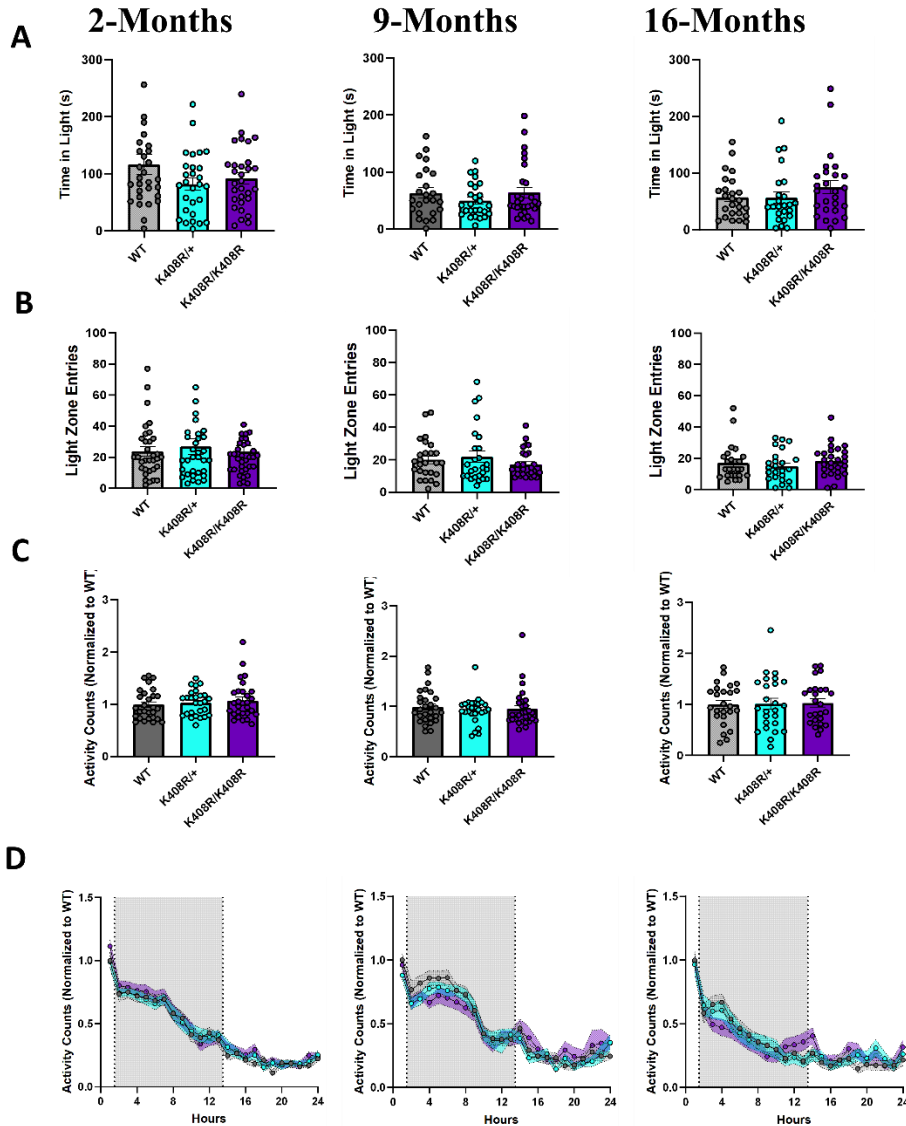


Figure 8. *Tdp-43*^{K408R} mutant mice do not show changes in light-dark box and beam break.

A) Time in the light box (seconds) **B)** and number of entries into the light box. **C)** Total horizontal activity counts normalized to the mean of wild-type animals **D)** Horizontal activity counts across 24 hours in 1-hour bins normalized to the mean of wild-type animals in the first hour. Statistical analyses for A-C are via Brown-Forsythe and Welch One-Way ANOVA with Dunnett’s post-hoc test. Mean +/- SEM is shown. Each dot represents one animal. Statistical analyses for D are via Two-Way ANOVA with Tukey’s post-hoc test. Mean +/- SEM is shown.

chamber) behind mesh. A social ratio was calculated by dividing the time spent in the social compared to the non-social chamber. An interaction ratio was calculated as the time the mouse spent in the interaction zone of the social compared to the non-social chamber. FTD patients often exhibit social withdrawal, and previously characterized FTD mouse models have demonstrated a loss of preference for interacting with the social target. At the 2-, 9-, and 16-month timepoints, there was no statistical difference between genotypes of the *Tdp-43*^{K408R} mice for either social or interaction ratios (Figure 10A, B). All mice across all testing ages, demonstrated a preference for interacting with the social rather than the non-social target. While the 3-chamber test explores social behaviour with a novel mouse, the tube test was used to assess social relationships between cage mates and social dominance hierarchy. Using a round robin approach, cage mates were placed on either end of an open tube. The mouse who steps all four feet out of the tube is declared the loser, and the one who remains in the tube is the winner. At the 2- and 9- month age points, there were no significant differences in battle wins between controls and *Tdp-43*^{K408R/+} or *Tdp-43*^{K408R/K408R} mice compared with the expected 50% (Figure 10C). At 16-months of age, there was a nonsignificant trend for *Tdp-43*^{K408R/+} mice, and a statistically significant increase in *Tdp-43*^{K408R/K408R} wins against wildtype animals (Figure 10C). These results may indicate an age dependent effect of blocking TDP-43 SUMOylation to reduce social dominance in mice living together in their home cage. However, it is important to note that at the 16-month age timepoint, some mice in the behaviour cohort had died, reducing the number of battles thus affecting the statistical power of this test.

Tdp-43^{+/+} *Tdp-43*^{K408R/+} *Tdp-43*^{K408R/K408R}

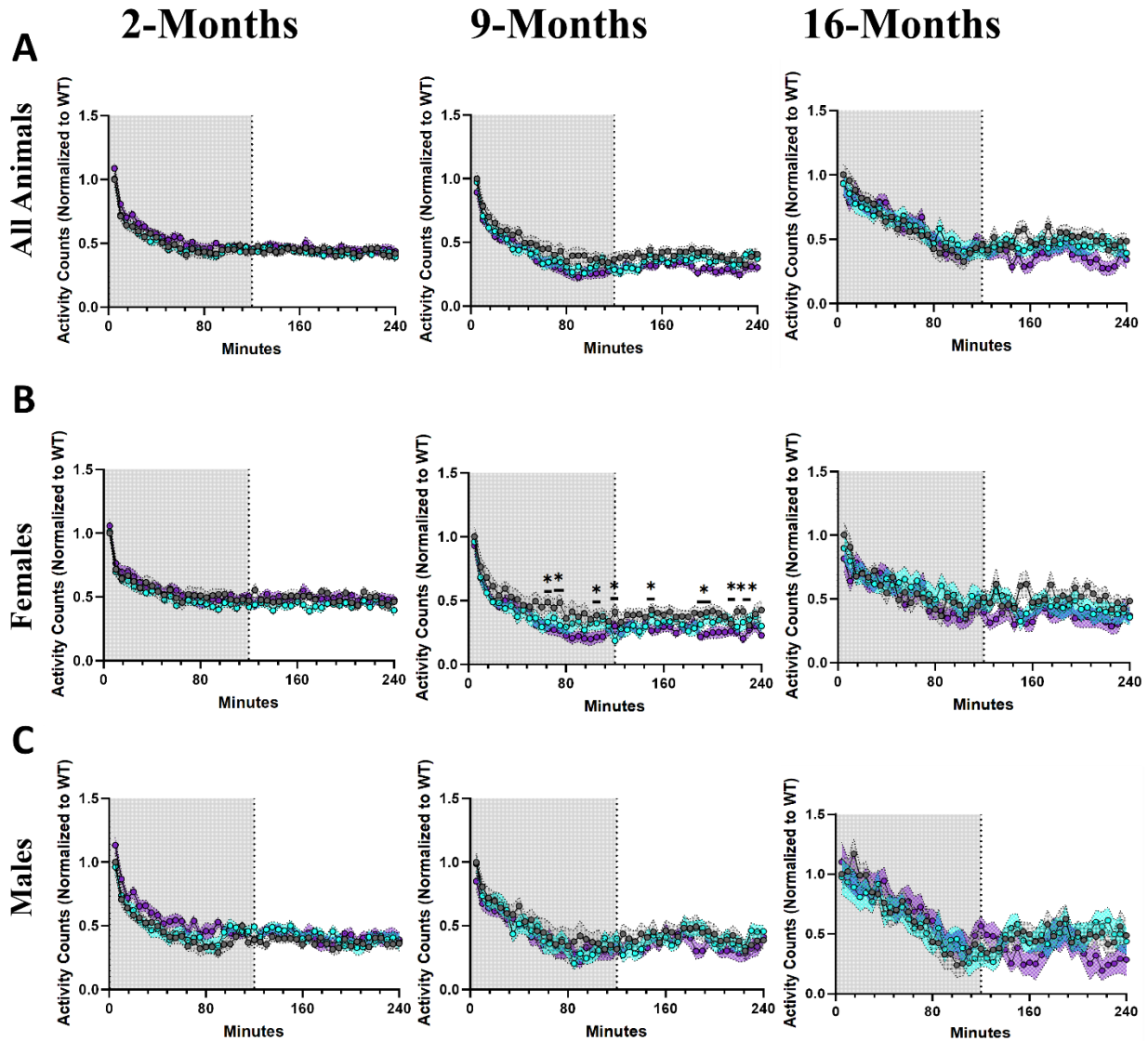


Figure 9. Female *Tdp-43*^{K408R} mutant mice show changes in habituation behaviour at middle age in beam break. A) All animals B) females only C) and males only horizontal activity counts for the first four hours in 5-minute bins normalized to the mean of wild-type animals in the first 5 minutes. Statistical analyses are via Two-Way ANOVA with Tukey’s post-hoc test. Mean +/- SEM is shown. (*P<0.05 **P<0.01).

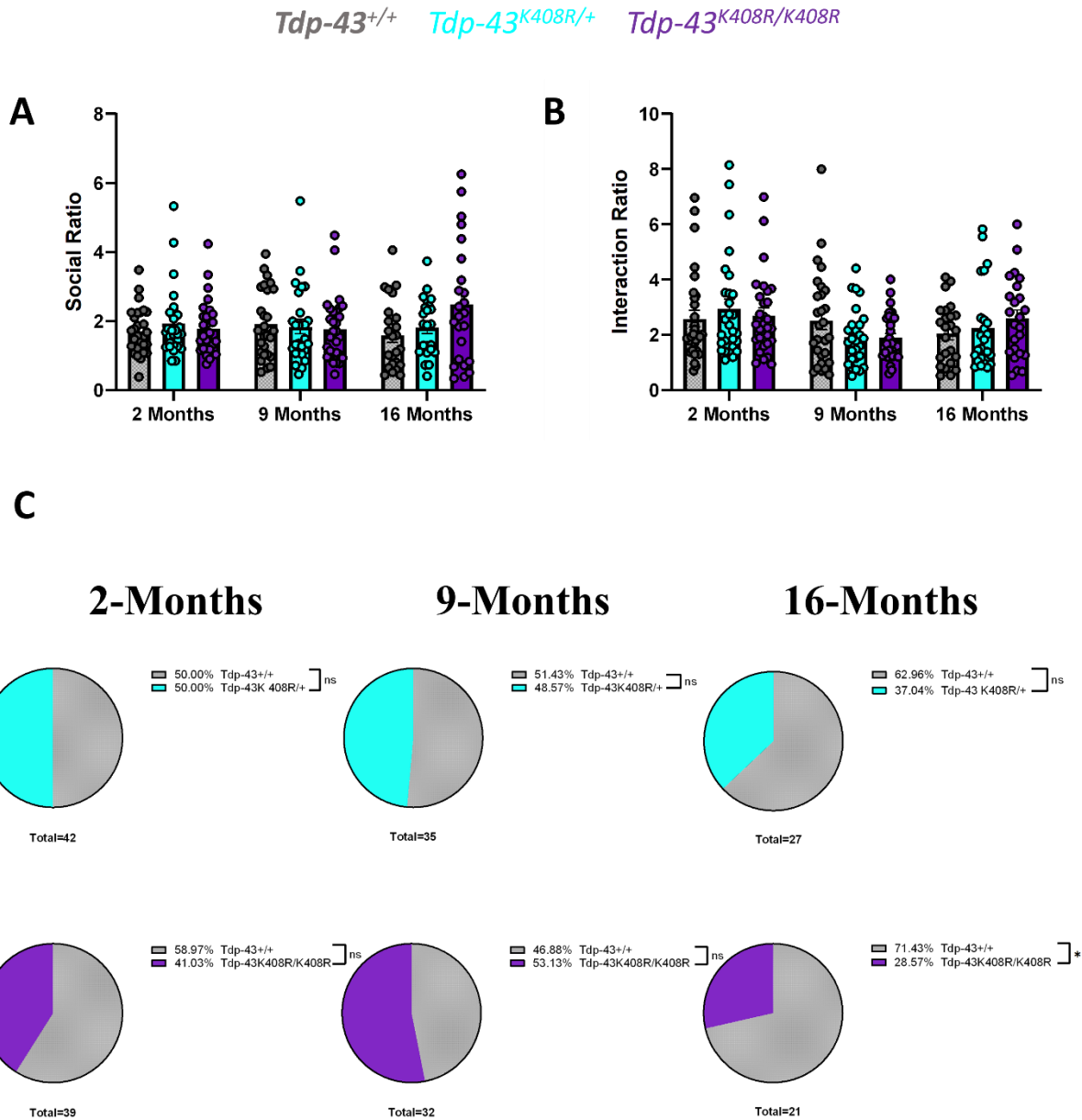


Figure 10. *Tdp-43^{K408R}* mutant mice display reduced dominance within cages at old age. A) Social ratio and **B)** interaction ratio from 3-chamber sociability test for 2-, 9-, and 16- month age points. **C)** Percentage of wins between genotypes in tube test. Statistical analyses for A-B are via Two-Way ANOVA with Tukey's post-hoc test. Mean +/- SEM is shown. Each dot represents one animal. Statistical analyses for C via Binomial test where expected results are 50% for each genotype in a battle. One-tailed P-value is reported (*P<0.05).

6.2.6 Working Memory of *Tdp-43*^{K408R} Mice

Particularly in bvFTD, the loss of executive function including working memory is the most common feature of disease and have been linked to dysfunction in the frontal lobe.^{202,203} Such deficits have been demonstrated in various preclinical animal models of FTD. To assess the *Tdp-43*^{K408R} mice for spatial working memory, the spontaneous Y-Maze test was used. Mice were allowed to explore all 3 identical arms, and if they have intact working memory, will explore a novel arm each entry. A mouse completes a spontaneous alternation when they enter a novel arm three times in a row. At the 2- and 9-month timepoints, there were no differences between the genotypes, or split by sex, for the percentage of spontaneous alternations (Figure 11). At the 16-month timepoint a sex difference was observed. There was a significant reduction in percentage alternations of female *Tdp-43*^{K408R/K408R} mice compared to controls, suggesting a working memory impairment (Figure 11B). In the 16-month male mice, the *Tdp-43*^{K408R/+} were found to have a significantly increased number of spontaneous alternations compared to controls (Figure 11C). However, the number of arm entries was assessed at all testing time points to ensure any result was not due to lack of exploration. Exclusively for the 16-month mice age, the male *Tdp-43*^{K408R/+} mice entered arms at significantly reduced frequency (Supplementary Figure 2A). Therefore, the male result is likely not related to working memory.

6.2.7 Emotional Processing of *Tdp-43*^{K408R} Mice

Patients with FTD display emotion blunting, or impaired responses to aversive stimuli.²⁰⁴ To explore emotional processing in the *Tdp-43*^{K408R} mice, they were subjected to tail suspension and fear conditioning paradigms. For tail suspension, the tail of the mouse was taped to a metal force meter, suspending the mouse above the ground for 6 minutes. The time the mouse spent

immobile during testing, or not actively trying to escape, was calculated as the main measure. There were no significant differences between genotypes at 2-, 9-, or 16-months of age (Figure 12A). In fear conditioning, both contextual and cued memory was tested. A foot shock was delivered to the mice, in a specific context and paired with a cue. The time the mice spent freezing in fear when exposed to the context or cue independent of the shock was measured. At the three age points tested, there were no differences between genotype in the time spent freezing in the novel environment prior to exposure to the shock (Figure 12B). There were no differences between genotypes at any age for time spent freezing on the context or cue testing days (Figure 12B). The time spent freezing on these days was increased from baseline, indicating the mice learnt and remembered the shock associations but responded similarly. Overall, no differences in emotional processing were observed in the *Tdp-43^{K408R}* mice.

6.2.8 Wellness Monitoring of Adult *Tdp-43^{K408R}* Mice

To monitor progression of ALS and FTD disease phenotypes, *Tdp-43^{K408R}* mice were regularly monitored across their lifespan. Genotype was not a main effect for body weight or hindlimb clasp scoring in adult mice (Figure 13A, B). No signs of kyphosis were observed in the mice (data not shown). All mice followed a pattern of increasing weight with age, except for period of active behaviour testing. Interestingly, in female mice signs of barbering, or excessive grooming by other cage mates, was observed. Specifically, bald patches on the neck, back, and chest area. Looking at the cumulative probability, the *Tdp-43^{K408R/+}* and *Tdp-43^{K408R/K408R}* genotypes were significantly more likely to be barbered by their cage mates compared to controls (Figure 13C). Barbering is a complex behaviour, and there could be multiple explanation for this result. This may reflect changes in social relationships or dominance within the cage, in line with results from the tube test. However, barbering was observed in cages with and without control animals

Tdp-43^{+/+} *Tdp-43*^{K408R/+} *Tdp-43*^{K408R/K408R}

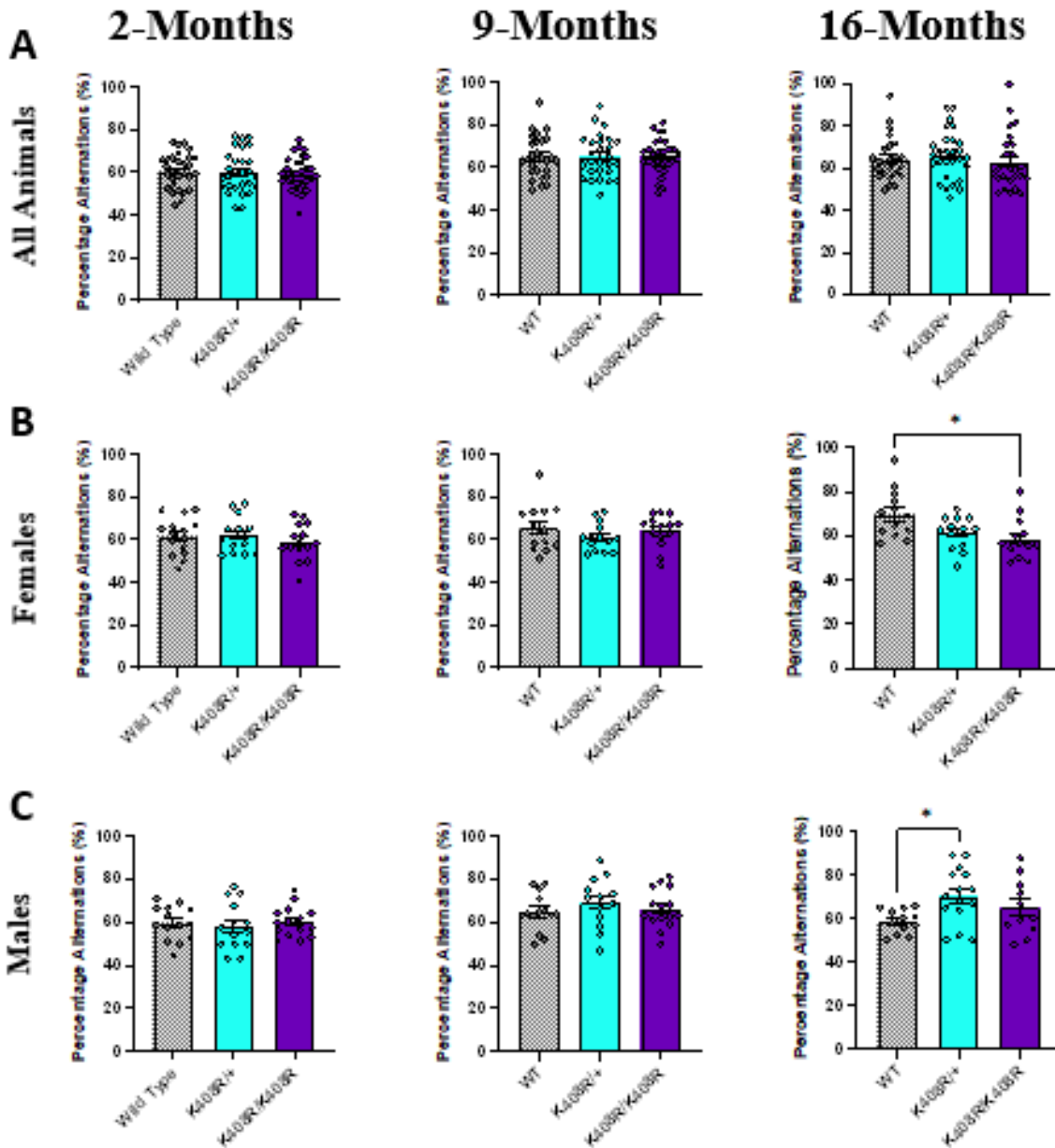


Figure 11. *Tdp-43*^{K408R} mutant female mice have cognitive deficit in Y-maze at old age. A) All animals B) females only C) and males only for the percentage of alternations completed in spontaneous Y-Maze test. All statistical analyses are via Brown-Forsythe and Welch One-Way ANOVA with Dunnett's post-hoc test. Mean +/- SEM is shown. Each dot represents one animal. (*P<0.05)

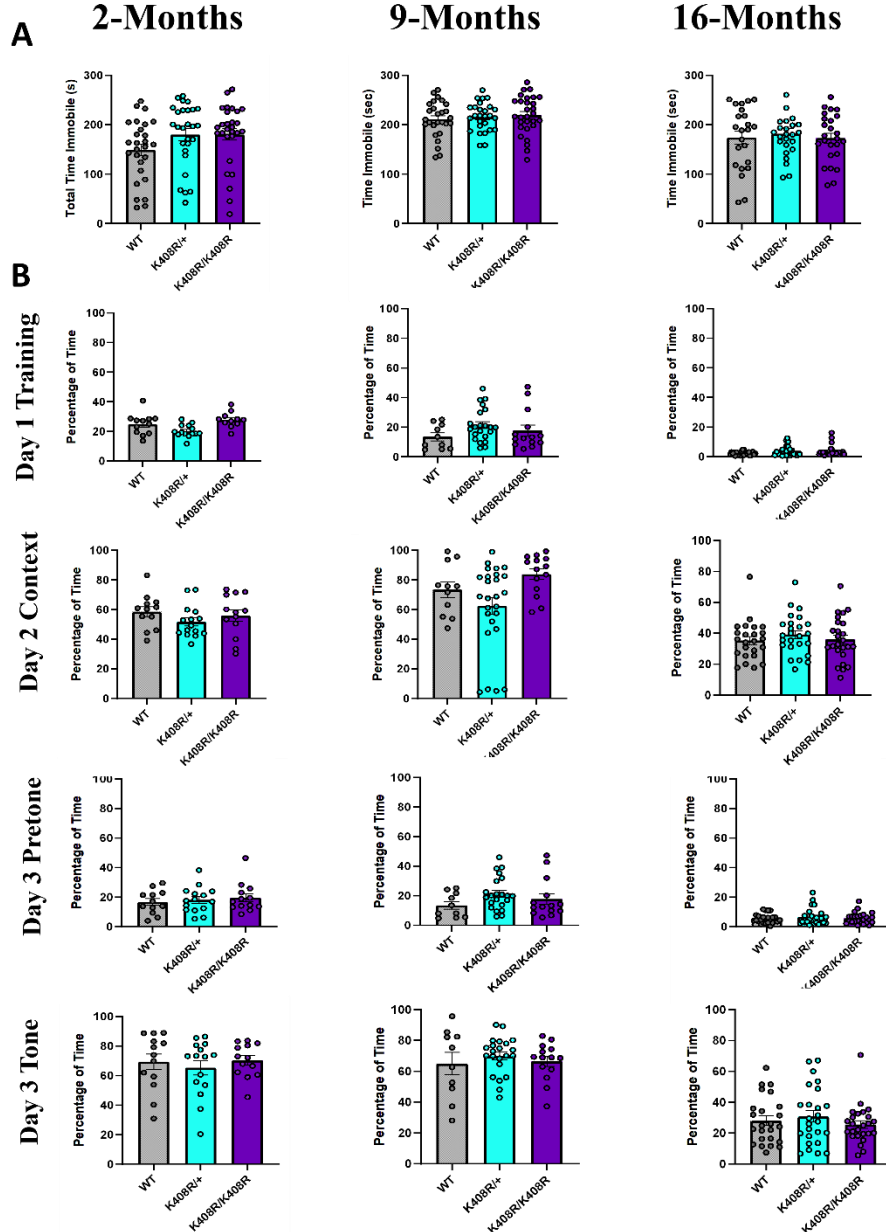


Figure 12. *Tdp-43*^{K408R} mutant mice do not display changes in emotional processing. A) Total time mice spent immobile (seconds) in tail suspension test at 2-, 9-, 16- month age time points. **B)** All animals **C)** females only **D)** and males only for the time spent freezing in the three-day fear conditioning paradigm. All statistical analyses are via Brown-Forsythe and Welch One-Way ANOVA with Dunnett’s post-hoc test. Mean +/- SEM is shown. Each dot represents one animal.

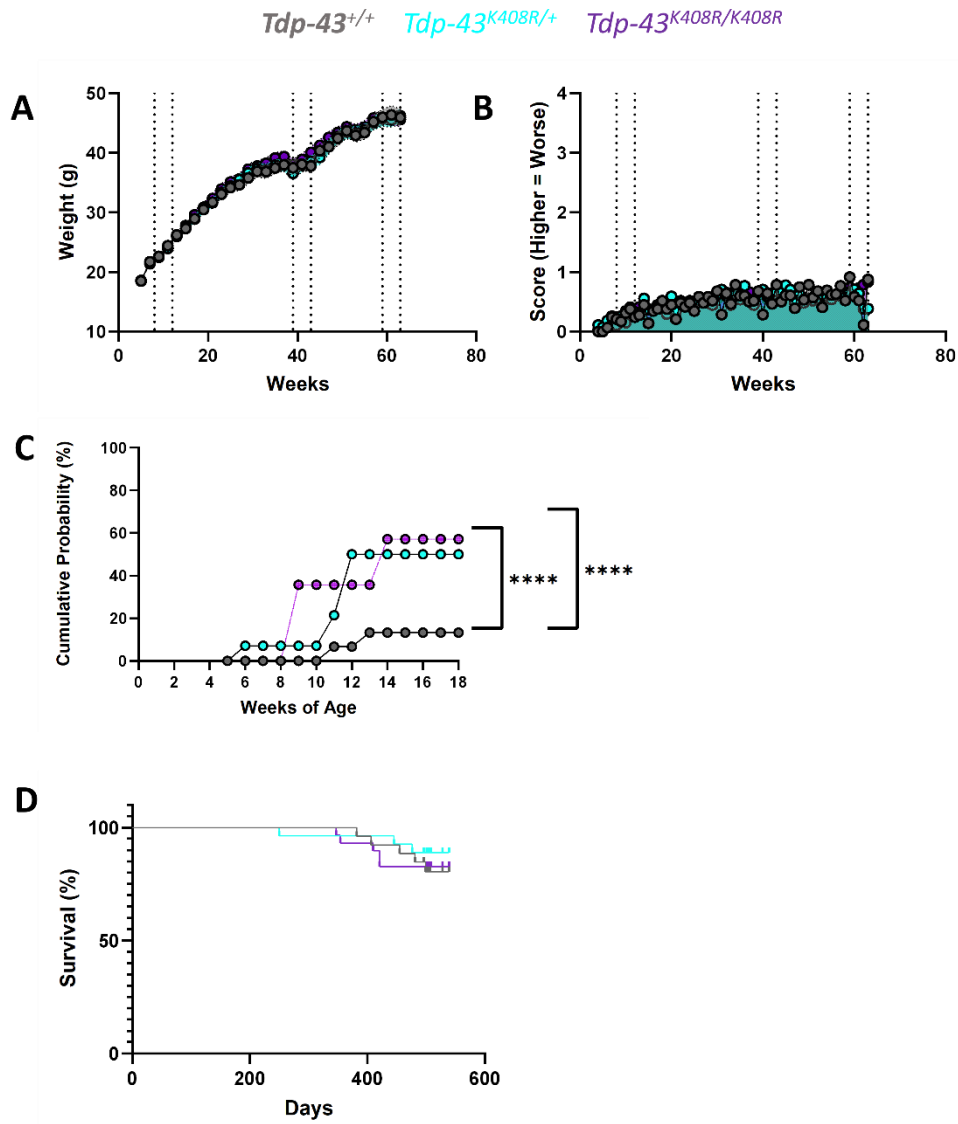


Figure 13. *Tdp-43^{K408R}* mutant mice neuromuscular impairments but female mice show changes in barbering behaviour. A) Adult body weight (grams) across lifespan. Gridlines indicate periods of active behaviour testing. **B)** Hindlimb claspings scores (out of 4) across lifespan. Gridlines indicate periods of active behaviour testing. **C)** Cumulative probability (percentage) of female mice for *Tdp-43^{+/+}*, *Tdp-43^{K408R/+}*, and *Tdp-43^{K408R/K408R}* in the first 18 weeks. **D)** Kaplan-Meier survival curve for all mice in behaviour colony up to 16-months of age. Statistical analyses for A-C are via Two-Way ANOVA with Tukey's post-hoc test. Mean +/- SEM is shown for A and B. (****P<0.0001)

and could therefore reflect behavioural differences in the mutant animals themselves. Finally, a survival curve was plotted but there was no difference between genotypes for the overall lifespan of the animals (Figure 13D).

6.3 Histological Characterization

6.3.1 Cortical Neurodegeneration in 5-Month Female *Tdp-43^{K408R}* Mice

Cortical atrophy is a clinical feature in both ALS and FTD.²⁰⁵ Cortical neurodegeneration was assessed broadly in the prefrontal and motor cortices of the *Tdp-43^{K408R}* mice. Measures of cortical thickness revealed no difference between *Tdp-43^{K408R/K408R}* and controls (Figure 14A, B). Additionally, there was no differences in neuronal counts for either of the areas (Figure 14C, D). Specific to ALS pathogenesis, layer V upper motor neurons are lost. Ctip2 as a marker of this cortical layer was used in the motor cortex to assess degeneration of upper motor neurons. There were no significant differences in Ctip2 positive cells counts between *Tdp-43^{K408R/K408R}* and controls (Figure 15).

6.3.2 Hippocampal Pathology in 5-Month Female *Tdp-43^{K408R}* Mice

There has been increasing evidence that hippocampal pathology is found in ALS and FTD based on neuroimaging and post-mortem studies.^{206–208} As a novel mouse model, the consequences of the K408R mutation on the hippocampus was explored. Interestingly, there was a non-significant increase in the number of pyknotic cells in the subgranular zone of the dentate gyrus of the *Tdp-43^{K408R/K408R}* (Figure 16A, B). There was no significant astrogliosis as measured by GFAP positive astrocytes in the dentate gyrus (Figure 16A, C).

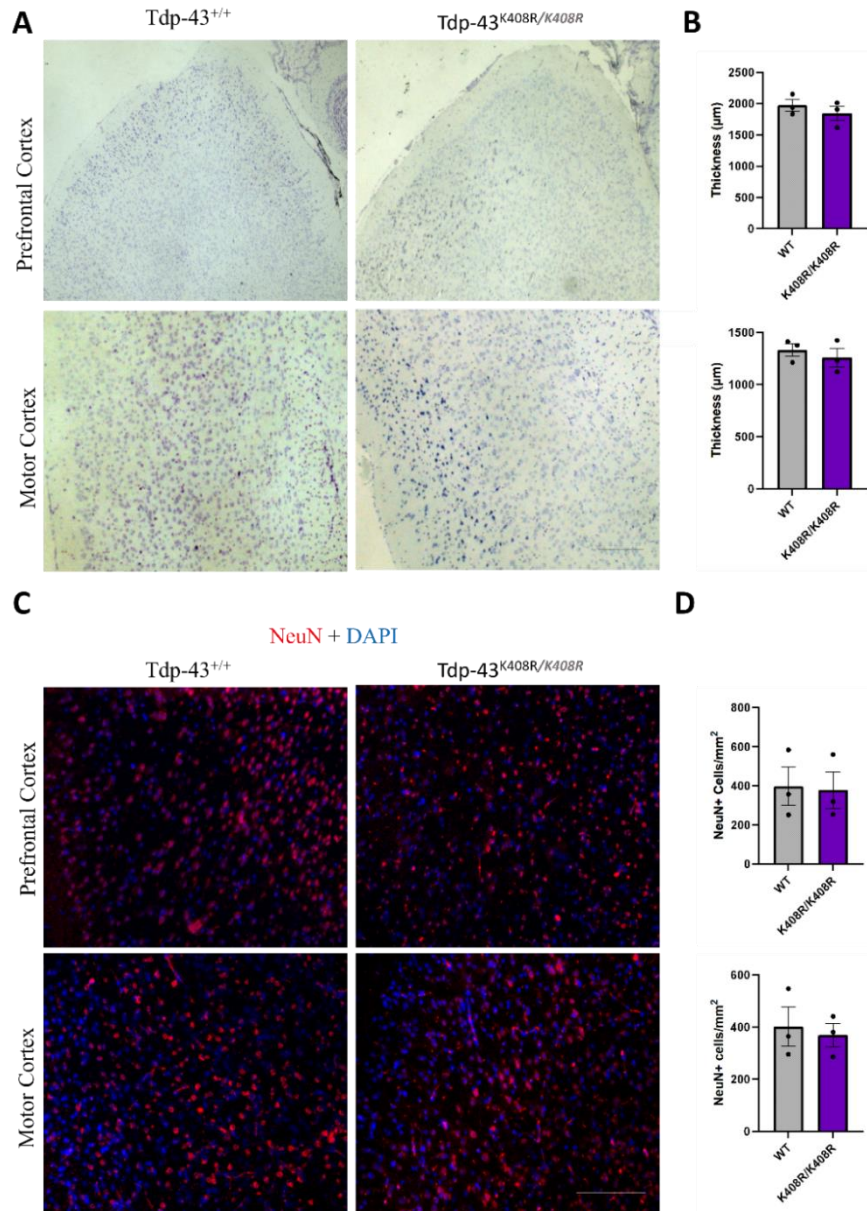


Figure 14. *Tdp-43*^{K408R} mutant female mice do not display cortical neurodegeneration at 5-months. **A)** Cresyl violet staining of prefrontal and motor cortices. **B)** Quantification of cortical thickness measurements (micrometers) of prefrontal and motor cortices. **C)** Neuronal staining (NeuN, red) of prefrontal and motor cortices. **D)** Quantification of neuronal counts (NeuN positive counts) of prefrontal and motor cortices. Scale bar represents 200μm. Statistical analyses are via Student's T-test. Mean +/- SEM is shown. Each dot represents one animal.

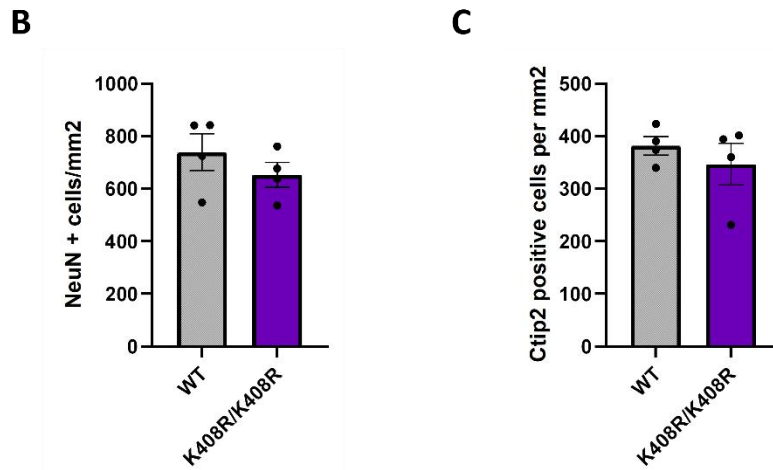
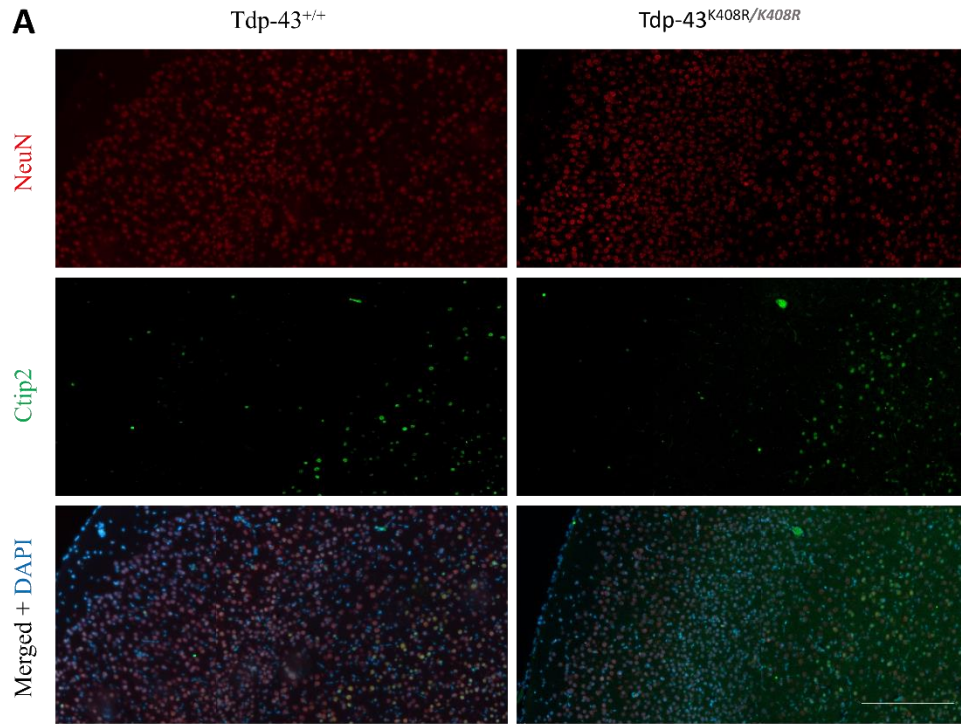


Figure 15. *Tdp-43*^{K408R} mutant female mice do not display loss of upper motor neurons. A) Staining of layer V (Ctip2, green) neurons (NeuN, red) in the motor cortex. **B)** Quantification of neurons and **C)** Ctip2 positive cells. Scale bar represents 200 μ m. Statistical analyses are via Student's T-test. Mean +/- SEM is shown. Each dot represents one animal.

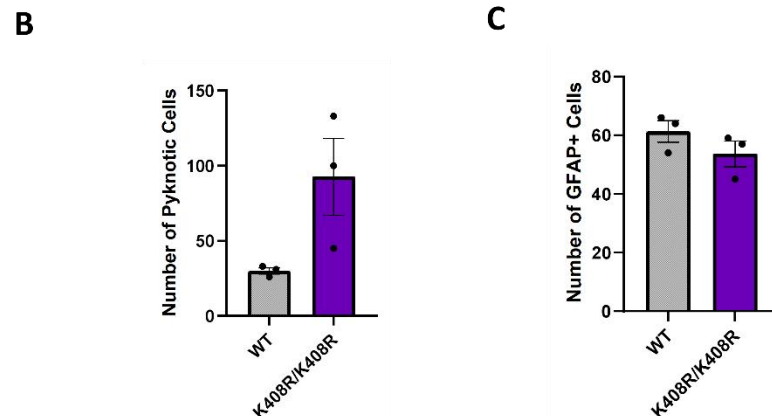
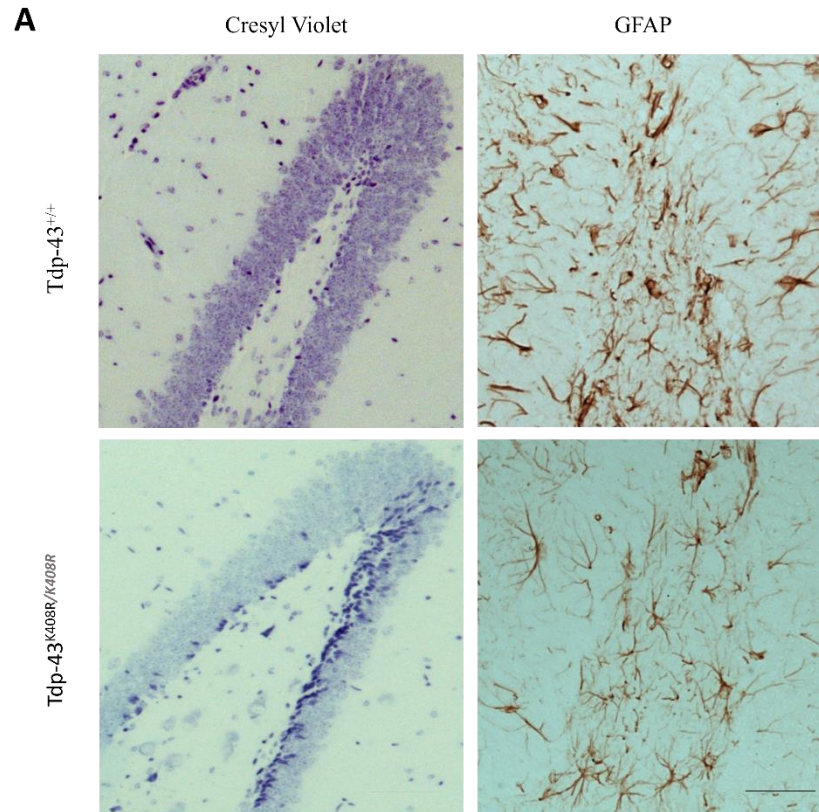


Figure 16. *Tdp-43^{K408R}* mutant female mice do not display significant hippocampal pathology at 5-months. A) Cresyl violet and GFAP staining of the hippocampal dentate gyrus. **B)** Quantification of the number of pyknotic cells in the dentate gyrus. **C)** Quantification of the number of GFAP positive astrocytes in the dentate gyrus. Scale bar represents 200 μ m. Statistical analyses are via Student's T-test. Mean +/- SEM is shown. Each dot represents one animal.

6.3.3 CNS Myelination in 5-Month Female *Tdp-43^{K408R}* Mice

Oligodendrocytes have been implicated in the pathogenesis of ALS and FTD. The loss of TDP-43 in oligodendrocytes results in their death and subsequently a reduction in myelination which has been reproduced in animal models.^{150,209} Myelin staining was assessed in the cerebellum, hippocampus, cortex, and spinal cord. Qualitatively, there were no differences in white matter staining intensity across genotypes suggesting no demyelination with the loss of TDP-43 SUMOylation (Figure 17).

6.3.4 Pathological TDP-43 in 5-Month Female *Tdp-43^{K408R}* Mice

TDP-43 mislocalization and phosphorylation are pathological hallmarks in ALS/FTD patients. In the cortex, full-length TDP-43 was qualitatively assessed for its cellular localization. In both the motor and prefrontal cortex, cells with cytoplasmic mislocalized TDP-43 were identified in the *Tdp-43^{K408R}* mice but not controls. Furthermore, in the spinal cord, mislocalized phosphorylated TDP-43 at S403/404 was observed in large (motor neuron) cells. These results suggest that blocking TDP-43 SUMOylation results in histopathological phenotypes reminiscent of ALS/FTD.

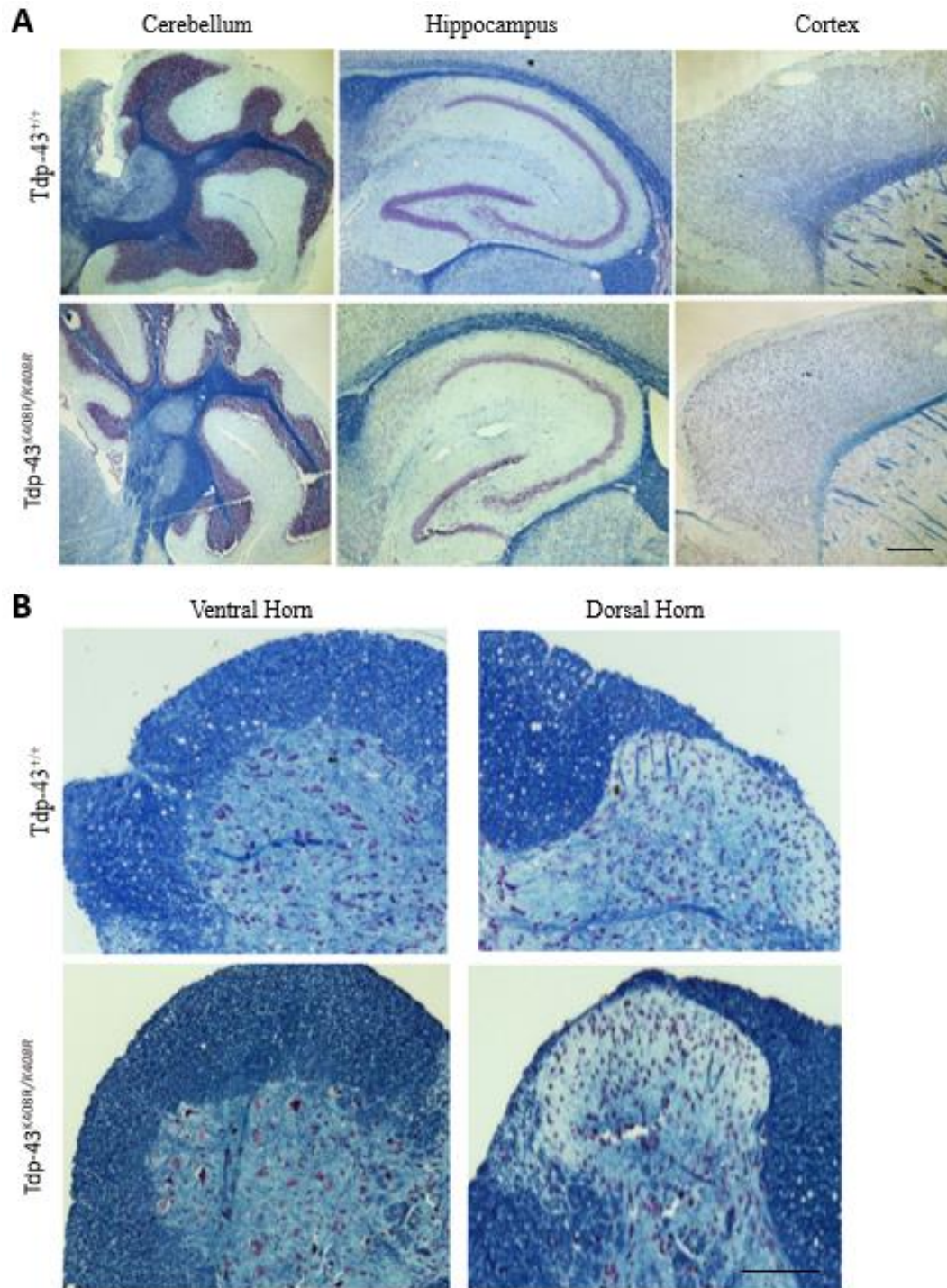


Figure 17. *Tdp-43*^{K408R} mutant female mice do not display central nervous system demyelination at 5-months. **A)** Luxol Fast Blue staining of myelin in the cerebellum, hippocampus, and cortex. **B)** Luxol Fast Blue staining of the myelin in the ventral and dorsal horn of the spinal cord. Scale bar represents 200 μ m.

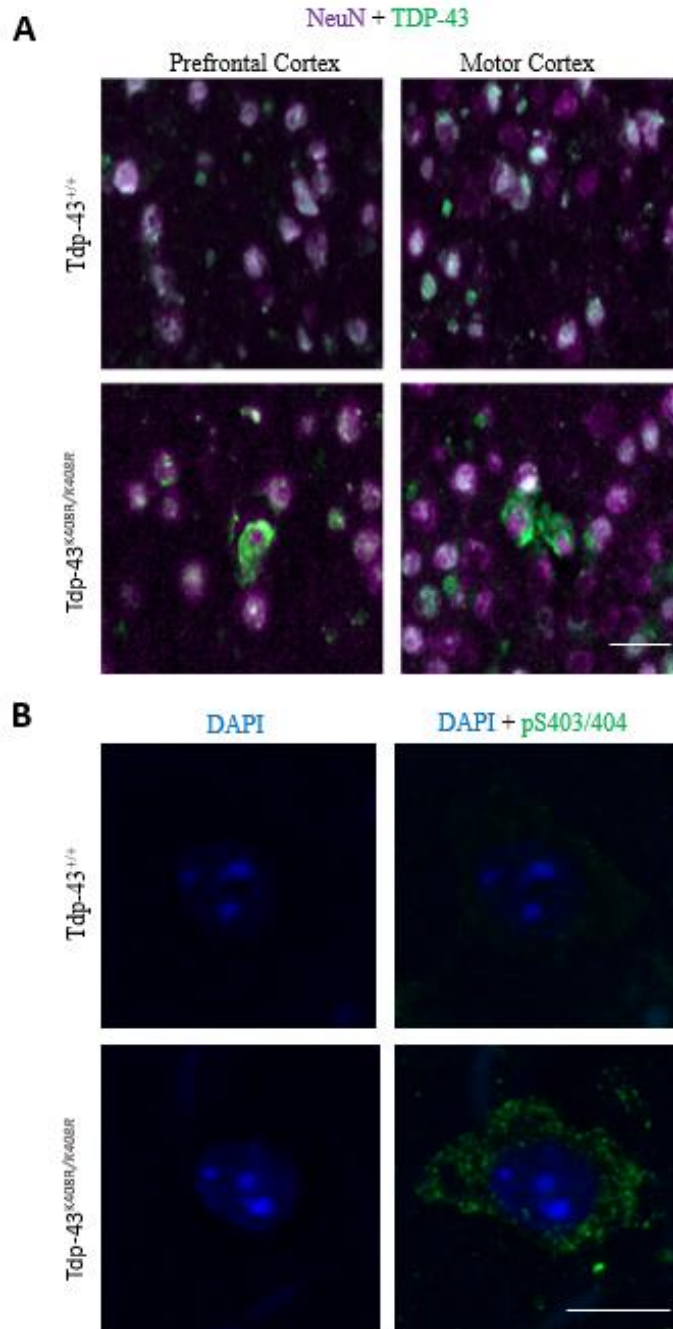


Figure 18. *Tdp-43*^{K408R} mutant female mice display pathological TDP-43 at 5-months. A)

Staining for full-length TDP-43 (green) and neurons (NeuN, purple) in the prefrontal and motor cortices.

Scale bar represents 30 μm . **B)** Staining for pS403/404 TDP-43 (green) in ventral spinal cord. Scale bar

represents 10 μm .

6.3.5 Lower Motor Neurons in 9-Month *Tdp-43*^{K408R} Mice

Pathologically, ALS leads to the loss of motor neurons in the ventral horn of the spinal cord, producing motor impairment. And as previously, discussed, TDP-43 pathology is a hallmark of almost all ALS cases. To investigate these disease features in the *Tdp-43*^{K408R} mice, ChAT positive lower motor neurons in spinal cord sections were quantified at 9-months of age. There was no significant difference in number between *Tdp-43*^{K408R/K408R} and controls (Figure 19). Qualitatively, full-length TDP-43 was assessed in these cells and there was no mislocalization or aggregation observed (Figure 19).

6.3.6 C-Terminal TDP-43 in 9-Month *Tdp-43*^{K408R} Mice

TDP-43 can be N-terminally cleaved to produce C-terminal fragments (CTF) of varying molecular weights.¹²⁰ In patients, CTFs have been detected within TDP-43 inclusions in brains and less commonly spinal cords. While their role in the pathogenesis of disease is not completely understood, some studies suggest they are toxic and promote neuronal death. This species of TDP-43 was specifically investigated in the spinal cord ventral roots of *Tdp-43*^{K408R} mice at 9-months old. Qualitatively, the number of large soma cells (presumed lower-motor neurons) with C-terminal TDP-43 mislocalization was significantly increased in *Tdp-43*^{K408R/K408R} mice compared to controls (Figure 19). This result may underly the mild behavioural phenotypes observed in the mice at this age, especially the onset of motor deficits in rotarod.

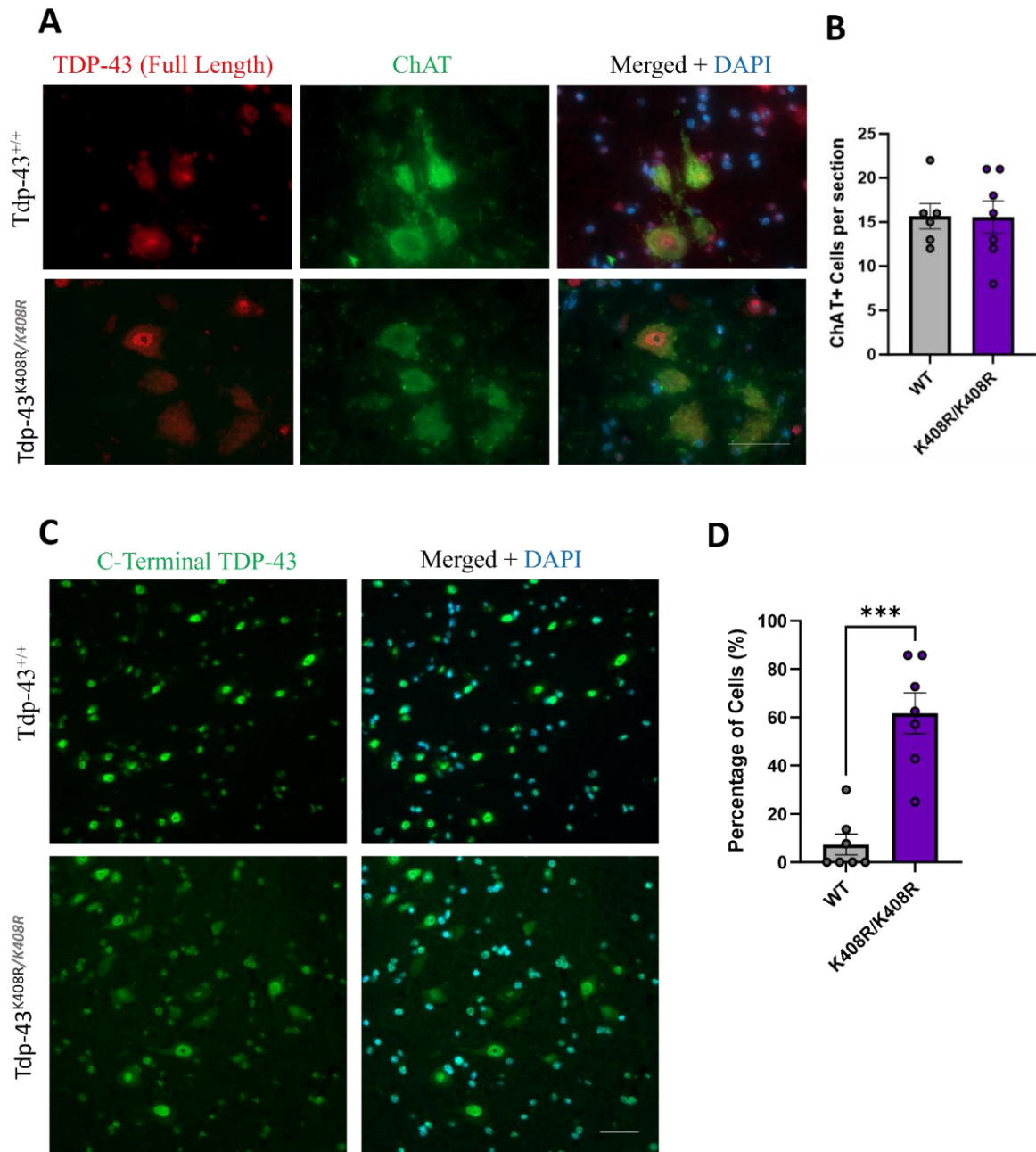


Figure 19. *Tdp-43*^{K408R} mutant mice display mislocalized TDP-43 at 9-months. **A)** Staining for full-length TDP-43 (red) and lower motor neurons (ChAT, green) in the ventral horn. **B)** Quantification of ChAT positive cells for each spinal cord section. Dots represent one animal as an average of three slices. **C)** Staining for c-terminal TDP-43 (green) in the ventral horn. **D)** Quantification of large (motor neuron) cells with mislocalized c-terminal TDP-43. Dots represent one animal. Scale bars represents 20 μ m.

5. Discussion

ALS and FTD are two debilitating neurodegenerative diseases existing on a clinical spectrum. ALS is caused by the degeneration of motor neurons in the central nervous system, producing neuromuscular symptoms and is inherently fatal.¹⁵ FTD results in behavioral and cognitive changes due to the loss of cortical neurons.⁷⁸ Despite ALS being the most common adult-onset motor neuron disease and FTD the second most common form of dementia, there are currently very limited biomarkers and therapeutic interventions to improve the quality and quantity of life for patients. An important connection between these diseases at the genetic and pathological level is the protein TDP-43, making it a relevant target in the development of novel therapeutics.²¹⁰ However, there is still a need for mouse models of ALS/FTD to translate basic science findings to clinical benefit. ALS and FTD are challenging diseases to model because of the many layers of heterogeneity. Patients have diverse clinical presentations, symptoms, progression, and positions along the ALS/FTD spectrum. Additionally, numerous genes and associated proteins have been implicated in disease pathogenesis. Furthermore, most patient cases are sporadic, of which there is no defined genetic mutation to model in animals.

In this present work, the *Tdp-43^{K408R}* mouse line was characterized as a novel model of ALS/FTD. Disturbances in TDP-43 yield detrimental phenotypes and thus, understanding TDP-43 misregulation could uncover novel targets to correct this. TDP-43 is regulated by post-translational modifications. However, the post-translational modification of TDP-43 by SUMOylation is not well understood and no animal models exist to study this. To fill this knowledge gap, the *Tdp-43^{K408R}* allele was generated. By blocking endogenous SUMOylation with a point mutation in TDP-43 at lysine 408 (K408R), the *Tdp-43^{K408R}* mouse line facilitated the investigation of whether ALS/FTD phenotypes were recapitulated at the histological level.

5.1 TDP-43 Animal Models have Variable Onset of ALS and FTD Disease

Features

Established animal models with altered TDP-43 have varied outcomes in terms of motor and non-motor phenotypes and timing of their emergence.¹⁶⁰ The characterization of the *Tdp-43^{K408R}* mutant mice was performed with a longitudinal approach to capture potential phenotypes. *Tdp-43^{K408R}* mice do not exhibit motor deficits at P8 based on weight, righting reflex, or limb suspension or at P21 based on weight or latency to fall in the hanging wire test. Some TDP-43 animal models observe significant phenotypes around this age. The overexpression of human mutant TDP-43 with a known disease mutation resulted in hindlimb clasping deficits at 14 days of age with poor gait and rotarod performance at 22 days.²¹¹ Between 26 and 30 days old, these mice develop paralysis and die. Additionally, mice with a homozygous, but not heterozygous, knock-in of a disease mutation in TDP-43 (N390D) were not able to survive past three weeks of age.¹⁸⁴ Across the adult lifespan of the *Tdp-43^{K408R}* mutant mice, there were no significant differences in weight, hindlimb clasping, or survival up to approximately 16 months of age. An absence of weight differences was observed in endogenous knock-in models of TDP-43 and post-natal knockout of TDP-43 did not alter survival.^{184,212} However, survival differences have previously been detected after 20 months in knock-in models and thus extending the survival study of the *Tdp-43^{K408R}* mice may give more insight. Overall, no robust neuromuscular deficits were found in the *Tdp-43^{K408R}* model. The unexpected barbering phenotype that was observed significantly more in the *Tdp-43^{K408R}* mutant mice has been noted in non-TDP-43 mouse models of FTD but not exclusively in females.^{193,213} However, this phenotype has not been extensively characterized and is not well understood in the context of FTD. Moving forward, planning cages

with different genotype ratios and scoring barbering could help parse out its relation to social behaviours.

In the *Tdp-43^{K408R}* mutant mice, cognitive related phenotypes preceded deficits in motor performance. This pattern of progression is seen in human patients as well as a mouse model overexpressing human TDP-43.¹⁹⁶ Female *Tdp-43^{K408R/K408R}* mice exhibited increased distance travelled, and time spent in the center of the open field test at 2-months suggesting a hyperactive, disinhibited phenotype. Related behaviors have been found in multiple Tau based models of FTD.^{214,215} At 9-months of age, there was reduced locomotion of the female *Tdp-43^{K408R/K408R}* mice during habituation to a novel cage-like environment which may indicate changes in cognitive processing.²¹⁶ At this age, male *Tdp-43^{K408R/+}* buried significantly less marbles, suggestive of apathetic behavior. Deficits in marble burying presenting at 5 months has been well-characterized in other models.¹⁵¹ At 9-months of age the mutant male mice develop a rotarod deficit, falling off the rod faster than controls. TDP-43 knock-in and overexpression models have observed rotarod deficits starting at 6-8 months as well. However, unlike in previously characterized models, the impaired rotarod performance did not persist or progress with age in the *Tdp-43^{K408R}* mutant suggesting that this motor deficit is mild whereas in other models, the motor deficit significantly worsened in an age-dependent manner. Additionally, there was no reduction in their grip strength which is a common feature of ALS models.^{150,212} The mild motor impairment in the mice was supported by a reduced distance travelled in the open field test at 9-months of age. Finally, at the 16-months age point, *Tdp-43^{K408R}* mutant mice displayed further cognitive and social behavioral changes. Female *Tdp-43^{K408R/K408R}* mice performed poorly in the Y-maze test of spatial working memory. In the tube test, *Tdp-43^{K408R/K408R}* mutant mice were less dominant, winning less battles against control cage mates. While TDP-43 models of FTD have

explored social behavior and found deficits, the tube test has been characterized specifically in progranulin models.¹⁹⁷ Similar results of reduced dominance at older age points were found.

Akin to the behavioral phenotypes, TDP-43 based models of ALS and FTD have heterogeneous features. Motor neuron loss has been detected in various TDP-43 models with overexpression systems showing this the earliest before 1-month of age.²¹¹ However, knock-in mutant TDP-43 models display behavioral impairments, but motor neuron degeneration is absent up to 2 years of age in the mice.²¹⁷ No neurodegeneration was detected in *Tdp-43^{K408R}* mutants up to 9-months but it is possible this was too early in the disease progression. However, while lower motor cell body counts were investigated in this study, the distal neuromuscular junctions were not. There is evidence to support that neuromuscular precedes motor neuron death.²¹⁸ Therefore, future work will examine the neuromuscular junctions in the *Tdp-43^{K408R}* mouse line to determine whether the loss of TDP-43 SUMOylation contributes to pathology in this region. Astrogliosis is a well characterized feature of ALS/FTD pathogenesis and replicated in mouse models.^{184,211}

Additionally, oligodendrocyte dysfunction including a cell-autonomous role has more recently been implicated, resulting in white matter loss.²⁰⁹ A recent study has investigated white matter in a wild-type TDP-43 overexpression model and found progressive demyelination with age.¹⁵⁰

Neither of these glial features were observed in this work. Regarding TDP-43 pathology, overexpression of humanized wild-type TDP-43 produced nuclear clearing in motor neurons at 1-month of age, whereas in animals with endogenous knock-in mutations of TDP-43, subtle mislocalization at 6-months and aggregation at 24-months has been found.^{184,211} However, other knock-in models lacked TDP-43 pathology.²¹⁷ *Tdp-43^{K408R}* mutants display mislocalization and phosphorylation between 5- and 9-months of age. This result suggests that this model may be promising for modeling ALS/FTD TDP-43 pathology for future studies.

Although it was not significant in this study, *Tdp-43^{K408R}* mutants were trending for an increased number of pyknotic cells in the sub-granular zone of the dentate gyrus, the site of adult neurogenesis. A recent study of a TDP-43 knock-in model found significantly impaired neurogenesis in the hippocampus.²¹⁹ Furthermore, there has been growing evidence that adult neurogenesis is impaired across many neurodegenerative diseases and this could be a potential therapeutic target.²²⁰

In summary, blocking endogenous SUMOylation of TDP-43 in mice reproduces mild ALS/FTD phenotypes for motor and non-motor behavior as well as histopathological features.

5.1.2 Investigation Limitations

It is important to note that this study has limitations. Firstly, in comparison to ALS/FTD patients and other animals, blocking SUMOylation in the *Tdp-43^{K408R}* mutant mice had mild behavioural and histological phenotypes despite promising signs of TDP-43 pathology in various regions of the CNS. There could be several explanations for why more robust changes are not observed. TDP-43 is known to be highly regulated by numerous mechanisms. Thus, other mechanisms including epigenetic effects or other post translational modifications could be compensating in the face of blocked SUMOylation. Another explanation could be that phenotypes resulting from the loss of TDP-43 SUMOylation could be partially penetrant where some mice have stronger phenotype compared to others of the same genotype. Although inbred laboratory mice are isogenic, there have been mouse models of other diseases which display variable penetrance. Future studies with a larger sample size could investigate this possibility and look for correlations between behavioural and histological phenotypes. Lastly, the timepoints chosen for this study could have been too early for robust phenotypes to emerge. TDP-43 knock in mouse

models of known patient mutations sometimes do not show phenotypes until around 20 months of age. Therefore, this study may have missed changes past the 16-month time point selected. Adding to this, it was hypothesized that blocking SUMOylation of TDP-43 in a stress dependent system would lead to the recapitulation of ALS/FTD phenotypes, reflecting the idea that these diseases are a multistep process. Aging is a stressor for biological systems, and thus more advanced age combined with the loss of TDP-43 SUMOylation may produce neurodegenerative phenotypes. There are other ways to impose additional stressors on the *Tdp-43^{K408R}* mouse model and investigate ALS/FTD features as discussed in future directions.

Another limitation of this study was that heterozygous but not homozygous mutant *Tdp-43^{K408R}* mice have behavioural phenotypes in certain tests such as marble burying. It is possible that this was a false positive result especially since heterozygous mice were not statistically different in any other behaviour test. Another explanation could be that there is a dominant negative effect where the wildtype allele attempts to autoregulate the mutant allele. Previous studies have found that perturbed TDP-43 autoregulation can produce cognitive phenotypes in mice.¹⁵¹ Future studies could investigate the levels of wildtype and or mutant TDP-43 alleles in the mutant mice.

5.2 Future Directions

5.2.1 Sex Differences in ALS/FTD

In this present work, sex differences were present for several phenotypes. Mutant *Tdp-43^{K408R}* female mice showed significant alterations in multiple domains of cognition and male mice presented with more motor-like deficits. Histologically, many of the experiments featured only female mice which is a limitation of this study. The presence of mislocalized TDP-43 in the cortex and phosphorylated TDP-43 in the spinal cord need to be investigated in male

counterparts at 5-months. However, c-terminal TDP-43 was observed in both sexes at 9-months. With the male sex bias in ALS patients, disease models often focus more on phenotypes of male mice.¹⁸⁴ However, more recently studies have begun to specifically look at sex differences in models. This is particularly important in TDP-43 since the sex bias in FTD is not well characterized. There has been growing support that estrogens may play neuroprotective roles in various disorders of the nervous system, including ALS and FTD.^{221,222} Clinical evidence has found that increased exposure to estrogens and being pre-menopausal each reduces the risk of developing ALS.²²³ The relationship between estrogens and FTD is more controversial.²²⁴ In preclinical models, many report no sex differences. However, it was found that female sexed animals with a TDP-43 knock-in mutation have a significant delay in the motor and cognitive symptoms found in male counterparts.²²⁵ Furthermore, androgens have been proposed to play a detrimental role in ALS pathogenesis. Female patients have been reported to have higher androgen levels compared to healthy controls.²²⁶ In animal models, mutant TDP-43 downregulated androgen receptors in spinal cords of male mice.²²⁷ Overall, recapitulating sex differences in animal models can aid in understanding the interaction between sex, genetics, and selective cellular vulnerability in ALS/FTD risk. Future investigation with the *Tdp-43^{K408R}* allele could alter sex hormones through gonadectomized animals and hormone replacement, to understand their contribution to pathogenesis and may lend to identifying novel therapeutic targets to protect against disease.

5.2.2 Environmental Insults and Stress in ALS/FTD

An important consideration in the modelling of neurodegenerative disorders, including ALS and FTD, is that they are likely multistep processes in which their pathophysiology depends on the interaction between genetics, age, and environmental stressors.²²⁸ Therefore, the use of strictly

genetic models limits a wholistic understanding of the complexities of disease. From clinical data, while age is a strong risk factor for ALS and FTD, studies have also suggested factors including exposure to heavy metals, pesticides, cyanotoxins, and electromagnetic fields whereas lifestyle factors include military service, high intensity physical activity, traumatic brain injury and smoking.^{66,229} These studies are limited by their retrospective and correlational design, nevertheless, support environment as a contributor to disease. Stressors in ALS/FTD *in vivo* and *in vitro* models have been used to begin drawing connections with patient data. In a mouse model with mutant TDP-43, exposure to hyperthermic stress led to nuclear depletion and cytoplasmic mislocalization of TDP-43 with defective stress granule assembly.²³⁰ In cell models with mutant TDP-43, stress has been found to induce recruitment of TDP-43 to the cytoplasm where it can activate an early integrated stress response or increase cellular toxicity during stress recovery.²³¹ Under chronic stress conditions, cytoplasmic TDP-43 can be cleaved, phosphorylated, and form disease like aggregates.²³² SUMOylation as a post-translational modification has also been implicated in the cellular response to stress. Stress leads to an increase in SUMOylation of targets.²³³ There is currently little evidence linking SUMOylation to ALS. In one study, it was found that the ALS associated C9ORF72 mutant proteins were found to disrupt SUMOylation resulting in impaired cellular stress responses mechanisms.²³⁴ In this present characterization of the *Tdp-43^{K408R}* mouse model, the loss of TDP-43 SUMOylation was investigated using age as a stressor. However, the absence of other stressors for the mice to reflect the human experience (e.g. viral infection, head trauma, intense physical activity) may not have been sufficient to produce cellular disruption and recapitulate ALS/FTD pathogenesis. There could be several methods to impose additional stressors in the *Tdp-43^{K408R}* mice. For environmental stressors relevant to ALS/FTD, the mice could be exposed to toxins, forced exercise training, or a

concussion paradigm. However, genetic stressors like the *C9ORF72* repeat expansion may be amenable in a laboratory setting. Clinically, ALS/FTD patients with a *C9ORF72* mutation also present with TDP-43 pathology, and *C9ORF72* toxicity results in cellular stress. This therefore suggests a potential link between these two genes in the context of ALS/FTD. Future studies, crossing the *Tdp-43*^{K408R} mice to an established transgenic mouse model expressing the human *C9ORF72* hexanucleotide repeat expansion will help establish this link. The latter model has *C9ORF72* pathology but lacks behavioural and histological phenotypes relevant to ALS/FTD.²³⁵ Therefore, it is hypothesized that the combination of *C9ORF72* stress and the loss of TDP-43 SUMOylation will push the system together age leading to an amplification of phenotypes. This study design may reflect the multiple hits required in patients to develop disease.

5.2.3 Biomarker Development for ALS/FTD

As previously discussed, there is a pressing need for ALS and FTD biomarkers for the benefits of patients. These biomarkers can be integrated into the diagnostic workflow, monitor disease progression, and be used in clinical trials to evaluate the effectiveness of novel therapeutics.²³⁶

Overall, biomarkers are critical for early diagnosis and treatment of these diseases which still pose a great challenge for the field. Biofluid biomarkers are the most conventional approach for various diseases as they do not require highly advanced equipment and are relatively accessible to collect from patients.²³⁷ CSF was previously the focus in neurodegenerative diseases because it is in close contact with the nervous system. However, the CSF exchanges contents with the blood and recent studies have found there is generally a high correlation between the contents of CSF and blood.²³⁸ Blood has benefits over CSF as the process to collect it is less invasive and it can also contain potential systemic biomarkers of disease from other organ system involved such as muscle for ALS.^{237,238}

Proteomic-based approaches are a powerful, high-throughput tool in biofluid biomarker discovery.²³⁹ Proteomics involves characterizing the protein profile of a biological sample. Proteins can be seen as a bridge between genetics and phenotypes.²³⁹ Therefore, they are ideal targets for understanding and monitoring disease. Proteomics for the discovery of biomarkers involves the generation of many candidate proteins which have significant differences in experimental compared with control conditions and subsequent prioritization using bioinformatics and validation of these candidates.²³⁹ Clinically, proteomics is increasingly utilized to attempt to identify proteins that can serve as disease-specific biomarkers.²⁴⁰

The need for biomarker discovery extends to preclinical translational biomarkers. Most patient-centered biomarker discovery studies have focused on distinguishing patients based on genetic subtypes. These studies have been able to identify differentially expressed biomarker candidates. As TDP-43 pathological hallmark, identifying biomarkers associated with this feature would likely be applicable to most ALS/FTD cases. However, since TDP-43 pathology must be confirmed post-mortem, animal models offer a promising alternative approach. Translational biomarkers are those identified in animal models of disease and validated in patients as well. Presently, there have been numerous clinical trials for ALS/FTD which have failed, highlighting the need for enhanced preclinical and clinical study designs with a focus on translation.²³⁸ Translational biomarkers would not only improve understanding of disease pathophysiology but also inform clinical studies on dosage, time course, adverse reactions of drugs, and target engagement.²⁴¹ Unfortunately, most preclinical studies have focused on SOD1 mutant mice, translating to a small percentage of human patients. Galectin-3 was identified as a biomarker candidate in mutant SOD1 mice and was also found to be elevated in ALS patient biofluids.²⁴²

Additionally, a 7-amino acid endogenous protein responded to ASO treatment in SOD1 mutant mice, suggesting it could act as a pharmacological biomarker.²⁴³ However, one study focused on an endogenous TDP-43 knock-in mutant ALS/FTD model and characterized plasma extracellular vesicles and found the alterations could predict disease progression in ALS patients.²⁴⁴

Overall, the use of TDP-43 based animal models holds promise for preclinical biomarker discovery. Therefore, future work is planned to investigate whether there are changes in the proteome of the *Tdp-43^{K408R}* mice resulting from lost TDP-43 SUMOylation. With the critical functions of both TDP-43 and SUMOylation within cells, we may be able to uncover dysregulated pathways relevant to ALS/FTD pathogenesis. These results could be validated in ALS/FTD patient samples where discovery is more challenging due to patient variability. In fact, we have collected blood serum from the *Tdp-43^{K408R}* mouse line at three age points to monitor proteomic changes in a longitudinal approach which may give insight to progression in patients. Overall, preclinical biomarker discovery in mouse models can provide insights to better understand disease pathogenesis or translate to patients for clinical benefit.

5.3 Conclusion

In conclusion, we have successfully generated the *Tdp-43^{K408R}* mouse line which recapitulates some behavioral and histological features of ALS and FTD, including the TDP-43 pathology, a pathological hallmark. The results from this study suggest that SUMOylation of TDP-43 is likely implicated in the pathogenesis of these diseases. This mouse line may serve to model the familial cases of disease, which constitute most patients, as it is not linked to a known disease-causing mutation. This model may serve as a useful tool for understanding the misregulation of TDP-43 in disease and facilitate the development of novel biomarkers and therapeutics.

Table 1. Scoring For Hindlimb Clasping Phenotype

Hindlimb Score	Description
0	No limb clasping. Normal toe splay and escape extension.
1	One hind limb exhibits loss of mobility with incomplete splay. Toes exhibit normal splay.
2	Both hind limbs exhibit loss of mobility with incomplete splay. Toes exhibit normal splay.
3	Both hind limbs exhibit clasping, loss of mobility, and curled toes.
4	Fore and hindlimbs exhibit clasping, loss of mobility, curled toes, and retraction into the body.

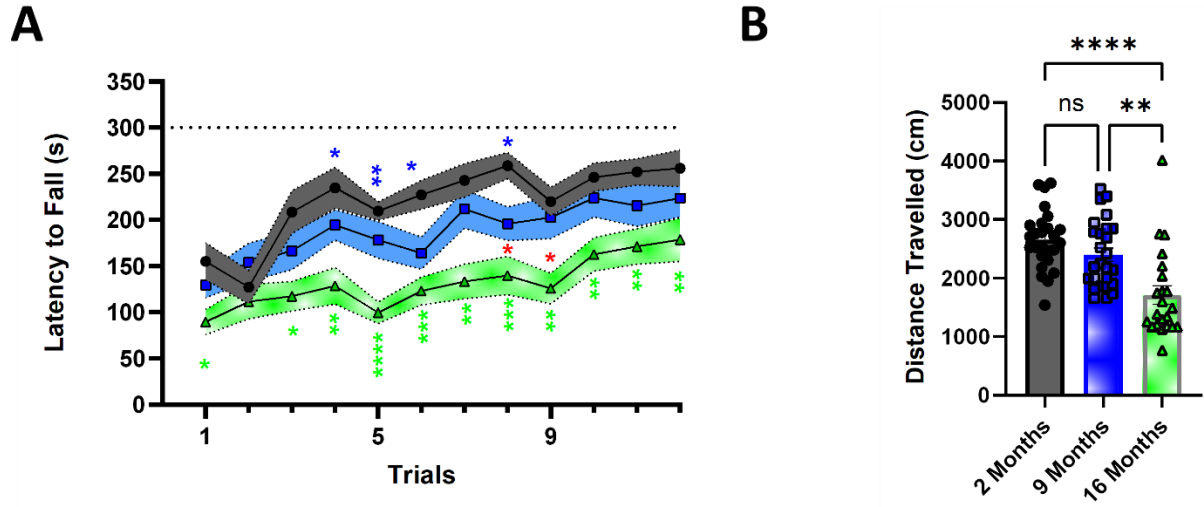
Table 2. Scoring for Kyphosis Phenotype

Hindlimb Score	Description
0	Spine is straight when mouse is walking. No kyphosis.
1	Mild spine curvature (kyphosis) but mouse is still able to straighten spine.
2	Mouse is unable to straighten spine completely and maintains persistent but mild curvature (kyphosis).
3	Mouse maintains pronounced spinal curvature (kyphosis) while walking and sitting.

Table 3. List of Primary Antibodies Used in Study

Antigen	Host Species	Dilution	Catalogue Number	Source
ChAT	Goat	1:200	AB144P	EMD Millipore
Ctip2	Rat	1:500	AB18465	Abcam
GFAP	Guinea Pig	1:200	173004(SY)	Synaptic Systems
NeuN	Mouse	1:1000	MAB377	EMD Millipore
TDP-43	Rabbit	1:500	10782-2-AP	Proteintech
TDP-43 (C-terminal)	Rabbit	1:200	12892-1-AP	Proteintech
pS403/404 TDP-43	Mouse	1:500	66079-1-Ig	Proteintech

2 Month *Tdp-43*^{+/+} 9 Month *Tdp-43*^{+/+} 16 Month *Tdp-43*^{+/+}



Supplementary Figure 1. Wild-type mice display motor decline in rotarod and open field with age.

Behaviour comparison between 2-, 9-, 16-month in **A**) rotarod **B**) and open field. All statistical analyses

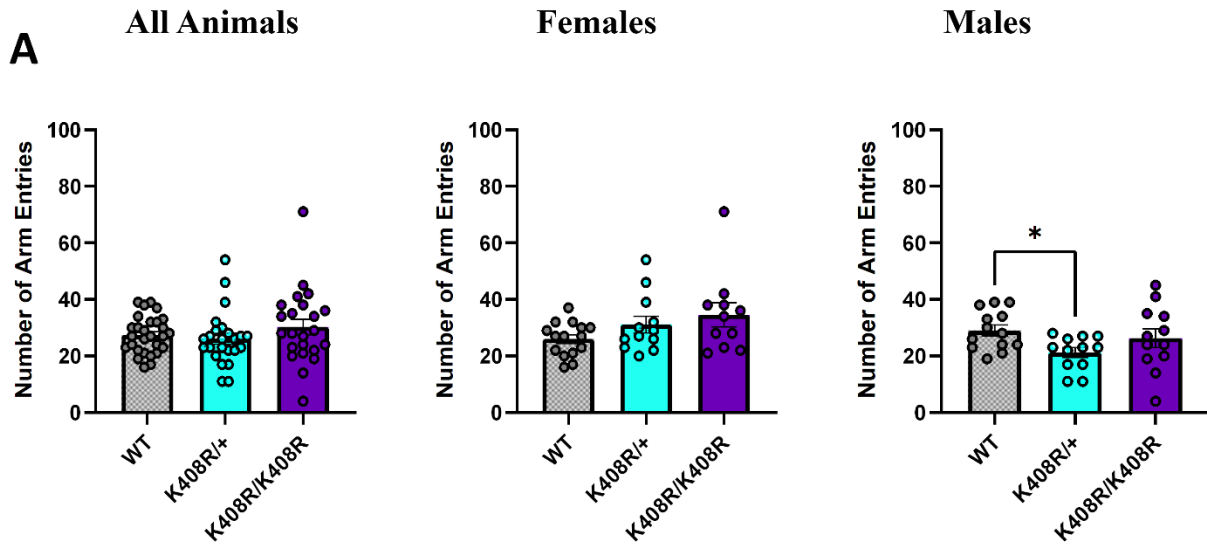
are via Two-Way ANOVA with Tukey's post-hoc test. Mean +/- SEM is shown. (* $P < 0.05$, ** $P < 0.01$)

*** $P < 0.001$, **** $P < 0.0001$). Green asterisks denote comparisons between 2- and 18-months. Blue

asterisks denote comparisons between 2- and 9-months. Red asterisks denote comparisons between 9- and

16-months.

Tdp-43^{+/+} *Tdp-43*^{K408R/+} *Tdp-43*^{K408R/K408R}



Supplementary Figure 2. Number of arm entries during Y-maze test at 16-months. A) Number of arm entries for all animals, females, or males only during the Y-maze test at 16-months of age. All statistical analyses are via Brown-Forsythe and Welch One-Way ANOVA with Dunnett's post-hoc test. Mean +/- SEM is shown. Each dot represents one animal. (*P<0.05).

6. References

1. Tiryaki E, Horak HA. ALS and Other Motor Neuron Diseases. *Contin Lifelong Learn Neurol*. 2014;20(5):1185. doi:10.1212/01.CON.0000455886.14298.a4
2. Longinetti E, Fang F. Epidemiology of amyotrophic lateral sclerosis: an update of recent literature. *Curr Opin Neurol*. 2019;32(5):771. doi:10.1097/WCO.0000000000000730
3. Ryan M, Heverin M, McLaughlin RL, Hardiman O. Lifetime Risk and Heritability of Amyotrophic Lateral Sclerosis. *JAMA Neurol*. 2019;76(11):1367-1374. doi:10.1001/jamaneurol.2019.2044
4. Rowland LP, Shneider NA. Amyotrophic lateral sclerosis. *N Engl J Med*. 2001;344(22):1688-1700. doi:10.1056/NEJM200105313442207
5. Rojas P, Ramírez AI, Fernández-Albarral JA, et al. Amyotrophic Lateral Sclerosis: A Neurodegenerative Motor Neuron Disease With Ocular Involvement. *Front Neurosci*. 2020;14. Accessed November 7, 2023. <https://www.frontiersin.org/articles/10.3389/fnins.2020.566858>
6. Talbott EO, Malek AM, Lacomis D. The epidemiology of amyotrophic lateral sclerosis. *Handb Clin Neurol*. 2016;138:225-238. doi:10.1016/B978-0-12-802973-2.00013-6
7. Xu L, Liu T, Liu L, et al. Global variation in prevalence and incidence of amyotrophic lateral sclerosis: a systematic review and meta-analysis. *J Neurol*. 2020;267(4):944-953. doi:10.1007/s00415-019-09652-y
8. Wolfson C, Gauvin DE, Ishola F, Oskoui M. Global Prevalence and Incidence of Amyotrophic Lateral Sclerosis: A Systematic Review. *Neurology*. 2023;101(6):e613-e623. doi:10.1212/WNL.0000000000207474
9. Niccoli T, Partridge L, Isaacs AM. Ageing as a risk factor for ALS/FTD. *Hum Mol Genet*. 2017;26(R2):R105-R113. doi:10.1093/hmg/ddx247
10. Manjaly ZR, Scott KM, Abhinav K, et al. The sex ratio in amyotrophic lateral sclerosis: A population based study. *Amyotroph Lateral Scler Off Publ World Fed Neurol Res Group Mot Neuron Dis*. 2010;11(5):439-442. doi:10.3109/17482961003610853
11. Grad LI, Rouleau GA, Ravits J, Cashman NR. Clinical Spectrum of Amyotrophic Lateral Sclerosis (ALS). *Cold Spring Harb Perspect Med*. 2017;7(8):a024117. doi:10.1101/cshperspect.a024117
12. Zakharova MN, Abramova AA. Lower and upper motor neuron involvement and their impact on disease prognosis in amyotrophic lateral sclerosis. *Neural Regen Res*. 2021;17(1):65-73. doi:10.4103/1673-5374.314289
13. Niedermeyer S, Murn M, Choi PJ. Respiratory Failure in Amyotrophic Lateral Sclerosis. *Chest*. 2019;155(2):401-408. doi:10.1016/j.chest.2018.06.035
14. Masrori P, Van Damme P. Amyotrophic lateral sclerosis: a clinical review. *Eur J Neurol*. 2020;27(10):1918-1929. doi:10.1111/ene.14393

15. Zarei S, Carr K, Reiley L, et al. A comprehensive review of amyotrophic lateral sclerosis. *Surg Neurol Int.* 2015;6:171. doi:10.4103/2152-7806.169561
16. Suzuki Y ichi, Shibuya K, Misawa S, et al. Fasciculation intensity and limb dominance in amyotrophic lateral sclerosis: a muscle ultrasonographic study. *BMC Neurol.* 2022;22(1):85. doi:10.1186/s12883-022-02617-1
17. Shellikeri S, Karthikeyan V, Martino R, et al. The Neuropathological Signature of Bulbar-onset ALS: A Systematic Review. *Neurosci Biobehav Rev.* 2017;75:378-392. doi:10.1016/j.neubiorev.2017.01.045
18. ALS with respiratory onset: Clinical features and effects of non-invasive ventilation on the prognosis. *Amyotroph Lateral Scler.* 2010;11(4):379-382. doi:10.3109/17482960903426543
19. Shoesmith CL, Findlater K, Rowe A, Strong MJ. Prognosis of amyotrophic lateral sclerosis with respiratory onset. *J Neurol Neurosurg Psychiatry.* 2007;78(6):629-631. doi:10.1136/jnnp.2006.103564
20. Hardiman O, Al-Chalabi A, Chio A, et al. Amyotrophic lateral sclerosis. *Nat Rev Dis Primer.* 2017;3:17071. doi:10.1038/nrdp.2017.71
21. Phukan J, Elamin M, Bede P, et al. The syndrome of cognitive impairment in amyotrophic lateral sclerosis: a population-based study. *J Neurol Neurosurg Psychiatry.* 2012;83(1):102-108. doi:10.1136/jnnp-2011-300188
22. Tsermentseli S, Leigh PN, Goldstein LH. The anatomy of cognitive impairment in amyotrophic lateral sclerosis: more than frontal lobe dysfunction. *Cortex J Devoted Study Nerv Syst Behav.* 2012;48(2):166-182. doi:10.1016/j.cortex.2011.02.004
23. Chiò A, Moglia C, Canosa A, et al. Cognitive impairment across ALS clinical stages in a population-based cohort. *Neurology.* 2019;93(10):e984-e994. doi:10.1212/WNL.0000000000008063
24. Crockford C, Newton J, Lonergan K, et al. ALS-specific cognitive and behavior changes associated with advancing disease stage in ALS. *Neurology.* 2018;91(15):e1370-e1380. doi:10.1212/WNL.0000000000006317
25. Rusina R, Vandenberghe R, Bruffaerts R. Cognitive and Behavioral Manifestations in ALS: Beyond Motor System Involvement. *Diagnostics.* 2021;11(4):624. doi:10.3390/diagnostics11040624
26. Chiò A, Moglia C, Canosa A, et al. Cognitive impairment across ALS clinical stages in a population-based cohort. *Neurology.* 2019;93(10):e984-e994. doi:10.1212/WNL.0000000000008063
27. Hardiman O, van den Berg LH, Kiernan MC. Clinical diagnosis and management of amyotrophic lateral sclerosis. *Nat Rev Neurol.* 2011;7(11):639-649. doi:10.1038/nrneurol.2011.153
28. Mead RJ, Shan N, Reiser HJ, Marshall F, Shaw PJ. Amyotrophic lateral sclerosis: a neurodegenerative disorder poised for successful therapeutic translation. *Nat Rev Drug Discov.* 2023;22(3):185-212. doi:10.1038/s41573-022-00612-2

29. Štětkářová I, Ehler E. Diagnostics of Amyotrophic Lateral Sclerosis: Up to Date. *Diagnostics*. 2021;11(2):231. doi:10.3390/diagnostics11020231
30. Yedavalli VS, Patil A, Shah P. Amyotrophic Lateral Sclerosis and its Mimics/Variants: A Comprehensive Review. *J Clin Imaging Sci*. 2018;8:53. doi:10.4103/jcis.JCIS_40_18
31. Williams JR, Fitzhenry D, Grant L, Martyn D, Kerr DA. Diagnosis pathway for patients with amyotrophic lateral sclerosis: retrospective analysis of the US Medicare longitudinal claims database. *BMC Neurol*. 2013;13(1):160. doi:10.1186/1471-2377-13-160
32. Wijesekera LC, Nigel Leigh P. Amyotrophic lateral sclerosis. *Orphanet J Rare Dis*. 2009;4(1):3. doi:10.1186/1750-1172-4-3
33. Srinivasan J, Scala S, Jones HR, Saleh F, Russell JA. Inappropriate surgeries resulting from misdiagnosis of early amyotrophic lateral sclerosis. *Muscle Nerve*. 2006;34(3):359-360. doi:10.1002/mus.20555
34. Kraemer M, Buerger M, Berlit P. Diagnostic problems and delay of diagnosis in amyotrophic lateral sclerosis. *Clin Neurol Neurosurg*. 2010;112(2):103-105. doi:10.1016/j.clineuro.2009.10.014
35. Richards D, Morren JA, Piro EP. Time to diagnosis and factors affecting diagnostic delay in amyotrophic lateral sclerosis. *J Neurol Sci*. 2020;417. doi:10.1016/j.jns.2020.117054
36. Diagnostic delay in amyotrophic lateral sclerosis - Gwathmey - 2023 - European Journal of Neurology - Wiley Online Library. Accessed November 16, 2023. <https://onlinelibrary-wiley-com.proxy.bib.uottawa.ca/doi/10.1111/ene.15874?af=R>
37. Brooks BR. El Escorial World Federation of Neurology criteria for the diagnosis of amyotrophic lateral sclerosis. Subcommittee on Motor Neuron Diseases/Amyotrophic Lateral Sclerosis of the World Federation of Neurology Research Group on Neuromuscular Diseases and the El Escorial "Clinical limits of amyotrophic lateral sclerosis" workshop contributors. *J Neurol Sci*. 1994;124 Suppl:96-107. doi:10.1016/0022-510x(94)90191-0
38. Belsh JM. ALS diagnostic criteria of El Escorial Revisited: do they meet the needs of clinicians as well as researchers? *Amyotroph Lateral Scler Mot Neuron Disord Off Publ World Fed Neurol Res Group Mot Neuron Dis*. 2000;1 Suppl 1:S57-60. doi:10.1080/14660820052415925
39. Costa J, Swash M, de Carvalho M. Awaji criteria for the diagnosis of amyotrophic lateral sclerosis: a systematic review. *Arch Neurol*. 2012;69(11):1410-1416. doi:10.1001/archneurol.2012.254
40. Li DW, Liu M, Cui B, et al. The Awaji criteria increases the diagnostic sensitivity of the revised El Escorial criteria for amyotrophic lateral sclerosis diagnosis in a Chinese population. *PLoS ONE*. 2017;12(3):e0171522. doi:10.1371/journal.pone.0171522
41. Pugdahl K, Camdessanché JP, Cengiz B, et al. Gold Coast diagnostic criteria increase sensitivity in amyotrophic lateral sclerosis. *Clin Neurophysiol*. 2021;132(12):3183-3189. doi:10.1016/j.clinph.2021.08.014

42. Shen D, Yang X, Wang Y, et al. The Gold Coast criteria increases the diagnostic sensitivity for amyotrophic lateral sclerosis in a Chinese population. *Transl Neurodegener.* 2021;10(1):28. doi:10.1186/s40035-021-00253-2
43. Goutman SA, Hardiman O, Al-Chalabi A, et al. Recent advances in the diagnosis and prognosis of ALS. *Lancet Neurol.* 2022;21(5):480-493. doi:10.1016/S1474-4422(21)00465-8
44. Maier A, Boentert M, Reilich P, et al. ALSFRS-R-SE: an adapted, annotated, and self-explanatory version of the revised amyotrophic lateral sclerosis functional rating scale. *Neurol Res Pract.* 2022;4:60. doi:10.1186/s42466-022-00224-6
45. Cedarbaum JM, Stambler N, Malta E, et al. The ALSFRS-R: a revised ALS functional rating scale that incorporates assessments of respiratory function. BDNF ALS Study Group (Phase III). *J Neurol Sci.* 1999;169(1-2):13-21. doi:10.1016/s0022-510x(99)00210-5
46. Fournier CN. Considerations for Amyotrophic Lateral Sclerosis (ALS) Clinical Trial Design. *Neurotherapeutics.* 2022;19(4):1180-1192. doi:10.1007/s13311-022-01271-2
47. Kiernan MC, Vucic S, Talbot K, et al. Improving clinical trial outcomes in amyotrophic lateral sclerosis. *Nat Rev Neurol.* 2021;17(2):104-118. doi:10.1038/s41582-020-00434-z
48. Corcia P, Beltran S, Lautrette G, Bakkouche S, Couratier P. Staging amyotrophic lateral sclerosis: A new focus on progression. *Rev Neurol (Paris).* 2019;175(5):277-282. doi:10.1016/j.neurol.2018.09.017
49. Fang T, Al Khleifat A, Stahl DR, et al. Comparison of the King's and MiToS staging systems for ALS. *Amyotroph Lateral Scler Front Degener.* 2017;18(3-4):227-232. doi:10.1080/21678421.2016.1265565
50. Johnson SA, Fang T, De Marchi F, et al. Pharmacotherapy for Amyotrophic Lateral Sclerosis: A Review of Approved and Upcoming Agents. *Drugs.* 2022;82(13):1367-1388. doi:10.1007/s40265-022-01769-1
51. Shoesmith C, Abrahao A, Benstead T, et al. Canadian best practice recommendations for the management of amyotrophic lateral sclerosis. *CMAJ Can Med Assoc J.* 2020;192(46):E1453-E1468. doi:10.1503/cmaj.191721
52. Miller RG, Mitchell JD, Moore DH. Riluzole for amyotrophic lateral sclerosis (ALS)/motor neuron disease (MND). *Cochrane Database Syst Rev.* 2012;2012(3):CD001447. doi:10.1002/14651858.CD001447.pub3
53. Hinchcliffe M, Smith A. Riluzole: real-world evidence supports significant extension of median survival times in patients with amyotrophic lateral sclerosis. *Degener Neurol Neuromuscul Dis.* 2017;7:61-70. doi:10.2147/DNND.S135748
54. <https://fyr.io>. Utilizing Real-World Data to Examine Outcomes in Patients With Amyotrophic Lateral Sclerosis. Practical Neurology. Accessed December 15, 2023. <https://practicalneurology.com/articles/2021-nov-dec/utilizing-real-world-data-to-examine-outcomes-in-patients-with-amyotrophic-lateral-sclerosis>

55. Nourelden AZ, Kamal I, Hagrass AI, et al. Safety and efficacy of edaravone in patients with amyotrophic lateral sclerosis: a systematic review and meta-analysis. *Neurol Sci.* 2023;44(10):3429-3442. doi:10.1007/s10072-023-06869-8
56. Sawada H. Clinical efficacy of edaravone for the treatment of amyotrophic lateral sclerosis. *Expert Opin Pharmacother.* 2017;18(7):735-738. doi:10.1080/14656566.2017.1319937
57. Cerillo JL, Parmar M. Tofersen. In: *StatPearls*. StatPearls Publishing; 2023. Accessed December 19, 2023. <http://www.ncbi.nlm.nih.gov/books/NBK594270/>
58. Hogden A, Foley G, Henderson RD, James N, Aoun SM. Amyotrophic lateral sclerosis: improving care with a multidisciplinary approach. *J Multidiscip Healthc.* 2017;10:205-215. doi:10.2147/JMDH.S134992
59. Tzeplaeff L, Wilfling S, Requardt MV, Herdick M. Current State and Future Directions in the Therapy of ALS. *Cells.* 2023;12(11):1523. doi:10.3390/cells12111523
60. Tsitkanou S, Della Gatta P, Foletta V, Russell A. The Role of Exercise as a Non-pharmacological Therapeutic Approach for Amyotrophic Lateral Sclerosis: Beneficial or Detrimental? *Front Neurol.* 2019;10:783. doi:10.3389/fneur.2019.00783
61. Muscaritoli M, Kushta I, Molfino A, Inghilleri M, Sabatelli M, Rossi Fanelli F. Nutritional and metabolic support in patients with amyotrophic lateral sclerosis. *Nutr Burbank Los Angel Cty Calif.* 2012;28(10):959-966. doi:10.1016/j.nut.2012.01.011
62. Gastrostomy in patients with amyotrophic lateral sclerosis (ProGas): a prospective cohort study. *Lancet Neurol.* 2015;14(7):702-709. doi:10.1016/S1474-4422(15)00104-0
63. Rimmer KP, Kaminska M, Nonoyama M, et al. Home mechanical ventilation for patients with Amyotrophic Lateral Sclerosis: A Canadian Thoracic Society clinical practice guideline. *Can J Respir Crit Care Sleep Med.* 2019;3(1):9-27. doi:10.1080/24745332.2018.1559644
64. Fahrner-Scott K, Zapata C, O'Riordan DL, et al. Embedded Palliative Care for Amyotrophic Lateral Sclerosis. *Neurol Clin Pract.* 2022;12(1):68-75. doi:10.1212/CPJ.0000000000001124
65. Zwicker J, Smith IC, Rice J, et al. Palliative care at any stage of amyotrophic lateral sclerosis: a prospective feasibility study. *Front Med.* 2023;10. Accessed December 18, 2023. <https://www.frontiersin.org/articles/10.3389/fmed.2023.1204816>
66. Oskarsson B, Horton DK, Mitsumoto H. Potential Environmental Factors in Amyotrophic Lateral Sclerosis. *Neurol Clin.* 2015;33(4):877-888. doi:10.1016/j.ncl.2015.07.009
67. Prasad A, Bharathi V, Sivalingam V, Girdhar A, Patel BK. Molecular Mechanisms of TDP-43 Misfolding and Pathology in Amyotrophic Lateral Sclerosis. *Front Mol Neurosci.* 2019;12. Accessed November 28, 2023. <https://www.frontiersin.org/articles/10.3389/fnmol.2019.00025>
68. Sreedharan J, Blair IP, Tripathi VB, et al. TDP-43 mutations in familial and sporadic amyotrophic lateral sclerosis. *Science.* 2008;319(5870):1668-1672. doi:10.1126/science.1154584

69. 17. Chiò A, Battistini S, Calvo A, et al. Genetic counselling in ALS: facts, uncertainties and clinical suggestions. *J Neurol Neurosurg Psychiatry*. 2014;85(5):478-485. doi:10.1136/jnnp-2013-305546 - Google Search. Accessed December 15, 2023. [https://www.google.com/search?q=17.+Chi%C3%B2+A%2C+Battistini+S%2C+Calvo+A%2C+et+al.+Genetic+counselling+in+ALS%3A+facts%2C+uncertainties+and+clinical+suggestions.+J+Neurol+Neurosurg+Psychiatry.+2014%3B85\(5\)%3A478-485.+doi%3A10.1136%2Fjnnp-2013-305546&oq=17.%09Chi%C3%B2+A%2C+Battistini+S%2C+Calvo+A%2C+et+al.+Genetic+counselling+in+ALS%3A+facts%2C+uncertainties+and+clinical+suggestions.+J+Neurol+Neurosurg+Psychiatry.+2014%3B85\(5\)%3A478-485.+doi%3A10.1136%2Fjnnp-2013-305546&gs_lcrp=EgZjaHJvbWUyBggAEEUYOdIBBzIzMGowajSoAgCwAgA&sourceid=chrome&ie=UTF-8](https://www.google.com/search?q=17.+Chi%C3%B2+A%2C+Battistini+S%2C+Calvo+A%2C+et+al.+Genetic+counselling+in+ALS%3A+facts%2C+uncertainties+and+clinical+suggestions.+J+Neurol+Neurosurg+Psychiatry.+2014%3B85(5)%3A478-485.+doi%3A10.1136%2Fjnnp-2013-305546&oq=17.%09Chi%C3%B2+A%2C+Battistini+S%2C+Calvo+A%2C+et+al.+Genetic+counselling+in+ALS%3A+facts%2C+uncertainties+and+clinical+suggestions.+J+Neurol+Neurosurg+Psychiatry.+2014%3B85(5)%3A478-485.+doi%3A10.1136%2Fjnnp-2013-305546&gs_lcrp=EgZjaHJvbWUyBggAEEUYOdIBBzIzMGowajSoAgCwAgA&sourceid=chrome&ie=UTF-8)
70. Abramzon YA, Fratta P, Traynor BJ, Chia R. The Overlapping Genetics of Amyotrophic Lateral Sclerosis and Frontotemporal Dementia. *Front Neurosci*. 2020;14. Accessed April 1, 2023. <https://www.frontiersin.org/articles/10.3389/fnins.2020.00042>
71. Scotter EL, Chen HJ, Shaw CE. TDP-43 Proteinopathy and ALS: Insights into Disease Mechanisms and Therapeutic Targets. *Neurother J Am Soc Exp Neurother*. 2015;12(2):352-363. doi:10.1007/s13311-015-0338-x
72. Kabashi E, Valdmanis PN, Dion P, et al. TARDBP mutations in individuals with sporadic and familial amyotrophic lateral sclerosis. *Nat Genet*. 2008;40(5):572-574. doi:10.1038/ng.132
73. Van Deerlin VM, Leverenz JB, Bekris LM, et al. TARDBP mutations in amyotrophic lateral sclerosis with TDP-43 neuropathology: a genetic and histopathological analysis. *Lancet Neurol*. 2008;7(5):409-416. doi:10.1016/S1474-4422(08)70071-1
74. Arai T, Hasegawa M, Akiyama H, et al. TDP-43 is a component of ubiquitin-positive tau-negative inclusions in frontotemporal lobar degeneration and amyotrophic lateral sclerosis. *Biochem Biophys Res Commun*. 2006;351(3):602-611. doi:10.1016/j.bbrc.2006.10.093
75. Neumann M, Sampathu DM, Kwong LK, et al. Ubiquitinated TDP-43 in frontotemporal lobar degeneration and amyotrophic lateral sclerosis. *Science*. 2006;314(5796):130-133. doi:10.1126/science.1134108
76. Onyike CU, Diehl-Schmid J. The Epidemiology of Frontotemporal Dementia. *Int Rev Psychiatry Abingdon Engl*. 2013;25(2):130-137. doi:10.3109/09540261.2013.776523
77. Leroy M, Bertoux M, Skrobala E, et al. Characteristics and progression of patients with frontotemporal dementia in a regional memory clinic network. *Alzheimers Res Ther*. 2021;13(1):19. doi:10.1186/s13195-020-00753-9
78. Weder ND, Aziz R, Wilkins K, Tampi RR. Frontotemporal Dementias: A Review. *Ann Gen Psychiatry*. 2007;6(1):15. doi:10.1186/1744-859X-6-15
79. Llorca-Bofí V, Illán-Gala I, González RB. Sex-related differences in the clinical diagnosis of frontotemporal dementia. Published online September 11, 2019:19005702. doi:10.1101/19005702

80. Finger EC. Frontotemporal Dementias. *Contin Lifelong Learn Neurol*. 2016;22(2 Dementia):464-489. doi:10.1212/CON.0000000000000300
81. Leyton CE, Hodges JR. Frontotemporal dementias: Recent advances and current controversies. *Ann Indian Acad Neurol*. 2010;13(Suppl2):S74-S80. doi:10.4103/0972-2327.74249
82. van Engelen MPE, Gossink FT, de Vijlder LS, et al. End Stage Clinical Features and Cause of Death of Behavioral Variant Frontotemporal Dementia and Young-Onset Alzheimer's Disease. *J Alzheimers Dis*. 77(3):1169-1180. doi:10.3233/JAD-200337
83. Bahia VS, Takada LT, Deramecourt V. Neuropathology of frontotemporal lobar degeneration: a review. *Dement Neuropsychol*. 2013;7(1):19-26. doi:10.1590/S1980-57642013DN70100004
84. Young JJ, Lavakumar M, Tampi D, Balachandran S, Tampi RR. Frontotemporal dementia: latest evidence and clinical implications. *Ther Adv Psychopharmacol*. 2018;8(1):33-48. doi:10.1177/2045125317739818
85. Sensitivity of revised diagnostic criteria for the behavioural variant of frontotemporal dementia - PMC. Accessed December 15, 2023. <https://www.ncbi.nlm.nih.gov.proxy.bib.uottawa.ca/pmc/articles/PMC3170532/>
86. Ghosh S, Lippa CF. Clinical Subtypes of Frontotemporal Dementia. *Am J Alzheimers Dis Dementias*®. 2015;30(7):653-661. doi:10.1177/1533317513494442
87. Peet BT, Spina S, Mundada N, La Joie R. Neuroimaging in Frontotemporal Dementia: Heterogeneity and Relationships with Underlying Neuropathology. *Neurotherapeutics*. 2021;18(2):728-752. doi:10.1007/s13311-021-01101-x
88. Whitwell JL. Neuroimaging across the FTD spectrum. *Prog Mol Biol Transl Sci*. 2019;165:187-223. doi:10.1016/bs.pmbts.2019.05.009
89. Bahia VS, Takada LT, Deramecourt V. Neuropathology of frontotemporal lobar degeneration: a review. *Dement Neuropsychol*. 2013;7(1):19-26. doi:10.1590/S1980-57642013DN70100004
90. Josephs KA, Whitwell JL, Parisi JE, et al. Caudate atrophy on MRI is a characteristic feature of FTLD-FUS. *Eur J Neurol*. 2010;17(7):969-975. doi:10.1111/j.1468-1331.2010.02975.x
91. Mackenzie IRA, Neumann M. Molecular neuropathology of frontotemporal dementia: insights into disease mechanisms from postmortem studies. *J Neurochem*. 2016;138(S1):54-70. doi:10.1111/jnc.13588
92. Neumann M, Rademakers R, Roeber S, Baker M, Kretschmar HA, Mackenzie IRA. A new subtype of frontotemporal lobar degeneration with FUS pathology. *Brain*. 2009;132(11):2922-2931. doi:10.1093/brain/awp214
93. Rademakers R, Neumann M, Mackenzie IRA. Recent advances in the molecular basis of frontotemporal dementia. *Nat Rev Neurol*. 2012;8(8):423-434. doi:10.1038/nrneurol.2012.117

94. Gowell M, Baker I, Ansorge O, Husain M. Young-onset frontotemporal dementia with FUS pathology. *Pract Neurol*. 2021;21(2):149-152. doi:10.1136/practneurol-2020-002730
95. Tan RH, Kril JJ, Fatima M, et al. TDP-43 proteinopathies: pathological identification of brain regions differentiating clinical phenotypes. *Brain*. 2015;138(10):3110-3122. doi:10.1093/brain/awv220
96. Neumann M, Lee EB, Mackenzie IR. FTLD-TDP pathological subtypes: clinical and mechanistic significance. *Adv Exp Med Biol*. 2021;1281:201-217. doi:10.1007/978-3-030-51140-1_13
97. Stecker M. A Perspective: Challenges in Dementia Research. *Med Kaunas Lith*. 2022;58(10):1368. doi:10.3390/medicina58101368
98. Tsai RM, Boxer AL. Treatment of Frontotemporal Dementia. *Curr Treat Options Neurol*. 2014;16(11):319. doi:10.1007/s11940-014-0319-0
99. Bott NT, Radke A, Stephens ML, Kramer JH. Frontotemporal dementia: diagnosis, deficits and management. *Neurodegener Dis Manag*. 2014;4(6):439-454. doi:10.2217/nmt.14.34
100. Barton C, Ketelle R, Merrilees J, Miller B. Non-pharmacological Management of Behavioral Symptoms in Frontotemporal and Other Dementias. *FOCUS*. 2016;14(4):492-498. doi:10.1176/appi.focus.140406
101. Strong MJ, Abrahams S, Goldstein LH, et al. Amyotrophic lateral sclerosis - frontotemporal spectrum disorder (ALS-FTSD): Revised diagnostic criteria. *Amyotroph Lateral Scler Front Degener*. 2017;18(3-4):153-174. doi:10.1080/21678421.2016.1267768
102. Sha SJ, Takada LT, Rankin KP, et al. Frontotemporal dementia due to C9ORF72 mutations. *Neurology*. 2012;79(10):1002-1011. doi:10.1212/WNL.0b013e318268452e
103. Turner MR, Kiernan MC, Leigh PN, Talbot K. Biomarkers in amyotrophic lateral sclerosis. *Lancet Neurol*. 2009;8(1):94-109. doi:10.1016/S1474-4422(08)70293-X
104. Verde F, Otto M, Silani V. Neurofilament Light Chain as Biomarker for Amyotrophic Lateral Sclerosis and Frontotemporal Dementia. *Front Neurosci*. 2021;15. Accessed December 18, 2023. <https://www.frontiersin.org/articles/10.3389/fnins.2021.679199>
105. Yuan A, Nixon RA. Neurofilament Proteins as Biomarkers to Monitor Neurological Diseases and the Efficacy of Therapies. *Front Neurosci*. 2021;15:689938. doi:10.3389/fnins.2021.689938
106. Xu Z, Henderson RD, David M, McCombe PA. Neurofilaments as Biomarkers for Amyotrophic Lateral Sclerosis: A Systematic Review and Meta-Analysis. *PLoS ONE*. 2016;11(10):e0164625. doi:10.1371/journal.pone.0164625
107. Feneberg E, Oeckl P, Steinacker P, et al. Multicenter evaluation of neurofilaments in early symptom onset amyotrophic lateral sclerosis. *Neurology*. 2018;90(1):e22-e30. doi:10.1212/WNL.0000000000004761
108. Behzadi A, Pujol-Calderón F, Tjust AE, et al. Neurofilaments can differentiate ALS subgroups and ALS from common diagnostic mimics. *Sci Rep*. 2021;11:22128. doi:10.1038/s41598-021-01499-6

109. Lee EH, Kwon HS, Koh SH, et al. Serum neurofilament light chain level as a predictor of cognitive stage transition. *Alzheimers Res Ther.* 2022;14(1):6. doi:10.1186/s13195-021-00953-x
110. Benatar M, Wu J, Andersen PM, Lombardi V, Malaspina A. Neurofilament light: A candidate biomarker of presymptomatic amyotrophic lateral sclerosis and phenoconversion. *Ann Neurol.* 2018;84(1):130-139. doi:10.1002/ana.25276
111. Mizuno Y, Amari M, Takatama M, Aizawa H, Mihara B, Okamoto K. Immunoreactivities of p62, an ubiquitin-binding protein, in the spinal anterior horn cells of patients with amyotrophic lateral sclerosis. *J Neurol Sci.* 2006;249(1):13-18. doi:10.1016/j.jns.2006.05.060
112. Arai T, Nonaka T, Hasegawa M, et al. Neuronal and glial inclusions in frontotemporal dementia with or without motor neuron disease are immunopositive for p62. *Neurosci Lett.* 2003;342(1-2):41-44. doi:10.1016/s0304-3940(03)00216-7
113. Cohen TJ, Lee VMY, Trojanowski JQ. TDP-43 functions and pathogenic mechanisms implicated in TDP-43 proteinopathies. *Trends Mol Med.* 2011;17(11):659-667. doi:10.1016/j.molmed.2011.06.004
114. François-Moutal L, Perez-Miller S, Scott DD, Miranda VG, Mollasalehi N, Khanna M. Structural Insights Into TDP-43 and Effects of Post-translational Modifications. *Front Mol Neurosci.* 2019;12. Accessed April 1, 2023. <https://www.frontiersin.org/articles/10.3389/fnmol.2019.00301>
115. Purice MD, Taylor JP. Linking hnRNP Function to ALS and FTD Pathology. *Front Neurosci.* 2018;12:326. doi:10.3389/fnins.2018.00326
116. Sephton CF, Good SK, Atkin S, et al. TDP-43 Is a Developmentally Regulated Protein Essential for Early Embryonic Development. *J Biol Chem.* 2010;285(9):6826-6834. doi:10.1074/jbc.M109.061846
117. Kuo PH, Doudeva LG, Wang YT, Shen CKJ, Yuan HS. Structural insights into TDP-43 in nucleic-acid binding and domain interactions. *Nucleic Acids Res.* 2009;37(6):1799-1808. doi:10.1093/nar/gkp013
118. Conicella AE, Zerze GH, Mittal J, Fawzi NL. ALS Mutations Disrupt Phase Separation Mediated by α -Helical Structure in the TDP-43 Low-Complexity C-Terminal Domain. *Struct Lond Engl 1993.* 2016;24(9):1537-1549. doi:10.1016/j.str.2016.07.007
119. Duan L, Zaepfel BL, Aksenova V, et al. Nuclear RNA binding regulates TDP-43 nuclear localization and passive nuclear export. *Cell Rep.* 2022;40(3):111106. doi:10.1016/j.celrep.2022.111106
120. Berning BA, Walker AK. The Pathobiology of TDP-43 C-Terminal Fragments in ALS and FTL. *Front Neurosci.* 2019;13. Accessed December 18, 2023. <https://www.frontiersin.org/articles/10.3389/fnins.2019.00335>
121. Jo M, Lee S, Jeon YM, Kim S, Kwon Y, Kim HJ. The role of TDP-43 propagation in neurodegenerative diseases: integrating insights from clinical and experimental studies. *Exp Mol Med.* 2020;52(10):1652-1662. doi:10.1038/s12276-020-00513-7
122. Ling SC, Polymenidou M, Cleveland DW. Converging mechanisms in ALS and FTD: Disrupted RNA and protein homeostasis. *Neuron.* 2013;79(3):416-438. doi:10.1016/j.neuron.2013.07.033

123. Frontiers | Failure to Deliver and Translate—New Insights into RNA Dysregulation in ALS. Accessed December 18, 2023. <https://www.frontiersin.org/articles/10.3389/fncel.2017.00243/full>
124. Ayala YM, De Conti L, Avendaño-Vázquez SE, et al. TDP-43 regulates its mRNA levels through a negative feedback loop. *EMBO J.* 2011;30(2):277-288. doi:10.1038/emboj.2010.310
125. Polymenidou M, Lagier-Tourenne C, Hutt KR, et al. Long pre-mRNA depletion and RNA missplicing contribute to neuronal vulnerability from loss of TDP-43. *Nat Neurosci.* 2011;14(4):459-468. doi:10.1038/nn.2779
126. Khalfallah Y, Kuta R, Grasmuck C, Prat A, Durham HD, Vande Velde C. TDP-43 regulation of stress granule dynamics in neurodegenerative disease-relevant cell types. *Sci Rep.* 2018;8(1):7551. doi:10.1038/s41598-018-25767-0
127. Wolozin B, Ivanov P. Stress granules and neurodegeneration. *Nat Rev Neurosci.* 2019;20(11):649-666. doi:10.1038/s41583-019-0222-5
128. Wolozin B. Regulated protein aggregation: stress granules and neurodegeneration. *Mol Neurodegener.* 2012;7(1):56. doi:10.1186/1750-1326-7-56
129. Marcelo A, Koppenol R, de Almeida LP, Matos CA, Nóbrega C. Stress granules, RNA-binding proteins and polyglutamine diseases: too much aggregation? *Cell Death Dis.* 2021;12(6):1-17. doi:10.1038/s41419-021-03873-8
130. Campos-Melo D, Hawley ZCE, Droppelmann CA, Strong MJ. The Integral Role of RNA in Stress Granule Formation and Function. *Front Cell Dev Biol.* 2021;9:621779. doi:10.3389/fcell.2021.621779
131. Dewey CM, Cenik B, Sephton CF, et al. TDP-43 is directed to stress granules by sorbitol, a novel physiological osmotic and oxidative stressor. *Mol Cell Biol.* 2011;31(5):1098-1108. doi:10.1128/MCB.01279-10
132. Colombrita C, Zennaro E, Fallini C, et al. TDP-43 is recruited to stress granules in conditions of oxidative insult. *J Neurochem.* 2009;111(4):1051-1061. doi:10.1111/j.1471-4159.2009.06383.x
133. McDonald KK, Aulas A, Destroismaisons L, et al. TAR DNA-binding protein 43 (TDP-43) regulates stress granule dynamics via differential regulation of G3BP and TIA-1. *Hum Mol Genet.* 2011;20(7):1400-1410. doi:10.1093/hmg/ddr021
134. Orrù S, Coni P, Floris A, et al. Reduced stress granule formation and cell death in fibroblasts with the A382T mutation of TARDBP gene: evidence for loss of TDP-43 nuclear function. *Hum Mol Genet.* 2016;25(20):4473-4483. doi:10.1093/hmg/ddw276
135. Dewey CM, Cenik B, Sephton CF, Johnson BA, Herz J, Yu G. TDP-43 Aggregation In Neurodegeneration: Are Stress Granules The Key? *Brain Res.* 2012;1462:16-25. doi:10.1016/j.brainres.2012.02.032
136. Dudman J, Qi X. Stress Granule Dysregulation in Amyotrophic Lateral Sclerosis. *Front Cell Neurosci.* 2020;14. Accessed December 18, 2023. <https://www.frontiersin.org/articles/10.3389/fncel.2020.598517>

137. Fernandes N, Nero L, Lyons SM, et al. Stress Granule Assembly Can Facilitate but Is Not Required for TDP-43 Cytoplasmic Aggregation. *Biomolecules*. 2020;10(10):1367. doi:10.3390/biom10101367
138. Zhang T, Hwang HY, Hao H, Talbot C, Wang J. Caenorhabditis elegans RNA-processing protein TDP-1 regulates protein homeostasis and life span. *J Biol Chem*. 2012;287(11):8371-8382. doi:10.1074/jbc.M111.311977
139. Diaper DC, Adachi Y, Sutcliffe B, et al. Loss and gain of Drosophila TDP-43 impair synaptic efficacy and motor control leading to age-related neurodegeneration by loss-of-function phenotypes. *Hum Mol Genet*. 2013;22(8):1539-1557. doi:10.1093/hmg/ddt005
140. Schmid B, Hruscha A, Hogl S, et al. Loss of ALS-associated TDP-43 in zebrafish causes muscle degeneration, vascular dysfunction, and reduced motor neuron axon outgrowth. *Proc Natl Acad Sci U S A*. 2013;110(13):4986-4991. doi:10.1073/pnas.1218311110
141. Wu LS, Cheng WC, Shen CKJ. Targeted Depletion of TDP-43 Expression in the Spinal Cord Motor Neurons Leads to the Development of Amyotrophic Lateral Sclerosis-like Phenotypes in Mice. *J Biol Chem*. 2012;287(33):27335. doi:10.1074/jbc.M112.359000
142. Donde A, Sun M, Ling JP, et al. Splicing repression is a major function of TDP-43 in motor neurons. *Acta Neuropathol (Berl)*. 2019;138(5):813-826. doi:10.1007/s00401-019-02042-8
143. Torres P, Ramírez-Núñez O, Romero-Guevara R, et al. Cryptic exon splicing function of TARDBP interacts with autophagy in nervous tissue. *Autophagy*. 2018;14(8):1398-1403. doi:10.1080/15548627.2018.1474311
144. Mehta PR, Brown AL, Ward ME, Fratta P. The era of cryptic exons: implications for ALS-FTD. *Mol Neurodegener*. 2023;18(1):16. doi:10.1186/s13024-023-00608-5
145. A panel of TDP-43-regulated splicing events verifies loss of TDP-43 function in amyotrophic lateral sclerosis brain tissue. *Neurobiol Dis*. 2023;185:106245. doi:10.1016/j.nbd.2023.106245
146. Krus KL, Strickland A, Yamada Y, et al. Loss of Stathmin-2, a hallmark of TDP-43-associated ALS, causes motor neuropathy. *Cell Rep*. 2022;39(13):111001. doi:10.1016/j.celrep.2022.111001
147. Ma XR, Prudencio M, Koike Y, et al. TDP-43 represses cryptic exon inclusion in the FTD-ALS gene UNC13A. *Nature*. 2022;603(7899):124-130. doi:10.1038/s41586-022-04424-7
148. Brown AL, Wilkins OG, Keuss MJ, et al. TDP-43 loss and ALS-risk SNPs drive mis-splicing and depletion of UNC13A. *Nature*. 2022;603(7899):131-137. doi:10.1038/s41586-022-04436-3
149. Steinacker P, Hendrich C, Sperfeld AD, et al. TDP-43 in Cerebrospinal Fluid of Patients With Frontotemporal Lobar Degeneration and Amyotrophic Lateral Sclerosis. *Arch Neurol*. 2008;65(11):1481-1487. doi:10.1001/archneur.65.11.1481
150. Yang C, Qiao T, Yu J, et al. Low-level overexpression of wild type TDP-43 causes late-onset, progressive neurodegeneration and paralysis in mice. *PLOS ONE*. 2022;17(2):e0255710. doi:10.1371/journal.pone.0255710

151. White MA, Kim E, Duffy A, et al. TDP-43 gains function due to perturbed autoregulation in a Tardbp knock-in mouse model of ALS-FTD. *Nat Neurosci*. 2018;21(4):552-563. doi:10.1038/s41593-018-0113-5
152. Ash PEA, Zhang YJ, Roberts CM, et al. Neurotoxic effects of TDP-43 overexpression in *C. elegans*. *Hum Mol Genet*. 2010;19(16):3206-3218. doi:10.1093/hmg/ddq230
153. Barmada SJ, Skibinski G, Korb E, Rao EJ, Wu JY, Finkbeiner S. Cytoplasmic Mislocalization of TDP-43 Is Toxic to Neurons and Enhanced by a Mutation Associated with Familial Amyotrophic Lateral Sclerosis. *J Neurosci*. 2010;30(2):639-649. doi:10.1523/JNEUROSCI.4988-09.2010
154. Walker AK, Spiller KJ, Ge G, et al. Functional recovery in new mouse models of ALS/FTLD after clearance of pathological cytoplasmic TDP-43. *Acta Neuropathol (Berl)*. 2015;130(5):643-660. doi:10.1007/s00401-015-1460-x
155. Alfieri JA, Pino NS, Igaz LM. Reversible Behavioral Phenotypes in a Conditional Mouse Model of TDP-43 Proteinopathies. *J Neurosci*. 2014;34(46):15244-15259. doi:10.1523/JNEUROSCI.1918-14.2014
156. Altman T, Ionescu A, Ibraheem A, et al. Axonal TDP-43 condensates drive neuromuscular junction disruption through inhibition of local synthesis of nuclear encoded mitochondrial proteins. *Nat Commun*. 2021;12(1):6914. doi:10.1038/s41467-021-27221-8
157. Johnson BS, Snead D, Lee JJ, McCaffery JM, Shorter J, Gitler AD. TDP-43 Is Intrinsically Aggregation-prone, and Amyotrophic Lateral Sclerosis-linked Mutations Accelerate Aggregation and Increase Toxicity. *J Biol Chem*. 2009;284(30):20329-20339. doi:10.1074/jbc.M109.010264
158. Moser JM, Bigini P, Schmitt-John T. The wobbler mouse, an ALS animal model. *Mol Genet Genomics*. 2013;288(5):207-229. doi:10.1007/s00438-013-0741-0
159. Schmitt-John T, Drepper C, Mussmann A, et al. Mutation of Vps54 causes motor neuron disease and defective spermiogenesis in the wobbler mouse. *Nat Genet*. 2005;37(11):1213-1215. doi:10.1038/ng1661
160. Morrice JR, Gregory-Evans CY, Shaw CA. Animal models of amyotrophic lateral sclerosis: a comparison of model validity. *Neural Regen Res*. 2018;13(12):2050-2054. doi:10.4103/1673-5374.241445
161. Fisher EMC, Greensmith L, Malaspina A, et al. Opinion: more mouse models and more translation needed for ALS. *Mol Neurodegener*. 2023;18(1):1-12. doi:10.1186/s13024-023-00619-2
162. Nonaka T, Suzuki G, Tanaka Y, et al. Phosphorylation of TAR DNA-binding Protein of 43 kDa (TDP-43) by Truncated Casein Kinase 1 δ Triggers Mislocalization and Accumulation of TDP-43. *J Biol Chem*. 2016;291(11):5473-5483. doi:10.1074/jbc.M115.695379
163. Buratti E. TDP-43 post-translational modifications in health and disease. *Expert Opin Ther Targets*. 2018;22(3):279-293. doi:10.1080/14728222.2018.1439923

164. Ren Y, Li S, Chen S, et al. TDP-43 and Phosphorylated TDP-43 Levels in Paired Plasma and CSF Samples in Amyotrophic Lateral Sclerosis. *Front Neurol.* 2021;12. Accessed December 18, 2023. <https://www.frontiersin.org/articles/10.3389/fneur.2021.663637>
165. Li HY, Yeh PA, Chiu HC, Tang CY, Tu BP hsien. Hyperphosphorylation as a Defense Mechanism to Reduce TDP-43 Aggregation. *PLOS ONE.* 2011;6(8):e23075. doi:10.1371/journal.pone.0023075
166. Renaud L, Picher-Martel V, Codron P, Julien JP. Key role of UBQLN2 in pathogenesis of amyotrophic lateral sclerosis and frontotemporal dementia. *Acta Neuropathol Commun.* 2019;7(1):103. doi:10.1186/s40478-019-0758-7
167. Hebron ML, Lonskaya I, Sharpe K, et al. Parkin ubiquitinates Tar-DNA binding protein-43 (TDP-43) and promotes its cytosolic accumulation via interaction with histone deacetylase 6 (HDAC6). *J Biol Chem.* 2013;288(6):4103-4115. doi:10.1074/jbc.M112.419945
168. Farina S, Esposito F, Battistoni M, Biamonti G, Francia S. Post-Translational Modifications Modulate Proteinopathies of TDP-43, FUS and hnRNP-A/B in Amyotrophic Lateral Sclerosis. *Front Mol Biosci.* 2021;8. Accessed December 18, 2023. <https://www.frontiersin.org/articles/10.3389/fmolb.2021.693325>
169. Enserink JM. Sumo and the cellular stress response. *Cell Div.* 2015;10:4. doi:10.1186/s13008-015-0010-1
170. Henley JM, Craig TJ, Wilkinson KA. Neuronal SUMOylation: Mechanisms, Physiology, and Roles in Neuronal Dysfunction. *Physiol Rev.* 2014;94(4):1249-1285. doi:10.1152/physrev.00008.2014
171. Liang YC, Lee CC, Yao YL, Lai CC, Schmitz ML, Yang WM. SUMO5, a Novel Poly-SUMO Isoform, Regulates PML Nuclear Bodies. *Sci Rep.* 2016;6(1):26509. doi:10.1038/srep26509
172. Geiss-Friedlander R, Melchior F. Concepts in sumoylation: a decade on. *Nat Rev Mol Cell Biol.* 2007;8(12):947-956. doi:10.1038/nrm2293
173. Dangoumau A, Veyrat-Durebex C, Blasco H, et al. Protein SUMOylation, an emerging pathway in amyotrophic lateral sclerosis. *Int J Neurosci.* 2013;123(6):366-374. doi:10.3109/00207454.2012.761984
174. Wilkinson KA, Henley JM. Mechanisms, regulation and consequences of protein SUMOylation. *Biochem J.* 2010;428(2):133-145. doi:10.1042/BJ20100158
175. Bernier-Villamor V, Sampson DA, Matunis MJ, Lima CD. Structural Basis for E2-Mediated SUMO Conjugation Revealed by a Complex between Ubiquitin-Conjugating Enzyme Ubc9 and RanGAP1. *Cell.* 2002;108(3):345-356. doi:10.1016/S0092-8674(02)00630-X
176. Foran E, Rosenblum L, Bogush AI, Trotti D. Sumoylation of critical proteins in amyotrophic lateral sclerosis: emerging pathways of pathogenesis. *Neuromolecular Med.* 2013;15(4):10.1007/s12017-013-8262-x. doi:10.1007/s12017-013-8262-x
177. Mandel N, Agarwal N. Role of SUMOylation in Neurodegenerative Diseases. *Cells.* 2022;11(21):3395. doi:10.3390/cells11213395

178. Multiplex SILAC analysis of a cellular TDP-43 proteinopathy model reveals protein inclusions associated with SUMOylation and diverse polyubiquitin chains - PubMed. Accessed December 18, 2023. <https://pubmed.ncbi.nlm.nih.gov/20047951/>
179. Maurel C, Chami AA, Thépault RA, et al. A role for SUMOylation in the Formation and Cellular Localization of TDP-43 Aggregates in Amyotrophic Lateral Sclerosis. *Mol Neurobiol.* 2020;57(3):1361-1373. doi:10.1007/s12035-019-01810-7
180. Maraschi A, Gumina V, Dragotto J, et al. SUMOylation Regulates TDP-43 Splicing Activity and Nucleocytoplasmic Distribution. *Mol Neurobiol.* 2021;58(11):5682-5702. doi:10.1007/s12035-021-02505-8
181. Chang CC, Tung CH, Chen CW, Tu CH, Chu YW. SUMOgo: Prediction of sumoylation sites on lysines by motif screening models and the effects of various post-translational modifications. *Sci Rep.* 2018;8(1):15512. doi:10.1038/s41598-018-33951-5
182. Miedel CJ, Patton JM, Miedel AN, Miedel ES, Levenson JM. Assessment of Spontaneous Alternation, Novel Object Recognition and Limb Clasping in Transgenic Mouse Models of Amyloid- β and Tau Neuropathology. *J Vis Exp JoVE.* 2017;(123):55523. doi:10.3791/55523
183. Guyenet SJ, Furrer SA, Damian VM, Baughan TD, La Spada AR, Garden GA. A Simple Composite Phenotype Scoring System for Evaluating Mouse Models of Cerebellar Ataxia. *J Vis Exp JoVE.* 2010;(39):1787. doi:10.3791/1787
184. Huang SL, Wu LS, Lee M, et al. A robust TDP-43 knock-in mouse model of ALS. *Acta Neuropathol Commun.* 2020;8(1):1-19. doi:10.1186/s40478-020-0881-5
185. Feather-Schussler DN, Ferguson TS. A Battery of Motor Tests in a Neonatal Mouse Model of Cerebral Palsy. *J Vis Exp JoVE.* 2016;(117):53569. doi:10.3791/53569
186. DMD_M_2.1.004.pdf. Accessed January 24, 2024. https://www.treat-nmd.org/wp-content/uploads/2023/07/DMD_M_2.1.004.pdf
187. Samaey C, Schreurs A, Stroobants S, Balschun D. Early Cognitive and Behavioral Deficits in Mouse Models for Tauopathy and Alzheimer's Disease. *Front Aging Neurosci.* 2019;11. Accessed January 24, 2024. <https://www.frontiersin.org/articles/10.3389/fnagi.2019.00335>
188. Xu YF, Gendron TF, Zhang YJ, et al. Wild-Type Human TDP-43 Expression Causes TDP-43 Phosphorylation, Mitochondrial Aggregation, Motor Deficits, and Early Mortality in Transgenic Mice. *J Neurosci.* 2010;30(32):10851. doi:10.1523/JNEUROSCI.1630-10.2010
189. Filiano AJ, Martens LH, Young AH, et al. Dissociation of Frontotemporal Dementia-Related Deficits and Neuroinflammation in Progranulin Haploinsufficient Mice. *J Neurosci.* 2013;33(12):5352-5361. doi:10.1523/JNEUROSCI.6103-11.2013
190. Wong P, Ho WY, Yen YC, Sanford E, Ling SC. The vulnerability of motor and frontal cortex-dependent behaviors in mice expressing ALS-linked mutation in TDP-43. *Neurobiol Aging.* 2020;92:43-60. doi:10.1016/j.neurobiolaging.2020.03.019

191. Kraemer BC, Schuck T, Wheeler JM, et al. Loss of murine TDP-43 disrupts motor function and plays an essential role in embryogenesis. *Acta Neuropathol (Berl)*. 2010;119(4):409-419. doi:10.1007/s00401-010-0659-0
192. Takeshita H, Yamamoto K, Nozato S, et al. Modified forelimb grip strength test detects aging-associated physiological decline in skeletal muscle function in male mice. *Sci Rep*. 2017;7(1):42323. doi:10.1038/srep42323
193. Van der Jeugd A, Vermaercke B, Halliday GM, Staufenbiel M, Götz J. Impulsivity, decreased social exploration, and executive dysfunction in a mouse model of frontotemporal dementia. *Neurobiol Learn Mem*. 2016;130:34-43. doi:10.1016/j.nlm.2016.01.007
194. Pond HL, Heller AT, Gural BM, McKissick OP, Wilkinson MK, Manzini MC. Digging behavior discrimination test to probe burrowing and exploratory digging in male and female mice. *J Neurosci Res*. 2021;99(9):2046-2058. doi:10.1002/jnr.24857
195. Deacon RM. Assessing nest building in mice. *Nat Protoc*. 2006;1(3):1117-1119. doi:10.1038/nprot.2006.170
196. Alfieri JA, Silva PR, Igaz LM. Early Cognitive/Social Deficits and Late Motor Phenotype in Conditional Wild-Type TDP-43 Transgenic Mice. *Front Aging Neurosci*. 2016;8. Accessed December 19, 2023. <https://www.frontiersin.org/articles/10.3389/fnagi.2016.00310>
197. Arrant AE, Filiano AJ, Warmus BA, Hall AM, Roberson ED. Progranulin haploinsufficiency causes biphasic social dominance abnormalities in the tube test. *Genes Brain Behav*. 2016;15(6):588-603. doi:10.1111/gbb.12300
198. Fan Z, Zhu H, Zhou T, Wang S, Wu Y, Hu H. Using the tube test to measure social hierarchy in mice. *Nat Protoc*. 2019;14(3):819-831. doi:10.1038/s41596-018-0116-4
199. Neely CLC, Pedemonte KA, Boggs KN, Flinn JM. Nest Building Behavior as an Early Indicator of Behavioral Deficits in Mice. *J Vis Exp JoVE*. 2019;(152). doi:10.3791/60139
200. Thomas A, Burant A, Bui N, Graham D, Yuva-Paylor LA, Paylor R. Marble burying reflects a repetitive and perseverative behavior more than novelty-induced anxiety. *Psychopharmacology (Berl)*. 2009;204(2):361-373. doi:10.1007/s00213-009-1466-y
201. Roberson ED. Mouse Models of Frontotemporal Dementia. *Ann Neurol*. 2012;72(6):837-849. doi:10.1002/ana.23722
202. Pasquier F, Grymonprez L, Lebert F, Van der Linden M. Memory impairment differs in frontotemporal dementia and Alzheimer's disease. *Neurocase*. 2001;7(2):161-171. doi:10.1093/neucas/7.2.161
203. Stopford CL, Thompson JC, Neary D, Richardson AMT, Snowden JS. Working memory, attention, and executive function in Alzheimer's disease and frontotemporal dementia. *Cortex J Devoted Study Nerv Syst Behav*. 2012;48(4):429-446. doi:10.1016/j.cortex.2010.12.002

204. Kumfor F, Piguet O. Disturbance of emotion processing in frontotemporal dementia: a synthesis of cognitive and neuroimaging findings. *Neuropsychol Rev.* 2012;22(3):280-297. doi:10.1007/s11065-012-9201-6
205. Mioshi E, Lillo P, Yew B, et al. Cortical atrophy in ALS is critically associated with neuropsychiatric and cognitive changes. *Neurology.* 2013;80(12):1117-1123. doi:10.1212/WNL.0b013e31828869da
206. de Souza LC, Chupin M, Bertoux M, et al. Is hippocampal volume a good marker to differentiate Alzheimer's disease from frontotemporal dementia? *J Alzheimers Dis JAD.* 2013;36(1):57-66. doi:10.3233/JAD-122293
207. Laakso MP, Frisoni GB, Könönen M, et al. Hippocampus and entorhinal cortex in frontotemporal dementia and Alzheimer's disease: a morphometric MRI study. *Biol Psychiatry.* 2000;47(12):1056-1063. doi:10.1016/s0006-3223(99)00306-6
208. Bocchetta M, Malpetti M, Todd EG, Rowe JB, Rohrer JD. Looking beneath the surface: the importance of subcortical structures in frontotemporal dementia. *Brain Commun.* 2021;3(3):fcab158. doi:10.1093/braincomms/fcab158
209. Wang J, Ho WY, Lim K, et al. Cell-autonomous requirement of TDP-43, an ALS/FTD signature protein, for oligodendrocyte survival and myelination. *Proc Natl Acad Sci U S A.* 2018;115(46):E10941-E10950. doi:10.1073/pnas.1809821115
210. Ferrari R, Kapogiannis D, Huey ED, Momeni P. FTD and ALS: a tale of two diseases. *Curr Alzheimer Res.* 2011;8(3):273-294.
211. Wils H, Kleinberger G, Janssens J, et al. TDP-43 transgenic mice develop spastic paralysis and neuronal inclusions characteristic of ALS and frontotemporal lobar degeneration. *Proc Natl Acad Sci U S A.* 2010;107(8):3858-3863. doi:10.1073/pnas.0912417107
212. Iguchi Y, Katsuno M, Niwa J ichi, et al. Loss of TDP-43 causes age-dependent progressive motor neuron degeneration. *Brain J Neurol.* 2013;136(Pt 5):1371-1382. doi:10.1093/brain/awt029
213. Frew J, Nygaard HB. Neuropathological and behavioral characterization of aged Grn R493X progranulin-deficient frontotemporal dementia knockin mice. *Acta Neuropathol Commun.* 2021;9(1):57. doi:10.1186/s40478-021-01158-x
214. Jul P, Volbracht C, de Jong IEM, Helboe L, Elvang AB, Pedersen JT. Hyperactivity with Agitative-Like Behavior in a Mouse Tauopathy Model. *J Alzheimers Dis JAD.* 2016;49(3):783-795. doi:10.3233/JAD-150292
215. Przybyla M, Stevens CH, Van Der Hoven J, et al. Disinhibition-like behavior in a P301S mutant tau transgenic mouse model of frontotemporal dementia. *Neurosci Lett.* 2016;631:24-29. doi:10.1016/j.neulet.2016.08.007
216. Robinson L, Plano A, Cobb S, Riedel G. Long-term home cage activity scans reveal lowered exploratory behaviour in symptomatic female Rett mice. *Behav Brain Res.* 2013;250:148-156. doi:10.1016/j.bbr.2013.04.041

217. Ebstein SY, Yagudayeva I, Shneider NA. Mutant TDP-43 Causes Early-Stage Dose-Dependent Motor Neuron Degeneration in a TARDBP Knockin Mouse Model of ALS. *Cell Rep.* 2019;26(2):364-373.e4. doi:10.1016/j.celrep.2018.12.045
218. Verma S, Khurana S, Vats A, et al. Neuromuscular Junction Dysfunction in Amyotrophic Lateral Sclerosis. *Mol Neurobiol.* 2022;59(3):1502-1527. doi:10.1007/s12035-021-02658-6
219. Lin Z, Kim E, Ahmed M, et al. MRI-guided histology of TDP-43 knock-in mice implicates parvalbumin interneuron loss, impaired neurogenesis and aberrant neurodevelopment in amyotrophic lateral sclerosis-frontotemporal dementia. *Brain Commun.* 2021;3(2):fcab114. doi:10.1093/braincomms/fcab114
220. Winner B, Winkler J. Adult Neurogenesis in Neurodegenerative Diseases. *Cold Spring Harb Perspect Biol.* 2015;7(4):a021287. doi:10.1101/cshperspect.a021287
221. Dubal DB, Wise PM. Estrogen and neuroprotection: from clinical observations to molecular mechanisms. *Dialogues Clin Neurosci.* 2002;4(2):149-161.
222. Mentis AFA, Bougea AM, Chrousos GP. Amyotrophic lateral sclerosis (ALS) and the endocrine system: Are there any further ties to be explored? *Aging Brain.* 2021;1:100024. doi:10.1016/j.nbas.2021.100024
223. Exposure to endogenous and exogenous sex hormones and reproductive history influence prognosis in women with ALS - Gonzalez Deniselle - 2023 - Muscle & Nerve - Wiley Online Library. Accessed December 19, 2023. <https://onlinelibrary.wiley.com/doi/abs/10.1002/mus.27942>
224. Levine AJ, Hewett L. Estrogen replacement therapy and frontotemporal dementia. *Maturitas.* 2003;45(2):83-88. doi:10.1016/S0378-5122(03)00142-7
225. Watkins J, Ghosh A, Keerie AFA, Alix JJP, Mead RJ, Sreedharan J. Female sex mitigates motor and behavioural phenotypes in TDP-43Q331K knock-in mice. *Sci Rep.* 2020;10(1):19220. doi:10.1038/s41598-020-76070-w
226. Trojsi F, D'Alvano G, Bonavita S, Tedeschi G. Genetics and Sex in the Pathogenesis of Amyotrophic Lateral Sclerosis (ALS): Is There a Link? *Int J Mol Sci.* 2020;21(10):3647. doi:10.3390/ijms21103647
227. McLeod VM, Chiam MDF, Perera ND, Lau CL, Boon WC, Turner BJ. Mapping Motor Neuron Vulnerability in the Neuraxis of Male SOD1G93A Mice Reveals Widespread Loss of Androgen Receptor Occurring Early in Spinal Motor Neurons. *Front Endocrinol.* 2022;13. Accessed December 19, 2023. <https://www.frontiersin.org/articles/10.3389/fendo.2022.808479>
228. Al-Chalabi A, Calvo A, Chio A, et al. Analysis of amyotrophic lateral sclerosis as a multistep process: a population-based modelling study. *Lancet Neurol.* 2014;13(11):1108-1113. doi:10.1016/S1474-4422(14)70219-4
229. Bozzoni V, Pansarasa O, Diamanti L, Nosari G, Cereda C, Ceroni M. Amyotrophic lateral sclerosis and environmental factors. *Funct Neurol.* 2016;31(1):7-19. doi:10.11138/FNeur/2016.31.1.007

230. Dubinski A, Gagné M, Peyrard S, Gordon D, Talbot K, Vande Velde C. Stress granule assembly in vivo is deficient in the CNS of mutant TDP-43 ALS mice. *Hum Mol Genet.* 2022;32(2):319-332. doi:10.1093/hmg/ddac206
231. Cytoplasmic TDP-43 is involved in cell fate during stress recovery | Human Molecular Genetics | Oxford Academic. Accessed December 19, 2023. <https://academic.oup.com/hmg/article/31/2/166/6347249>
232. Ratti A, Gumina V, Lenzi P, et al. Chronic stress induces formation of stress granules and pathological TDP-43 aggregates in human ALS fibroblasts and iPSC-motoneurons. *Neurobiol Dis.* 2020;145:105051. doi:10.1016/j.nbd.2020.105051
233. Frontiers | SUMOylation Connects Cell Stress Responses and Inflammatory Control: Lessons From the Gut as a Model Organ. Accessed December 19, 2023. <https://www.frontiersin.org.proxy.bib.uottawa.ca/articles/10.3389/fimmu.2021.646633/full>
234. Marmor-Kollet H, Siany A, Kedersha N, et al. Spatiotemporal Proteomic Analysis of Stress Granule Disassembly Using APEX Reveals Regulation by SUMOylation and Links to ALS Pathogenesis. *Mol Cell.* 2020;80(5):876-891.e6. doi:10.1016/j.molcel.2020.10.032
235. O'Rourke JG, Bogdanik L, Muhammad AKMG, et al. C9orf72 BAC Transgenic Mice Display Typical Pathologic Features of ALS/FTD. *Neuron.* 2015;88(5):892-901. doi:10.1016/j.neuron.2015.10.027
236. Sturme E, Malaspina A. Blood biomarkers in ALS: challenges, applications and novel frontiers. *Acta Neurol Scand.* 2022;146(4):375-388. doi:10.1111/ane.13698
237. Carlyle BC, Trombetta BA, Arnold SE. Proteomic Approaches for the Discovery of Biofluid Biomarkers of Neurodegenerative Dementias. *Proteomes.* 2018;6(3):32. doi:10.3390/proteomes6030032
238. Vu LT, Bowser R. Fluid-Based Biomarkers for Amyotrophic Lateral Sclerosis. *Neurotherapeutics.* 2017;14(1):119-134. doi:10.1007/s13311-016-0503-x
239. Birhanu AG. Mass spectrometry-based proteomics as an emerging tool in clinical laboratories. *Clin Proteomics.* 2023;20(1):32. doi:10.1186/s12014-023-09424-x
240. Vignaroli F, Mele A, Tondo G, et al. The Need for Biomarkers in the ALS–FTD Spectrum: A Clinical Point of View on the Role of Proteomics. *Proteomes.* 2023;11(1):1. doi:10.3390/proteomes11010001
241. Subramanyam M, Goyal J. Translational biomarkers: from discovery and development to clinical practice. *Drug Discov Today Technol.* 2016;21-22:3-10. doi:10.1016/j.ddtec.2016.10.001
242. Galectin-3 is a candidate biomarker for ALS: Discovery by a proteomics approach - PMC. Accessed December 19, 2023. <https://www.ncbi.nlm.nih.gov.proxy.bib.uottawa.ca/pmc/articles/PMC2948604/>
243. Gertsman I, Wu J, McAlonis-Downes M, et al. An endogenous peptide marker differentiates SOD1 stability and facilitates pharmacodynamic monitoring in SOD1 amyotrophic lateral sclerosis. *JCI Insight.* 4(10):e122768. doi:10.1172/jci.insight.122768

244. Pasetto L, Callegaro S, Corbelli A, et al. Decoding distinctive features of plasma extracellular vesicles in amyotrophic lateral sclerosis. *Mol Neurodegener.* 2021;16(1):1-21. doi:10.1186/s13024-021-00470-3